Validation and application of intravascular ultrasound in the study of percutaneous coronary intervention

Nicholas D Palmer

A thesis submitted to the University of Edinburgh for the degree of Doctor of Medicine

April 2002

For Juliette, Lucy, Katie and Christian

What makes a Great Physician?

I would answer that *he is a great physician who, above other men, understands diagnosis.* It is not he who promises to cure all maladies, who has a remedy ready for every symptom, or one remedy for all symptoms; who boasts that success never fails him, when his daily history gives the lie to such assertion. It is rather he, who, with just discrimination, looks at a case in all its difficulties; who to habits of correct reasoning, adds the acquirements obtained from study and observation; who is trustworthy in common things for his common sense, and in professional things for his judgement, learning and experience; who forms his opinion positive or approximative, according to the evidence; who looks at the necessary results of inevitable causes; who promptly does what man may do of good, and carefully avoids what he may do of evil.

Dr Jacob Bigelow
Nature in Disease, 1852.

INTRODUCTION

Intravascular ultrasound (IVUS) is a relatively new method of imaging coronary arteries which has several advantages over contrast angiography in the accurate quantification of coronary lumen and vessel dimensions and assessment of atherosclerotic plaque. Experimentally, IVUS has so far provided detailed insights into the distribution and composition of atheroma in the coronary circulation and its behaviour when subjected, particularly, to balloon dilatation. The technique is now regarded as a useful adjunct to angiography in the routine assessment of patients with atherosclerotic coronary disease as well as in the guidance of percutaneous coronary interventional techniques such as balloon angioplasty and intracoronary stent implantation. Additionally, the concept of three-dimensional reconstruction of IVUS images has recently been realized providing the opportunity for longitudinal as well as tomographic analysis.

Despite the wealth of information so far provided by IVUS most *in vitro* studies require cautious interpretation due to well-recognised limitations of studying animal models of atherosclerosis or human coronary disease in circumstances that do not accurately reflect the clinical setting. This thesis is based upon the development of a pulsatile flow system which is capable of accurately reproducing some of the important physiological properties of *in-vivo* flow in normal and diseased coronary arteries. Some characteristics of *in-vivo* coronary blood flow cannot be met, such as the effect of blood viscosity and extrinsic compression of the vessel by the beating heart. However, the system is designed to enable the study of human coronary atherosclerotic disease by IVUS in conditions which closely resemble those seen in the clinical setting. The initial chapters provide an overview of IVUS, including methods and rationale for three-dimensional reconstruction, and describe the development and validation of the flow system. Chapters 3 and 4 assess the qualitative accuracy of IVUS in the assessment of the composition of atherosclerotic plaque and also the reproducibility of IVUS assessments of vessel and lumen dimensions in diseased coronary arteries. There follows a study of coronary balloon angioplasty designed to assess the influence of procedural factors, such as balloon calibre and inflation pressure selection, and IVUS guidance on the initial success of the procedure. In the remaining chapters two studies

examine three-dimensional reconstruction of IVUS images and the influence of technical factors, which are inherent in IVUS imaging, on the accuracy of atherosclerotic plaque volume measurement and its use in assessing vascular injury following coronary balloon angioplasty. It should be emphasized that all patient donors died from causes other than cardiovascular disease such that the histopathological studies involved the use of coronary artery specimens which were not required for diagnostic purposes. The studies adhered to strict ethical standards of the day. Harvesting of specimens received ethical approval as part of the overall IVUS research programme being undertaken at the time. All specimens were retained by the Department of Pathology during the study period and disposed of appropriately following the final analyses.

Taken together these studies have helped to provide further insights into the quantitative and qualitative accuracy of IVUS in the assessment of coronary atherosclerosis and the technical factors which may confound these analyses. Furthermore, the value of IVUS in guiding, and assessing the outcome of, coronary balloon angioplasty is clearly demonstrated. Given the close correlation of the studies to the clinical setting the findings should be expected to influence our approach to clinical IVUS studies and utilize the technique more frequently in the guidance of percutaneous coronary intervention.

TABLE OF CONTENTS

Chapter 1

Intravascular ultrasound: an overview 1

1.1 Introduction 2
1.2 Limitations of coronary angiography 2
1.3 Intravascular ultrasound 3
1.3.1 Development and technology of IVUS 7
1.3.2 Image acquisition and interpretation 9
1.3.3 Insights into coronary artery disease 15
1.3.4 Diagnostic IVUS in clinical practice 18
1.3.5 Guidance of percutaneous intervention 19
1.3.6 Insights into transplant vasculopathy 24
1.3.7 Research applications of IVUS 25
1.3.8 Current technical limitations of IVUS 26
1.3.9 Future directions for IVUS 27
1.4 Conclusions 28
1.5 Three-dimensional reconstruction of IVUS images: an overview 29
1.5.1 Image acquisition 29
1.5.2 IVUS catheter characteristics 30
1.5.3 Continuous versus ECG-gated pullbacks 30
1.5.4 Image digitization and segmentation 32
1.5.5 Acoustic quantification system 32
1.5.6 Contour detection system 34
1.5.7 Challenges and future directions 35
1.5.8 Conclusion 38

Chapter 2

Methodology 39

2.1 Introduction 40

2.2 Development and validation of pulsatile flow system 41

2.2.1 Coronary flow 41

2.2.2 Perfusion pressure 43

2.2.3 Vessel distensibility 43

2.2.4 Saline perfusion 44

2.3 Harvesting and preparation of coronary artery specimens 45

2.4 Histological analysis 46

Chapter 3

Analysis of coronary atheromatous plaque by intravascular ultrasound. Reproducibility and histological correlation of lesion morphology 48

3.1 Introduction 49

3.2 Methods 49

3.2.1 IVUS image analysis 51

3.2.2 Histological analysis 52

3.2.3 Statistical analysis 52

3.3 Results 52

3.3.1 IVUS image quality 53

3.3.2 Intra-observer agreement 53

3.3.3 Inter-observer agreement 53

3.3.4 Predominant plaque composition 54
3.3.5 Histological correlation to plaque type 54
3.3.6 Focal calcium deposition 55
3.3.7 Influence of pulsatile flow 55
3.4 Discussion 55
3.4.1 Reproducibility 56
3.4.2 Histological correlation 57
3.5 Limitations of the study 57
3.6 Conclusions 58

Chapter 4

Clinical implications of interobserver variability in reference site selection in intravascular ultrasound-guided percutaneous intervention 66

4.1 Introduction 67
4.2 Methods 68
4.2.1 IVUS measurements 68
4.2.2 Statistical analysis 69
4.3 Results 69
4.3.1 Variability of measurements at minimum lumen area 70
4.3.2 Variability of measurements at reference sites 70
4.3.3 Implication of variability in IVUS measurements on balloon size selection 71
4.4 Discussion 71
4.4.1 A review of previous studies 73
4.4.2 Clinical implications 74
4.5 Study limitations 75
4.6 Conclusions 75

Chapter 5

Influence of balloon calibre and inflation pressure characteristics on arterial wall injury in intravascular ultrasound-guided percutaneous transluminal coronary angioplasty – histopathological observations 83

5.1 Introduction 84
5.2 Methods 84
5.3 Data and statistics 86
5.4 Results 87
5.4.1 Post-intervention analysis 87
5.4.2 Influence of plaque characteristics on outcome 88
5.5 Discussion 88
5.5.1 Influence of balloon calibre and inflation pressure 88
5.5.2 Influence of plaque characteristics 90
5.6 Study limitations 91
5.7 Conclusions 91

Overview of subsequent chapters 98

Chapter 6

An analysis of the influence of catheter shaft angulation on the accuracy of volume measurement by three-dimensional intravascular ultrasound 99

6.1 Introduction 100
6.2 Methods 101

6.2.1 Imaging methodology 102
6.2.2 Three-dimensional reconstruction and volume measurement 103
6.2.3 Data analysis and statistics 104
6.3 Results 104
6.3.1 Phantom study 104
6.3.2 Coronary artery study 105
6.3.3 Influence of transducer tip position 106
6.4 Discussion 106
6.4.1 Impact of catheter conformation 113
6.4.2 Impact of transducer tip position 114
6.4.3 Explanation of findings 114
6.4.4 Clinical implications 116
6.5 Conclusions 116

Chapter 7

Evaluation of arterial wall dissections in coronary angioplasty: a comparison of two- and three-dimensional intravascular ultrasound imaging 118

7.1 Introduction 119
7.2 Methods 120
7.2.1 Three-dimensional IVUS image interpretation 121
7.2.2 IVUS image analysis 121
7.2.3 Histopathological analysis 122
7.2.4 Statistical analysis 122
7.3 Results 123
7.3.1 Dissection type 123
7.3.2 Dissection length and depth 124

7.4 Discussion 124

7.4.1 Previous studies 126

7.4.2 Study limitations 127

7.4.3 Clinical implications 127

7.5 Conclusions 128

Chapter 8

General conclusions 134

8.1 General conclusions 135

Chapter 9

Bibliography 138

9.1 Bibliography 139

I confirm that, under the supervision of Professor Keith Fox and Dr David Northridge, I was solely responsible for the design and construction of the described pulsatile flow system and conducted all the studies contained in this thesis. This thesis was composed by myself and has not been submitted for any other degree or professional qualification

ACKNOWLEDGEMENTS

A chance conversation on a flight from Europe resulted in the opportunity for me to join the IVUS research programme in Edinburgh. For that I have Dr Roger Smith to thank. When my career path was unclear his encouragement and enthusiasm ensured that cardiology was to be my future!

I have several people to thank for their support during my time as a research fellow in Edinburgh. Firstly, Dave Northridge who took me under his wing and provided a direction for the research programme. His supervision of the work and friendship during this time were greatly appreciated. I am indebted to Professor Keith Fox who provided initial support for the studies and acted as my supervisor. Despite a very hectic schedule he always put time aside to advise on the projects undertaken and constantly encouraged me to publish the data. Thanks also to Dr Alistair Lessells for acquiring and processing the pathological specimens, and Drs Ian Starkey and Stuart Shaw for their teaching and support in the clinical area. I had the great privilege of working in a highly dedicated research environment in Edinburgh, a factor that I am sure was the key to the success of this thesis.

The continued encouragement, support and love of my parents is always appreciated. There really is no one who is *as* interested in what you are doing as your mum and dad and I have appreciated using them as a sounding-board for various decisions I have had to make in my career so far. My dad is mainly responsible for my enthusiasm for clinical medicine. Of all the physicians I have known he remains the "greatest". I only hope that I have acquired at least some of the high standards he had during his professional career.

Lastly, but certainly not least, I owe a great deal to my incredibly understanding wife, Jue, who has endured numerous lonely evenings as I wrote this thesis and unfortunately remains the ultimate "cath. lab widow" as I pursue a career in interventional cardiology. I couldn't have done all this with anyone else.

PUBLICATIONS

The studies performed for this thesis have produced the following publications:

Palmer ND, Lange A, Palka P, Ramo MP, Kearney PP, Fox KAA, Sutherland GR. Effect of catheter shaft position, angulation and pullback type on the volumetric analysis of IVUS images: a phantom study. Eur Heart J 1996; **17**: 186.

Palmer ND, Northridge DB, Lessells A, Fox KAA. Analysis of pre-interventional coronary stenoses by intracoronary ultrasound: an in vitro study with histological correlation using a novel pulsatile flow system. Scot Med J 1997; **42** (6): 188.

Palmer ND, Northridge DB, Kearney PP. Interobserver variability in reference segment selection and quantitation using intracoronary ultrasound. Heart 1998; **79** (suppl 1): 14.

Palmer ND, Fort S, Lessells A, Fox KAA, Northridge DB. High pressure versus larger calibre to achieve an optimal balloon size in coronary angioplasty: interim results of an in vitro intravascular ultrasound study. J Am Coll Cardiol 1998; **31** (2): 316A.

Palmer ND, Fort S, Lessells A, Fox KAA, Northridge DB. Evaluation of arterial wall dissections in coronary angioplasty: a comparison of two- and three-dimensional intravascular ultrasound imaging. Eur Heart J 1998; **19**: 550.

Palmer ND, Lessells A, Fox KAA, Northridge DB. Should balloon calibre/pressure strategies in coronary angioplasty be influenced by atherosclerotic plaque composition? In vitro observations with intravascular ultrasound. Scot Med J 1998; **82**: 34.

Palmer ND, Fort S, Fox KAA, Northridge DB. Do undersized balloons cause more dissections? An in vitro study of high pressure inflations in coronary angioplasty. Cardiology News 1998; **2** (2): 33.

Palmer ND, Northridge DB. Clinical applications of intravascular ultrasound: an overview. Cardiology News 1998; **1** (4): 4-6.

Palmer ND, Northridge DB, Lessells A, McDicken WN, Fox KAA. In vitro analysis of coronary atheromatous lesions by intravascular ultrasound: reproducibility and histological correlation of lesion morphology. Eur Heart J 1999; **20**: 1701-1706.

Palmer ND, Northridge DB, Lessells A, Fox KAA. Assessment of vessel wall injury following PTCA: a comparison of the accuracy of two- and three-dimensional intravascular ultrasound. Coronary Artery Disease 2003; **14**: 255-62.

Palmer ND, Northridge DB, Lessells A, Fox KAA. Influence of balloon calibre and inflation pressure characteristics on arterial wall injury in intravascular ultrasound-guided percutaneous transluminal coronary angioplasty – histopathological observations. Accepted for *J Intervent Cardiol,* 2003.

CHAPTER 1
Intravascular Ultrasound: an overview

1.1 Introduction

Coronary artery disease is the most dangerous medical condition in the Western World, causing over 100,000 deaths annually in the United Kingdom alone. Since the late 1950's the "gold standard" for the in-vivo diagnosis of coronary artery disease has been the angiogram. Coronary angiography is able to provide an overall map of the distribution of the coronary arteries and the location of atherosclerotic narrowings which is ideal for evaluating patients requiring coronary bypass surgery where the surgeon has only to decide which vessels to graft and where to place the anastomosis. In the last two decades major advances in our understanding of the pathogenesis of coronary artery disease and the development of more lesion-specific percutaneous, catheter-based techniques such as coronary balloon angioplasty (PTCA) have highlighted some of the basic limitations of angiography in assessing coronary atherosclerosis and prompted the development of other imaging modalities such as intravascular ultrasound (IVUS).

1.2 Limitations of coronary angiography

Assessment of the qualitative and quantitative impact of percutaneous coronary interventions and strategies used to promote atheroma regression demands a high degree of accuracy which can not be provided by the angiogram. Information regarding alterations in atheromatous plaque and visualization of the arterial wall is not possible. Although focal stenoses can be identified diffuse atheromatous disease is frequently not seen (Arnett *et al*, 1979). Additionally, the technique measures lumen diameter in calculating the degree of stenosis rather than lumen area which is generally regarded as the critical anatomical parameter defining the degree of stenosis (McPherson *et al*, 1987) [Figure 1a]. The variability of visual estimates of stenosis severity has been appreciated for many years (Zir *et al*, 1976). Bertrand *et al* assessed the accuracy of on line visual estimation of the results of PTCA and demonstrated that the reduction in stenosis severity was overestimated by 72% (61.8% stenosis reduction by visual estimation vs 36% by quantitative coronary angiography) [Bertrand *et al*, 1993]. Furthermore, clinically important stenoses of 50% or more were systematically overestimated whereas those less than 50% were underestimated by visual assessment. Computerized quantitative coronary angiography (QCA) of digital cineangiographic images provides

automated lumen edge detection and has been shown to be accurate and reproducible (Hermiller *et al*, 1992). However marked interobserver variability in identification of stenoses occurs in two-thirds of selected lesions largely due to differences in frame selection (Gurley *et al*, 1992). In over half the unanimously–identified stenoses failed automated edge detection occurred due to complex coronary anatomy and poor image quality (Figure 1b). There also remains the significant problem of identifying ostial lesions and those stenoses occurring in areas of significant vessel overlap despite the use of multiple orthogonal view planes.

1.3 Intravascular Ultrasound (IVUS)

Our understanding of the pathogenesis of coronary artery disease has changed dramatically over the last fifteen years. Additionally, minimally invasive, lesion-specific techniques such as balloon angioplasty have become very realistic alternatives to surgical revascularisation in certain patient subsets. It became clear from histologic, post-mortem studies that the extent of arterial narrowing by atherosclerotic plaque is only a weak indicator of whether that plaque will ultimately cause a myocardial infarction (Roberts *et al*, 1979; Fuster *et al*, 1992). The composition of the plaque, particularly the presence of a large lipid core, appears to predict plaque rupture and subsequent thrombotic occlusion (Davies *et al*, 1985 & 1993; Falk, 1989). Therefore, an angiographically mild stenosis may represent a more dangerous plaque than a more high grade lesion which is more likely to be composed of stable fibrous plaque. Dramatic advances in catheter-based therapies for coronary artery disease have further highlighted the limitations of angiography. The development of balloon angioplasty in the late 1970's was based on the concept that an atherosclerotic obstruction could be reduced by compression of plaque by high pressure balloon dilatation (Gruentzig *et al*, 1979). Subsequent studies have revealed that the mechanism of luminal enlargement is more complex, involving tearing and displacement of the plaque with stretching of the arterial wall (Farb *et al*, 1990; Hoshino *et al*, 1987; Lyon *et al*, 1987). These mechanisms vary in magnitude from lesion to lesion and are unpredictable from the angiographic appearance alone (Figure 2).

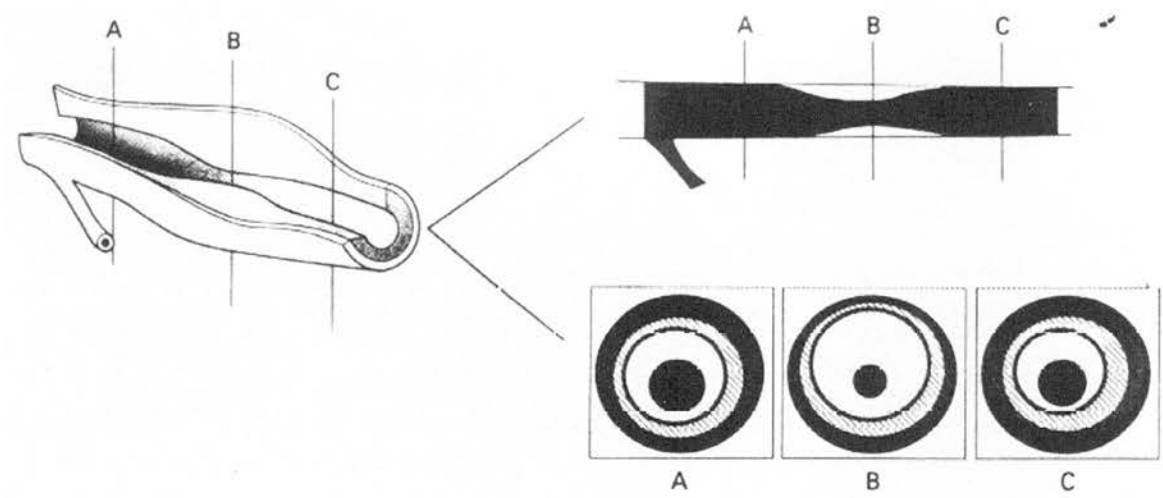

Figure 1a. ***Schematic diagram of a focally stenosed coronary arterial segment. Lines A and C transect the proximal and distal lumens. Line B transects the minimum lumen diameter site. The angiographic appearance (right upper panel) suggests normal reference segments (A&C) against which the diameter stenosis is calculated by contour detection methods. IVUS (right lower panel) shows considerable intimal thickening at these sites and vessel enlargement at the minimum lumen diameter site. The vessel area stenosis is calculated as >90% by IVUS whereas angiography suggests a lumen area stenosis of only 70% (reproduced with permission).***

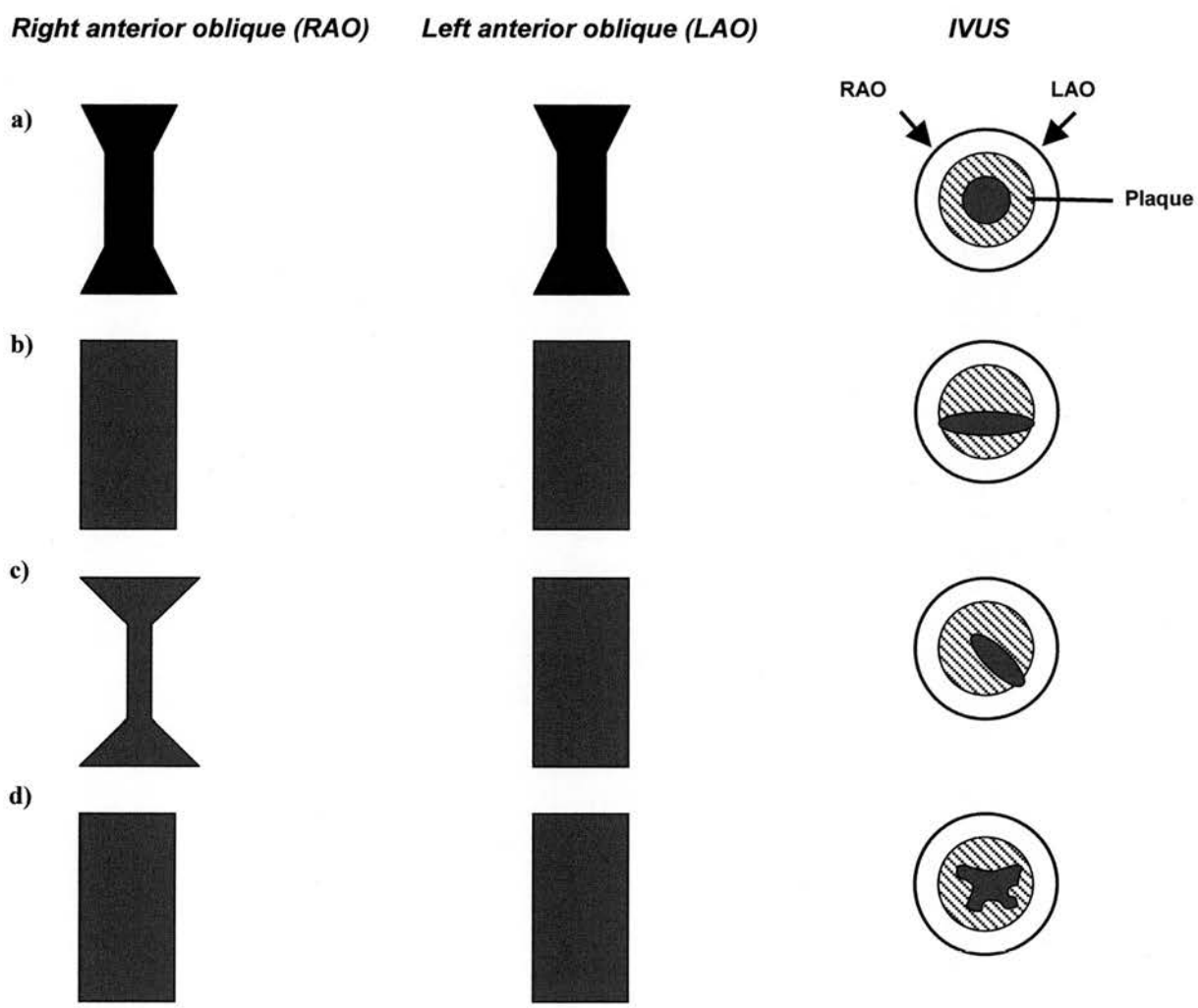

Figure 1b. ***Angiography versus IVUS in lumen assessment. In example a, mild concentric stenoses are identified using orthogonal angiographic views (RAO/LAO). Eccentric, elliptical lumens may not be evident in any (example b), or just one imaging plane (example c). Complex, irregular lumens are often missed by angiography (example d).***

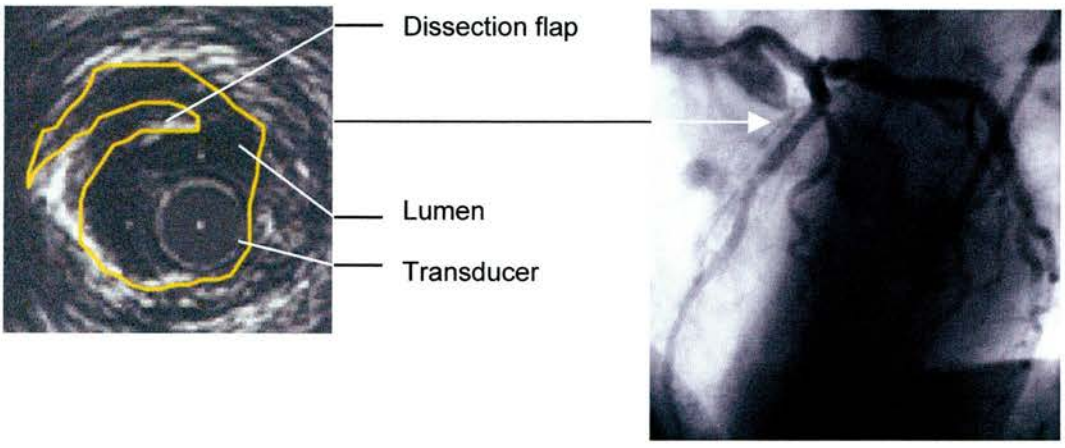

Figure 2. ***IVUS versus angiography post-PTCA. Following balloon dilatation of the proximal left anterior descending coronary artery (arrowed) the angiographic appearance suggests a smooth lumen. IVUS images at the tightest point of the original stenosis demonstrate a significant dissection flap extending into the medial layer.***

The proliferation of catheter-based techniques in the 1980's motivated the development of IVUS (Yock *et al*, 1988; Hodgson *et al*, 1989; Nissen *et al*, 1990). The technique enables detailed visualization of plaque morphology and composition in a cross-sectional or tomographic format with the ability to quantify lumen and vessel dimensions. The ability to view the arterial lumen has emphasized the limitations of angiography particularly in determining whether an apparently normal coronary artery is free of atherosclerotic disease. Numerous IVUS studies have demonstrated the presence of considerable atherosclerotic plaque, frequently causing significant luminal obstruction, in arterial segments that appear angiographically normal or only mildly diseased (Davidson *et al,* 1990; Ehrlich *et al,* 1991; Porter *et al,* 1993) [Figure 3].

1.3.1 *Development and Technology of IVUS*

Although endoluminal ultrasound had been described for many years the key challenge was to deliver high quality images from transducers that were small enough to navigate the coronary arteries. Clinical studies using IVUS really began in 1989 with the development of 5-6 French catheters which could negotiate relatively straight, proximal arterial segments (Bom *et al,* 1989). By 1994 sufficiently flexible and small catheters (2.9-3.2F or 0.9-1.0mm) had been developed that were able to access most lesions that required interrogation prior to a percutaneous revascularisation technique.

There are two types of intravascular ultrasound catheter: *solid state* (electronic) and *mechanical* (Figure 4). With the solid state approach, an array of ultrasound transducer elements is arranged in a cylinder at the tip of the catheter. Sequential firing of the elements produces a beam which rotates in a 360^0 arc producing a cross-sectional, tomographic image. Mechanical systems contain a single transducer at the catheter tip which is rotated by a flexible drive shaft running the length of the catheter. It is generally felt that mechanical systems provide better image quality since they operate at higher frequencies (30-40MHz), provide better image resolution, and have been miniaturized to a greater extent than solid state transducers. However mechanical systems are prone to image distortion due to binding of the drive shaft within the

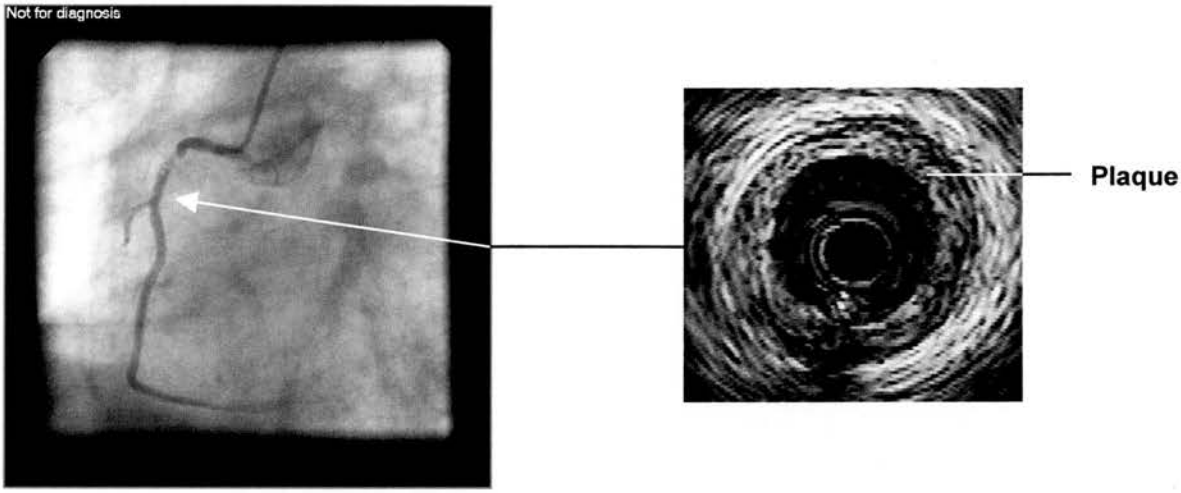

Figure 3. ***Occult disease detected by IVUS. In an angiographically normal segment of the right coronary artery distal to a severe stenosis significant atherosclerotic plaque is demonstrated by IVUS.***

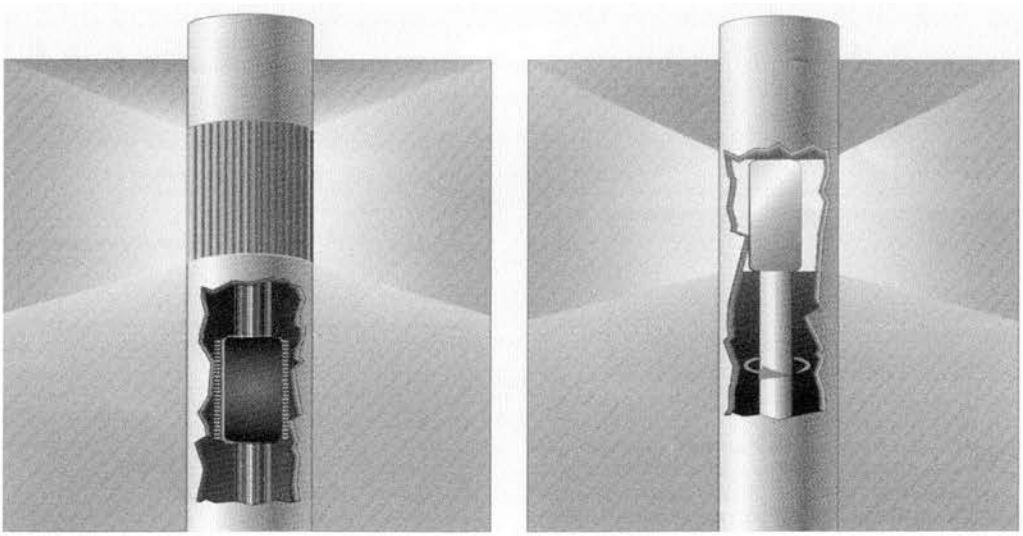

Figure 4. ***Mechanical and solid state state transducers (reproduced with permission).***

catheter (see Chapter 6) and suffer from image artefacts due to the guidewire. Electrical manipulation of the beam shape is an advantage of solid state systems. Commercially available systems using both approaches are available and have sufficiently good delivery and imaging characteristics to be useful in routine clinical practice.

1.3.2 *Image acquisition and interpretation*

The *acquisition* of IVUS images requires considerable experience in the practical aspect of cardiac catheterization and also in interpreting the images produced to provide sufficient information to enable clear clinical decisions to be made during a procedure. Before imaging, an intracoronary injection of isosorbide dinitrate (1-3mg) is performed to reduce the risk of spasm and induce maximal dilatation. An intravenous bolus of heparin (2000-5000 units) is administered prior to guidewire insertion. The short monorail catheters are advanced along the guidewire to a position distal to the lesion. They are usually able to cross tortuous proximal segments of the coronary artery although a stable guide catheter position that provides good support is important. Occasionally, problems are encountered when IVUS catheters are advanced into small distal vessels causing damage to the vessel wall, and when crossing stents as the relatively blunt catheter tip can disrupt the stent struts. A more central orientation of the catheter may be facilitated by adjustments in guide catheter position. Complications such as spasm and arterial wall dissections due to the catheter are, however, rare (Hausmann *et al,* 1995).

A standard imaging protocol should be followed for each IVUS examination. Whilst advancing the catheter distal to the segment of interest the image quality is optimized by adjustments of the gain settings. A common error is to reduce the near gain within the lumen to eliminate excessive backscatter from blood. This practice risks missing soft plaques around the catheter. The presented image may be electronically rotated such that anatomically correct images are produced. For instance, before entering the left anterior descending coronary artery from the left main coronary artery the image is rotated so that the left circumflex coronary artery branches in the 9 o'clock position such that diagonal artery branches will originate from the left between 8 to 12 o'clock and septal

branches originate at approximately 6 o'clock. Alternatively, in serial studies, topical landmarks such as calcium deposits, side-branches or adjacent veins can be used to ensure reproducible orientation of images (Figure 5). This process is particularly important clinically when selective plaque removal with atherectomy is performed or, in the research setting, when precise localization of plaque constituents is necessary in serial studies of atheroma regression techniques.

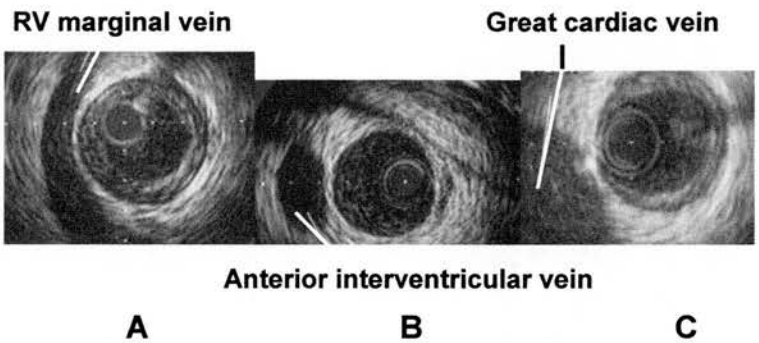

Figure 5. ***IVUS image orientation using adjacent veins. A right coronary artery; B, left anterior descending; C, left circumflex.***

The IVUS catheter is withdrawn manually or with the aid of a mechanical pullback device (0.5-1.0mm/sec) across the segment of interest. Mechanical pullbacks are particularly necessary where precise measurements of lesion length are required or when three-dimensional reconstruction is to be performed either on-line or from the recorded images. Analysis of the arterial segment is performed from the recorded images rather than the live image so as to minimize the time the IVUS catheter is positioned in the coronary artery. This is particularly important when a severe stenosis or very disrupted post-PTCA segment is being analyzed since prolonged, partial or complete vessel occlusion may result in myocardial ischaemia.

Image *interpretation* can be separated into qualitative and quantitative aspects.
<u>*Qualitative*</u> – it is important to understand normal arterial morphology before describing pathologic changes. In the normal intima, a superficial layer of endothelial cells covers a very thin subendothelial layer of connective tissue and smooth muscle cells. Its thickness increases with age, from a single layer at birth to 250μm at 40 years (Velican D *et al,*

1981). Diffuse intimal thickening is common in older patients and is histologically distinct from atherosclerosis (Becker, 1985). The muscular media thickness ranges from 125μm to 350μm although fibrous degeneration occurs in the elderly and in patients with atherosclerotic disease (Porter *et al,* 1994). The adventitia is composed of loose collagen and elastic tissue and is 300-500μm thick. Two sheets of elastic tissue separate the media from the intima (internal elastic lamina) and the adventitia (external elastic lamina).

The sudden change in acoustic impedance between adjacent tissue layers plays an important part in the determination of the characteristics of the ultrasound image of the vessel wall (Siegel *et al,* 1993). The leading edge of the intimal layer and the adventitia are well visualized with ultrasound. Elastic lamina layers are not well visualized so that only two layers are distinguishable, the intima-media complex and the adventitial layer (Isner *et al,* 1986) [Figure 6].

The pathology of atherosclerotic plaque development by IVUS has been well described (Di Mario *et al,* 1992; Peters *et al,* 1994). Early fatty streaks or degeneration of the internal elastic lamina do not change the ultrasonic appearance of the vessel wall. With further progression of atherosclerosis an increase in intimal thickness can be detected by IVUS (Figure 6). These arteries usually look normal angiographically however numerous studies have demonstrated that mild intimal thickening is associated with an abnormal response to vasoactive stimuli. In advanced atherosclerosis three basic lesion types are distinguished: (1) soft or fibrolipid plaques which have diffuse lipid infiltration and show low echoreflectivity; (2) hard or fibrodense plaques which produce contain predominantly fibrous tissue and show relatively high reflectivity equivalent to, or greater than, the surrounding adventitia and (3) calcified lesions which produce intensely bright reflections with acoustic shadowing (Figure 7). These classifications do not however reflect the mechanical characteristics of the plaque and their responses to balloon dilatation remain unpredictable (Hiro *et al,* 1995). Assessment of the accuracy and reproducibility of such a classification is described in Chapter 3. Focal calcification is very accurately detected by ultrasound. Deposits are described by their number, their depth within the plaque and their circumferential extent and axial distribution. IVUS has

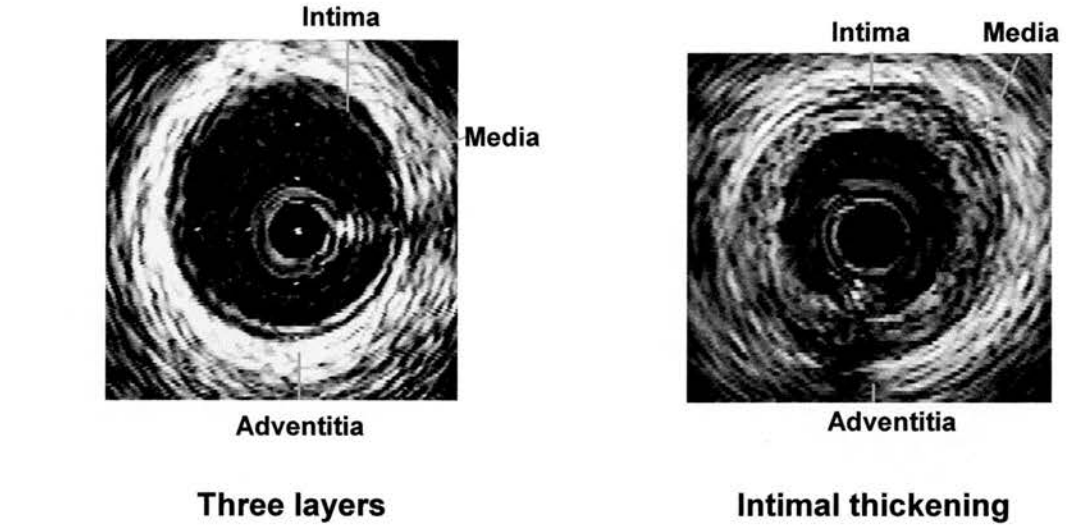

Figure 6. ***The normal three-layered appearance and intimal thickening as depicted by IVUS***

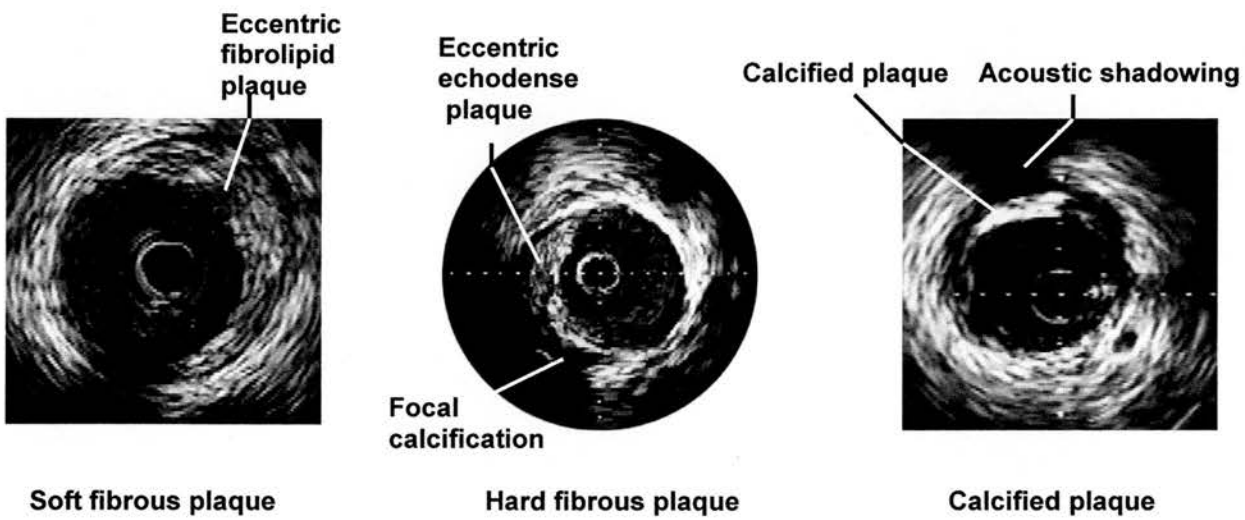

Figure 7. ***Atherosclerotic plaque composition by IVUS***

revealed that localized calcification is present much more commonly than is appreciated by angiography, occurring in 70-80% of lesions treated (Tuczu *et al,* 1996). Calcium deposits are important predictors of the way a particular lesion will respond to catheter-based interventions, particularly balloon dilatation and subsequently can influence device selection prior to percutaneous intervention (Fitzgerald *et al,* 1992 & 1992). Lipid pools can also be identified as completely echolucent areas often covered with a thin fibrous cap. Thrombus appears as a bright speckled reflection within the arterial lumen which is often mobile although it is frequently the case that it cannot be reliably distinguished from other plaque types (Kearney *et al,* 1996) [Figure 8].

Eccentric plaques are very commonly seen and are defined as ratio (thinnest / thickest portion of plaque) <0.5). This is despite their frequently concentric appearance on the angiogram (Mintz *et al,* 1996). Detection of eccentric plaques is of importance as these lesions are more likely to dissect following balloon dilatation and identification of the thickest portion of plaque is necessary in guiding selective plaque removal interventions.

With improvements in image quality, spontaneous plaque ruptures or fissures are increasingly observed mainly in unstable, ischaemic syndromes (Erbel *et al,* 1995). Wall disruption or dissection are frequently the result of percutaneous intervention. Simple radial tears and dissections are well-defined (Chapters 5&7). Dissection is diagnosed as a visible intimal flap and/or presence of blood flow, often confirmed by contrast injection, in the newly created lumen (Figure 9).

Quantitative – very high accuracy and inter/intraobserver reproducibility has been demonstrated for IVUS quantitation of vessel dimensions (Nishimura *et al,* 1990; Potkin *et al,* 1990; Hausmann *et al,* 1994) although a number of problems exist which need to be recognized. IVUS systems are usually calibrated however, ideally, accuracy of measurements needs confirming in vitro prior to its use in clinical studies. Catheter malignment such that the transducer lies eccentrically in the lumen results in an elliptical rather than circular cross-section leading to overestimation of area and diameter measurements. However, comparison of IVUS with quantitative coronary angiography in normal arteries demonstrated no significant inaccuracy due to a non-coaxial catheter

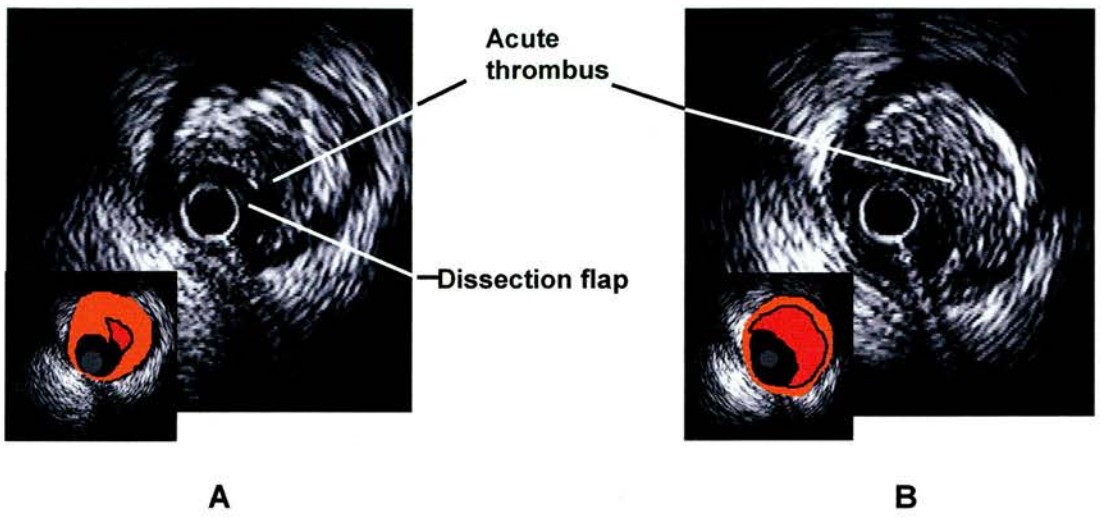

Figure 8. ***Thrombus detected by IVUS. A, following PTCA; B, following plaque rupture in a patient presenting with an acute coronary syndrome.***

Figure 9. ***IVUS assessment of arterial injury post-PTCA***

position. This is probably due to the small size of the coronary artery lumen relative to the length of the intracoronary segment of the imaging catheter which prevents significant malalignment (Di Mario *et al,* 1993). However this source of error should be considered in left main coronary artery studies, in tortuous segments, in large, ectatic vessels or when measuring close to acute bends. Rotation angle artefacts as a result of non-uniform rotation of a mechanical catheter drive shaft may distort images. Reliable quantitation is not possible when such artifacts are present. Pulsatile changes in vessel dimensions due to systole and diastole can influence quantitation. This variation is significantly reduced when plaque is present (Weissman *et al,* 1995). The most practical approach is to measure lumen dimensions in systole, when the lumen is maximally distended and ultrasound catheter movement within the lumen is minimal making the image more easily interpretable. Vessel and lumen dimension measurements are summarized in Table 1 and illustrated in Figure 10.

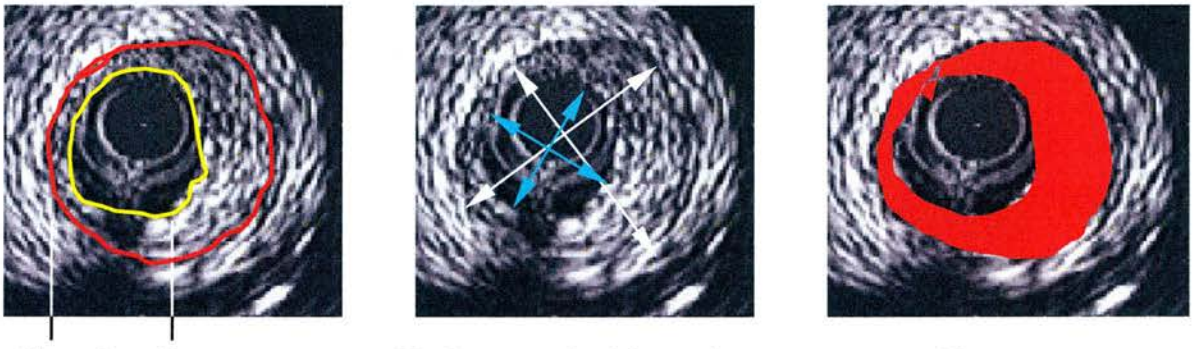

Figure 10. ***IVUS assessment of lumen and vessel dimensions***

1.3.3 *Insights into coronary artery disease*

The cross-sectional images of coronary arteries by IVUS provide a precise characterization of the location and extent of atherosclerotic plaque within the arterial wall. IVUS demonstrates the tremendous extent of plaque burden that is not evident on the angiogram. The presence of a plaque on angiography is inferred by seeing a segment that is narrowed compared to an adjacent "reference" segment. Unfortunately, the reference segment itself is almost always diseased. By IVUS it is evident that the average reference segment has 35-40% of its cross-sectional area filled with plaque,

despite the fact that it appears normal angiographically (Losordo *et al,* 1994). Furthermore, even at locations where the angiogram shows definite narrowing, IVUS demonstrates that the amount of plaque actually present is much greater than would be predicted on the basis of the narrowing alone. At these sites remodelling, or local expansion, of the vessel has occurred. This is an adaptive mechanism which results in less severe compromise of the lumen than would be expected given the amount of plaque burden (Glagov *et al,* 1986; Ge *et al*, 1993; Gerber *et al,* 1993) [Figure 11]. More recent data has suggested that coronary stenoses may remodel as described or demonstrate shrinkage resulting in marked luminal compromise at an earlier stage in the natural development of the atherosclerotic lesion (Pasterkamp *et al*, 1995a). In clinical practice different modes of remodelling may influence the response of a lesion to balloon dilatation during a percutaneous procedure (Pasterkamp *et al*, 1995b).

Table 1. Intravascular ultrasound measurements in common use

Measurement	Abbreviation	Comments
Lumen area	LA, mm^2	
Total vessel area	VA, mm^2	Area inside leading edge of brighter adventitia do not trace if >90 degrees of vessel circumference not visible (shadowing/attenuation)
Plaque area	PA, mm^2	Area included between the two contours indicated above (VA-LA)
Percent plaque area	%PA, %	Percentage of VA occupied by plaque, calculated as (VA-LA)/VA x 100
Max. lumen diameter	MaxLD, mm	
Min. lumen diameter	MinLD, mm	
Mean lumen diameter	MeanLD, mm	Calculated as: $(\sqrt{LA}/\pi) \times 2$
Lumen symmetry index	MinD/MaxD	1 indicates circular lumen, <1 indicates increasing ellipitical lumen shape
Max. plaque thickness	MaxPT, mm	
Min. plaque thickness	Min PT, mm	
Plaque eccentricity index	Min/max PT	1 indicates concentric plaque, <1 indicates increasing plaque eccentricity

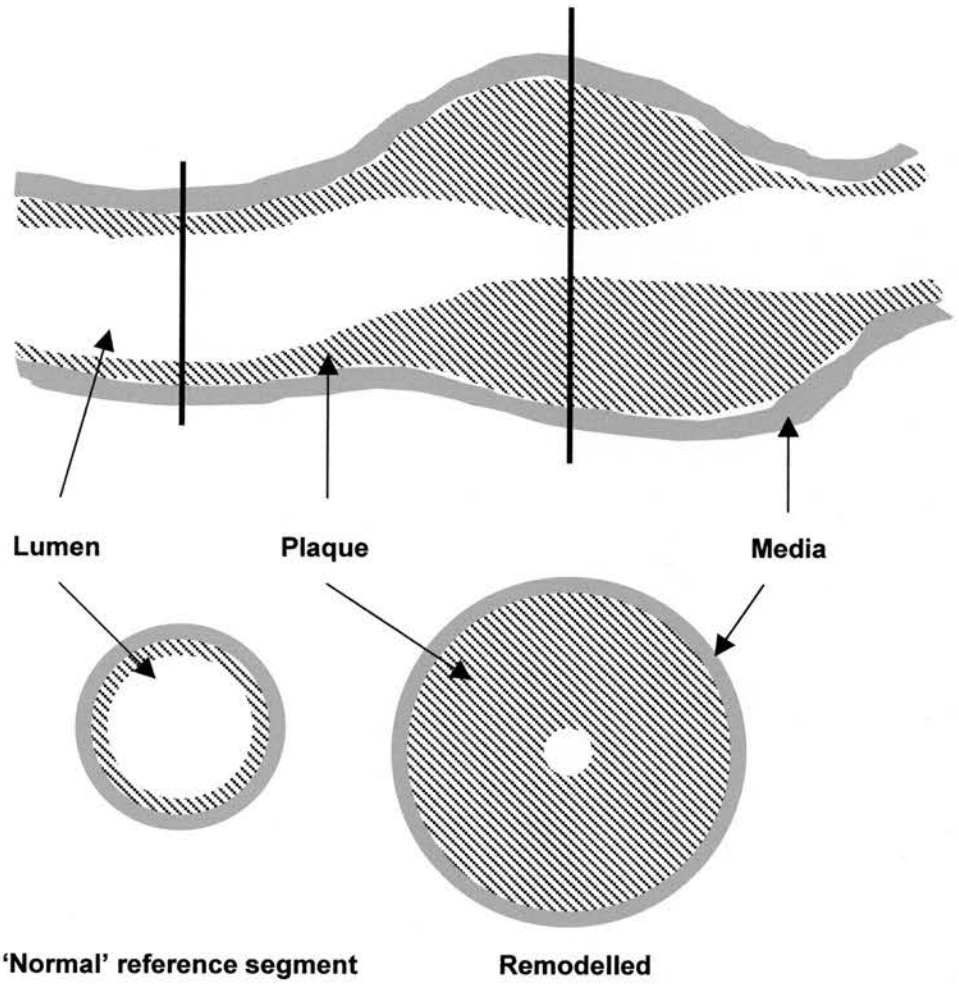

Figure 11. ***Compensatory remodeling within a coronary stenosis. Vessel expansion occurs to accommodate plaque accumulation and preserve the arterial lumen until over 40% of vessel area is occupied by plaque. It can be seen that this mechanism is not detected by angiographic assessment.***

1.3.4 *Diagnostic IVUS in clinical practice*

Normal angiograms - normal coronary angiograms are present in 10-15% of patients undergoing coronary angiography because of suspected coronary disease. Plaque formation has been noted by IVUS in as much as 50% of these patients (Erbel *et al*, 1996) and 36% have impaired functional parameters such as coronary flow reserve. This suggests that patients with typical chest pain and a normal angiogram (Syndrome X) may have significant atherosclerosis although the clinical relevance of this is uncertain. IVUS can also be used to evaluate other vessel abnormalities such as myocardial bridging (Ge *et al*, 1994), spontaneous coronary dissection (Kearney *et al*, 1994) and abnormal contrast opacification within the vessel lumen.

Intermediate stenoses and ambiguous lesions – Suboptimal angiographic visualization impairs accurate assessment of stenosis severity. Ostial stenoses of the right and left coronary arteries, the left main bifurcation or at the origin of side-branches are often poorly visualized because of guide catheter wedging, vessel overlap or foreshortening. Occasionally, insufficient quality of the angiogram results from extreme obesity, emphysema or chest deformities. Extreme eccentricity of stenoses results in discrepancies in the estimate of stenosis severity between orthogonal angiographic views. Measurements of lumen dimensions in such lesions by IVUS is straightforward and the examination frequently solves the problem of ambiguous or intermediate lesions by showing obviously normal or severely diseased vessels (Ge *et al*, 1995).

In two large prospective series, in more than 20% of the examinations before coronary interventions, IVUS changed the management strategy (treatment of angiographically non-significant lesions and vice-versa) [Lee *et al*, 1995; Mintz *et al*, 1994]. However, the IVUS criteria used to define the severity of the lesion had not been objectively defined such that the real impact of IVUS for clinical decision making was unclear. Recently it has become clear that luminal dimensions derived from IVUS are well correlated with physiological parameters of coronary flow (Abizaid *et al*, 1998; Takagi *et al*, 1999).

1.3.5 *Guidance of percutaneous coronary intervention*

The strongest role for IVUS is in the selection and guidance of catheter-based coronary interventions. IVUS has provided crucial new information concerning the mechanisms of balloon angioplasty and newer techniques, such as directional coronary atherectomy, which was previously inferred from animal models or histologic studies of post-mortem specimens. IVUS has clearly demonstrated that tearing of the atherosclerotic plaque occurs in 60-80% of coronary angioplasty cases (Gerber *et al*, 1992). Furthermore, tears have been demonstrated to originate at the interface of normal artery and thin portions of plaque and adjacent to focal calcium deposits where shear forces are highest (Potkin *et al*, 1992). Extensive dissections which extend deep into the arterial media and into superficial adventitial layers often provoke marked spasm, resulting in abrupt vessel closure, and a more profound smooth muscle proliferative response, resulting in restenosis (Jain *et al*, 1994). However, plaque tears and dissections are not necessarily an unfavourable outcome following balloon angioplasty. Limited disruption is invariably useful in producing an adequate lumen gain by releasing the segment of vessel from the constriction caused by a rigid, concentric plaque. IVUS has demonstrated that lesions that tear after PTCA have a greater lumen gain than lesions that simply stretch but do not tear (Honye *et al*, 1992). The use of IVUS to accurately quantify vessel and lumen dimensions has enabled the safe use of larger balloon calibres to maximize lumen gain without excessive vessel injury resulting in reduced long-term restenosis rates (Stone *et al*, 1997; Abizaid *et al*, 1997).

The problem of late lumen loss after balloon angioplasty is one of the most extensively studied areas in the last decade of research in catheter-based revascularisation techniques. Depending on the type of lesion and the location restenosis may occur in 20-50% of lesions within six months of the procedure (Baim *et al*, 1986). Initial research suggested that the primary mechanism of restenosis was aggressive proliferation of smooth muscle cells in the intimal and medial layers triggered by injury and growth factors originating in part from circulating blood cells (Faxon *et al*, 1987). This prompted the identification and testing of agents to inhibit this response. Recent clinical studies using IVUS, however, have drawn attention to another mechanism in the

restenosis response in addition to intimal proliferation: namely, late negative remodelling or contraction of the arterial wall in the originally dilated segment. Early data suggest that half or more of the late loss in lumen calibre can be attributed to segmental contraction occurring one to three months following the procedure (Post *et al,* 1994). Although there is no evidence yet for a specific mechanism, it may be that deep wall injury at the time of the balloon dilatation triggers a scarring process, perhaps originating in the adventitia, that progressively narrows the artery (Andersen *et al,* 1996). This may help account for the fact that the acute gains obtained by tearing a segment with a balloon are lost in the first months of follow-up. As more detailed studies of angioplasty by ultrasound become available, it may be possible to predict which types of injury are most likely to cause a late restenosis response. These cases may be more favourably approached by some of the other catheter techniques.

Besides triggering a huge effort in the pharmaceutical industry, the recognition of the restenosis problem launched the development of a number of non-balloon catheter approaches to reducing atherosclerotic narrowings. The first of these approaches was directional atherectomy (DCA). This catheter is a plaque extraction device which uses a rotating cutter to shave the plaque from one portion of the vessel at a time. The small pieces of plaque are stored in a collection chamber at the tip of the catheter and are ultimately removed with the catheter. Despite widespread initial use, randomized studies comparing balloon angioplasty and DCA suggested that, despite the ability of the atherectomy device to actually remove plaque from the artery wall, there was no major advantage in terms of long-term outcome (Adelman *et al,* 1993; Simonton *et al,* 1995). Just as in the case of balloon angioplasty, recent studies with IVUS have clarified the actual effect of the atherectomy device on the vessel wall and have provided new insight into the somewhat disappointing long-term results from these initial randomized trials (Umans *et al,* 1995; Di Mario *et al,* 1995).

The IVUS studies have shown that despite the excellent angiographic appearance following treatment with DCA, the actual plaque burden remaining is large. On average, over 55% of the cross-sectional area of the vessel is still filled with plaque at the end of the procedure. This remaining plaque burden is invisible angiographically because of the

remodelling process and because the treated segment is being compared to a reference segment which itself has moderate, angiographically occult disease. Preliminary follow-up data have suggested that the percent plaque residual is the most powerful predictor of outcome at six months. Using ultrasound guidance, more accurate and aggressive plaque removal can be performed compared to angiographic guidance where selection of sites to make cuts is often hampered by the marked eccentricity of the lesion (Sumitsuji *et al,* 1997). Cutting too deeply in an area of minimal plaque may result in vessel perforation. It is unclear whether ultrasound guidance of DCA will influence restenosis rates although plaque removal followed by implantation of an intracoronary stent has demonstrated some advantage over balloon predilatation (Moussa *et al,* 1998).

Rotational atherectomy, a device which comprises a high-speed rotating, diamond-tipped burr, is designed to enlarge the luminal area particularly in calcified plaques, which tend to be resistant to balloon dilatation, and in the treatment of diffuse in-stent restenosis. Ultrasound guidance enables more aggressive burr sizing to maximize luminal gain (Kovach *et al,* 1993). Again, however, there is no evidence that this technique reduces restenosis rates when compared to balloon dilatation.

IVUS has had a pivotal role in the development of intracoronary stent implantation. Stents comprise an expandable metal lattice, in the form of a short tube that is inserted into a stenosis mounted on a balloon catheter. The stent is deployed by balloon dilatation and left behind as a permanent prosthesis in the vessel, with the rigid metal struts of the stent holding open the segment that was previously narrowed. The improved luminal gain achieved by stenting reduces the impact of the neointimal hyperplasia that occurs in the months following implantation. The problem of negative remodelling is also negated. As a result, restenosis rates after coronary stenting are significantly lower than for balloon angioplasty (Serruys *et al,* 1994; Fischman *et al,* 1994).

During the early years of stent implantation an important problem was encountered. Up to 20% of patients experienced thrombosis of the stent, often in the few days after the procedure. This prompted the use of aggressive parenteral anticoagulant regimes and the combined use of warfarin and an antiplatelet agent in the weeks following the stent

implantation. Although this approach had some success the relatively high incidence of bleeding complications led to prolonged hospital stays. IVUS studies of stents that appeared well-deployed by angiography suggested that two occult problems were frequently occurring: *incomplete apposition* and *incomplete expansion* (Nakamura *et al*, 1994).

Incomplete apposition describes the situation where a portion of the stent is not directly in contact with the vessel wall. This results in a disruption of blood flow in the arterial lumen and also exposes a greater surface area of the metallic stent to blood. These factors are likely to promote local thrombus formation (Figure 12).

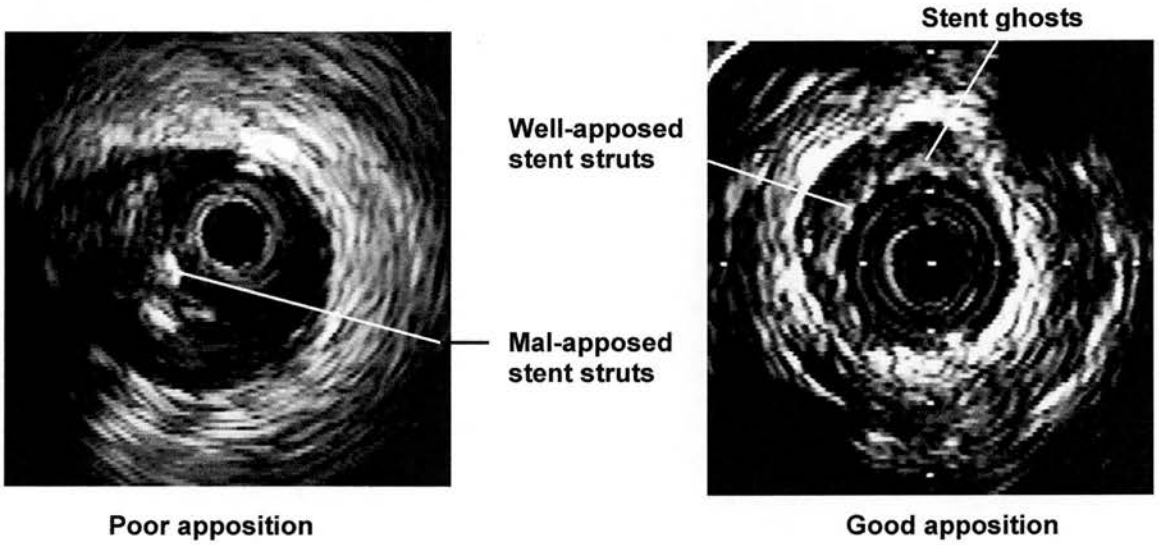

Figure 12. *Stent apposition assessed by IVUS*

Incomplete expansion refers to the situation in which some portion of the stent remains constricted despite the expansion of other areas of the stent by the balloon. Not surprisingly, this occurs in the most rigid portions of a plaque, typically where there is a localized area of calcification.

Recognition of the existence of these factors by IVUS has prompted a significant change in the approach to coronary stenting, with the routine use of much higher pressure balloon inflations than was originally recommended. This has led to a considerable reduction in the rates of subacute thrombosis (to less than 1% in most studies) [Colombo

et al, 1995; Belli *et al*, 1995; Wong *et al*, 1995]. As a result oral antiplatelet agents are now sufficient as adjunctive antithrombotic therapy. Furthermore, rates of restenosis have been further reduced. Even with high pressure deployment IVUS has demonstrated that a significant proportion of stents still have areas of underexpansion which require further balloon dilatation with larger calibre balloons (Albiero *et al,* 1997).

A number of clinical trials have evaluated IVUS guidance for stent implantation. The MUSIC (Multicentre Ultrasound Stenting in Coronaries) trial (de Jaegere *et al,* 1998) was a prospective, non-randomised, observational study designed to evaluate the added value of IVUS in determining optimal stent deployment in vessels larger that 3mm diameter. Optimal expansion by oversized balloon post-dilatation was difficult to achieve yet the angiographic restenosis rate at six months was only 8.3% which is half that observed in stent trials involving angiographic guidance. There have been three randomised trials of ultrasound guided stenting. CRUISE (Can Routine Ultrsound Influence Stent Expansion, Fitzgerald PJ *et al,* 2000) involved IVUS guidance [N=249] compared to a cohort who had angiographic guidance with IVUS only to document the final result [N=250]. Larger balloon sizes and higher inflation pressures for post-dilatation were observed in the IVUS guidance group ($p<0.001$). In addition 36% of subjects in this group had a change in stent deployment strategy as a result of the IVUS appearances resulting in superior stent expansion and a 44% relative reduction in target vessel revascularisation at nine month follow up. Important study limitations which cast doubt on the results were the lack of angiographic follow-up and the presence of more multivessel coronary disease in the angiographically guided group. Angiographic follow up was undertaken in OPTICUS (Optimisation with ICUS to reduce stent restenosis, Mudra H *et al,* 1999). A total of 550 patients were involved with six month follow up. Despite the achievement of optimal stent deployment in 64% of IVUS guided subjects no significant differences in clinical or angiographic endpoints between the two groups. Although these results were initially disappointing it was observed that interventionists tended to use aggressive post-dilatation techniques in the angiographically guided group to help achieve an "IVUS –like" result. Finally, 759 subjects were studied in the AVID (Angiography versus intravascular ultrasound-directed stent placement, Russo RJ *et al,* 1999) trial. After optimal, angiography guided stent deployment subjects were

randomised to IVUS guidance of post-dilatation with larger balloons or only documentation of the final result by IVUS. IVUS guidance resulted in a larger minimum stent lumen area and reduced target lesion revascularisation at 12 months. Overall, these trials demonstrated reductions in clinical restenosis using IVUS guidance Consequently, some interventionists still rely on IVUS guidance for stent deployment. The main perceived drawbacks of the technique in this setting are the prolongation of procedure times for IVUS pullbacks, the need for experienced operators and technical staff and the additional procedural costs incurred. Randomised trials have so far not demonstrated a clear clinical and cost-related advantage for IVUS although more recent studies of cost efficacy should prompt its more widespread use as a routine strategy for monitoring stent deployment (Choi *et al,* 2001). Furthermore, in-stent restenosis remains a significant problem particularly where longer stents are implanted, in small calibre vessels (<2.5mm), in diffuse coronary disease and following treatment of total occlusions (Figure 13). In these high risk groups the additional lumen gain that can be achieved by IVUS guidance may provide improved long term outcomes.

1.3.6 *Insights into transplant vasculopathy*

IVUS has been utiilised in recipients of heart transplants in whom the progression of coronary disease is particularly aggressive. These patients suffer an accelerated process of intimal thickening which is histologically very distinct from atherosclerosis (Johnson *et al,* 1991). This process is the major cause of death in transplant recipients. Furthermore, IVUS has shown that 25% of transplanted hearts have early atherosclerotic lesions (Chenzbraun *et al,* 1995). Serial studies of these lesions after transplantation show no greater progression of vasculopathy in these patients than in patients who received hearts which were free of atherosclerotic disease (Rickenbacher *et al,* 1995a).

Within the first year after transplantation, approximately 40% of patients have extensive intimal thickening. Preliminary studies suggest that greater degrees of intimal disease predispose patients to cardiac events (Rickenbacher *et al,* 1995b). Vasculopathy is widely thought to be related to the rejection process and/or its therapy. In many centres IVUS is now being routinely used for annual surveillance to directly assess the process

and guide the use of different combinations of anti-rejection therapies with the ultimate goal of controlling the rate of intimal proliferation (Pinto *et al,* 1994).

1.3.7 *Research applications of IVUS*

While the application of IVUS in guiding different therapeutic approaches is receiving

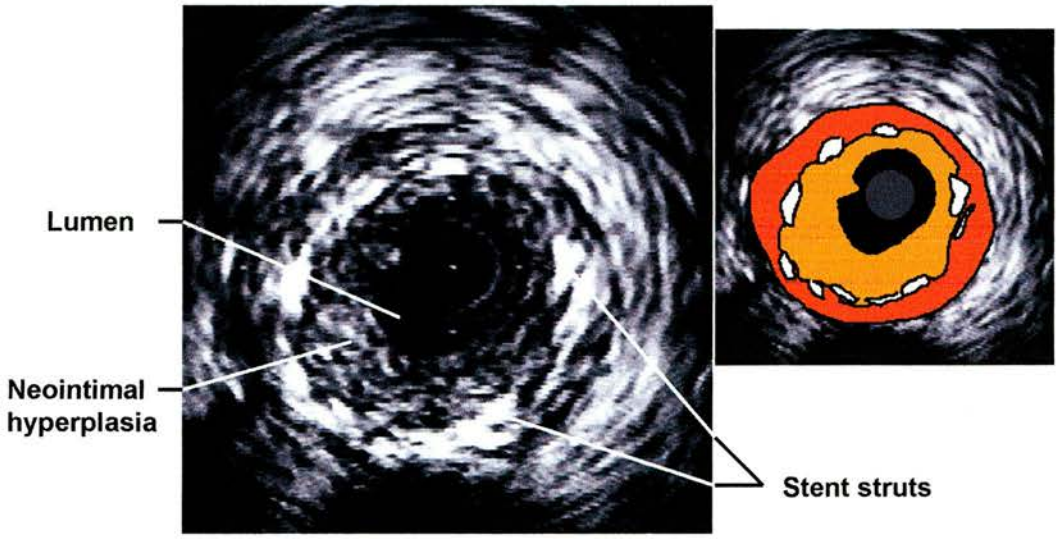

Figure 13. ***Demonstration of in-stent restenosis produced by neointimal hyperplasia***

the most practical attention at present, its use in understanding and characterizing different plaque types may have more far-reaching significance. Observations from post-mortem and serial angiographic studies suggest that the substrate for myocardial infarction, a ruptured plaque, occurs most often in only mildly stenosed segments of coronary arteries. These relatively small plaques appear to rupture as a result of ongoing physical forces associated with arterial pulsations and movements of the heart associated with factors that weaken the fibrous cap that separates the lipid-rich plaque core from the arterial lumen (Falk *et al,* 1989). Local factors affecting this process are the degree of inflammation of the tissue within the plaque and the biomechanical properties of the cap and lipid pool. Technical developments in IVUS transducers have enabled fairly reliable assessment of the thickness of the fibrous cap and the size of the lipid pool. Recent data

(Ge *et al,* 1999) suggests there may be a role for IVUS in stratifying such lesions based on the risk of plaque rupture, which has been demonstrated to occur more frequently with a fibrous cap thickness of <0.7mm and where the lipid pool (echolucent area) below the cap is >1mm^2, such that revascularisation therapies can be prioritized accordingly. However, it appears difficult to determine how such a process can be applied to the clinical setting in terms of which patient should be selected for assessment.

Clinical trials using lipid-lowering therapies, such as statins, have demonstrated marked benefit in reducing cardiac events. However serial angiographic studies have revealed virtually no reduction in the degree of stenosis which suggested that changes in plaque composition and stability was responsible for conveying the observed benefit (Tamura *et al,* 1997). A number of serial IVUS studies are underway which are exploring whether there are demonstrable differences in plaque constituents following a period of treatment with lipid-lowering therapies (Schortl *et al,* 2001).

1.3.8 *Current technical limitations of IVUS*

Quantitative. Although IVUS enables fairly accurate measurement of lumen and vessel dimensions there is a tendency to overestimate lumen dimensions due to a number of factors inherent in clinical IVUS studies. Firstly, a weak intimal signal, causing endoluminal border dropout, can arise due to the low dynamic range of some IVUS systems. Secondly, due to vessel tortuousity, transducers are usually eccentrically positioned causing a more pronounced rotation angle artefact. Finally, direct splinting of the vessel wall may abnormally distend the lumen.

Qualitative. Precise characterisation of atheroma requires high frequency IVUS imaging. Current transducers are sufficient to depict the major plaque types for clinical studies but are inadequate for studies of atheroma regression. The development of 40MHz transducers is likely to overcome some of this limitation but computerized post-processing of ultrasound data is necessary for detailed analyses to be performed (see Chapter 3)

Safety. Despite its invasive nature, the potential limitation of IVUS with respect to vessel wall injury and other complications during clinical studies has never really been demonstrated. In an early review of 2207 cases performed in a number of different centres, 92% were free of complications (Hausmann *et al,* 1995). Vasospasm (2.9%) was the most common problem but vessel dissection, thrombosis, embolisation and occlusion occurred in 0.3% of cases. Myocardial infarction and the requirement for emergency coronary bypass surgery occurred in 0.1% of cases. There is no evidence that accelerated intimal thickening results from instrumenting the vessel (Pinto *et al*, 1993).

1.3.9 *Future directions for IVUS*

Continuing technological improvements in IVUS image processing have enabled the production of three-dimensional images from sequential two dimensional IVUS scans. In the case of catheter imaging this requires a controlled pullback through the arterial segment of interest. The process remains problematic due to the practical difficulties in tracking the precise movement of the transducer in curved segments of artery and due to the beat-to-beat movement of the heart. The use of ECG-gating of image acquisition has overcome some of these problems and the use of combined information from IVUS images and angiography is showing some promise in improving the quality of reconstructions (Slager *et al,* 1995). Several commercially available systems have been introduced which provide reasonably precise reconstructions for clinical use (see later). Image acquisition and post-processing is however time-consuming and requires additional expertise. Consequently, there is little enthusiasm to incorporate the technique into routine clinical practice and it remains predominantly a very useful research tool.

Another active area of development in image processing is tissue characterization, which is a general description for a set of computer-based techniques for enhanced tissue recognition from the ultrasound signal. In one approach, the raw radiofrequency signal reflected back from the plaque to the transducer is diverted directly to a computer before entering the chain of signal processing that ultimately forms the image. The combined amplitude and frequency data in the radiofrequency signal is compared to a known statistical profile for a given tissue subtype. This type of analysis provides a higher

sensitivity for identification of subtle tissue characteristics than is available from the image alone, because the image is developed purely from the amplitude envelope of the signal (Spencer *et al,* 1997).

Currently, efforts are underway to further miniaturize the imaging element and to incorporate imaging directly into therapeutic catheters. An imaging/balloon combination catheter has been developed which allows the operator to adjust the pressure and duration of the balloon inflation according to the plaque morphology and dimensions (Mudra *et al,* 1994). This combination has had limited ability to date, but may have more utility in combination with new balloon designs that allow the effective diameter of the balloon to be altered during the procedure. Alterations are made in response to information from the ultrasound images. Another approach to a combined therapeutic/imaging platform is an imaging core or guidewire which can run in the central lumen of a balloon or stent deployment catheter and can visualize the treated segment through the wall of the catheter. Clinical trial evidence for the benefit of such devices is awaited.

1.4 Conclusions

It is clear that IVUS is established as a new standard for the visualization and measurement of coronary atherosclerosis in clinical practice. The ability to observe the disease process continues to provide the basis for key studies evaluating new pharmacologically- and catheter-based techniques to treat atherosclerotic plaque. In the meantime. IVUS is being utilized on a day-to-day basis in many catheterization laboratories to monitor and optimize existing coronary procedures.

1.5 Three-dimensional reconstruction of IVUS images: an overview

The natural history and progression or regression of coronary atherosclerosis after pharmacologic or percutaneous interventions have most often been assessed by coronary angiography (Stone *et al*, 1993; Waller *et al*, 1988; Waters *et al*, 1993). The limitations of this technique in assessing atherosclerotic plaque were described in detail in the introductory chapter. The use of two-dimensional IVUS enables detailed assessment of the lumen and arterial wall (Gussenhoven *et al*, 1989). Atherosclerotic remodelling of lesions, which is angiographically undetectable until significant luminal encroachment has occurred (Stiel *et al*, 1989), can be accurately measured in single tomographic image slices by manual tracing of lumen and vessel boundaries. A reasonable assessment of plaque composition can be made and the ability to provide a detailed assessment of the response of the arterial wall to balloon dilatation has resulted in in vivo descriptions of the mechanisms involved in balloon angioplasty and stent deployment (The *et al*, 1992; Nakamura *et al*, 1989). The most important limitation of conventional IVUS imaging is the selection of target sites for serial measurements in pre/post studies. Reliance is placed upon local landmarks such as focal calcium deposits or arterial side-branches to match sites. Furthermore, assessment of an entire coronary segment requires the analysis of serial tomographic slices during a recorded pullback sequence. This requires mental reconstruction of the linear extent of changes in plaque and luminal architecture which is a difficult process and therefore prone to some degree of intra- and inter-observer error. A major part of the problem is caused by the lack of a third dimension in conventional IVUS imaging. Three-dimensional reconstruction of IVUS images enables a more advanced assessment of vessel, lumen and plaque morphology. During on-line reconstruction measurements of the target lesion and reference segments may be accessed immediately in a longitudinal view. Additionally, the same sites are more easily identified in follow-up studies.

1.5.1 *Image acquisition*

All the current commercially available systems possess similar processing steps to obtain a three-dimensional reconstruction. The quality of the reconstruction is dependent upon the quality of the two-dimensional IVUS images. Accordingly system settings

must be optimized prior to performing the image acquisition stage. Gain settings must be set to enable clear delineation of the endoluminal and external elastic lamina borders. To reconstruct images the entire circumference of both borders must be visible within the circular display of the IVUS system. This is a potential problem where the transducer, which is positioned centrally on the display, lies eccentrically against the lumen wall in areas of coronary artery with particularly large dimensions such as ectatic segments or within saphenous vein grafts (Figure 1).

1.5.2 *IVUS catheter characteristics*

Image acquisition is performed either on-line, as the IVUS imaging catheter is withdrawn from distal to the stenosis through the arterial segment to be reconstructed, or off-line from recorded images on video tape. Mechanized pull-backs of 0.1mm/second are possible. The catheter design mainly used for repeated pull-backs is of relatively small calibre (2.9F) and has a 15cm long transparent distal sheath which houses the transducer enabling the transducer to be readvanced across the lesion without coming into direct contact with the vessel wall. This design also has the advantage of stabilizing the transducer pull-back trajectory and therefore reducing the risk of a non-uniform pull-back speed during catheter withdrawal. Despite this the pull-back must be commenced well before the segment to be reconstructed (5-10 seconds) to allow for straightening of the imaging core inside the catheter before a constant withdrawal speed is attained.

1.5.3 *Continuous versus ECG-gated pullbacks*

Different pullback methods can be applied. The most frequent approach is the use of a continuous pull-back speed which results in an equidistant spacing of adjacent images (Fuessel *et al,* 1996). In serial studies side-branches or calcium deposits are used as topographic landmarks to ensure reliable comparison of the same arterial segment. A modified concept of the continuous pull-back is ECG-triggered video labelling during the pull-back sequence. Video frames coinciding with the R-wave of the ECG are automatically labelled and images acquired at the same phase of the cardiac cycle are

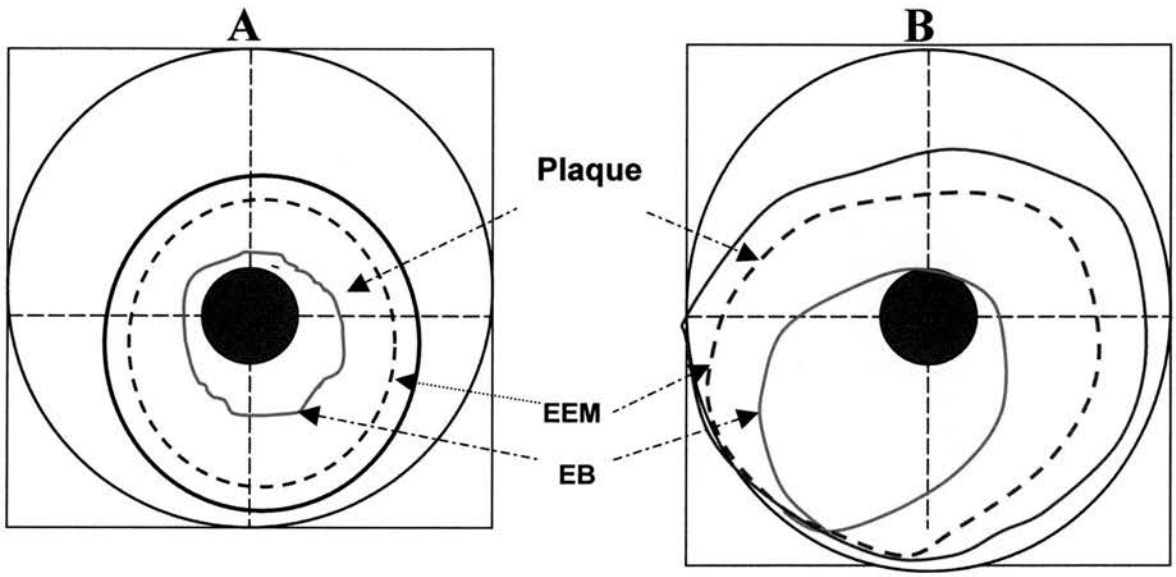

Figure 1. ***Diagram A, IVUS image in which the entire endoluminal (EB) and external elastic lamina (EEM) borders are visible within the circular display. In diagram B the EEM is incomplete due to eccentric catheter positioning within the lumen of a large calibre vessel.***

used for offline three-dimensional reconstruction. This method minimizes the systolic-diastolic artifacts which are frequently observed in non-triggered uniform-speed pull-backs giving the endoluminal border of the reconstructed image a sawtooth appearance rather than a smooth contour which potentially influences accurate measurement of lumen and vessel volumes (Figure 2). These cyclic motion artifacts can be further overcome by the use of both the ECG-triggered pull-back device and ECG-gated image acquisition (Roelandt *et al,* 1994b Bruining *et al,* 1995). A dynamic three-dimensional reconstruction system can dynamically display the arterial segment, showing the motion of an entire cardiac cycle. This is achieved by defining the upper and lower limits of the R-R interval prior to image acquisition. Within this range 25 IVUS images per cardiac cycle can be sampled, digitized and stored to create the final reconstruction sequence (Figure 3). The one drawback of such a technique is the need to sample and process a large amount of data which requires a slightly longer analysis time than for a conventional study.

1.5.4 *Image digitization and segmentation*

Image digitization can be performed on- or off-line. Acquired frames are sampled with a framegrabber at a defined digitization frame rate (typically 8.5 frames/sec). The segmentation step involves the identification of structures within the IVUS image by applying dedicated computer algorithms which discriminate between the blood pool inside the lumen and structures of the vessel wall (Chandrasekaran *et al,* 1992). The quality of these algorithms determines the final quality of the three-dimensional reconstruction. Segmentation is currently achieved by using either an *acoustic quantification* algorithm (Hausmann *et al,* 1994) or a *contour detection* algorithm (Li *et al,* 1994b).

1.5.5 *Acoustic quantification system*

This system (EchoQuant, INDEC, CA,USA) distinguishes between the blood pool and vessel wall using an algorithm for statistical pattern recognition. Essentially the algorithm is able to distinguish between the ultrasound speckle pattern of flowing blood and that of the vessel wall (Li *et al,* 1994a). As a result the interface between the lumen

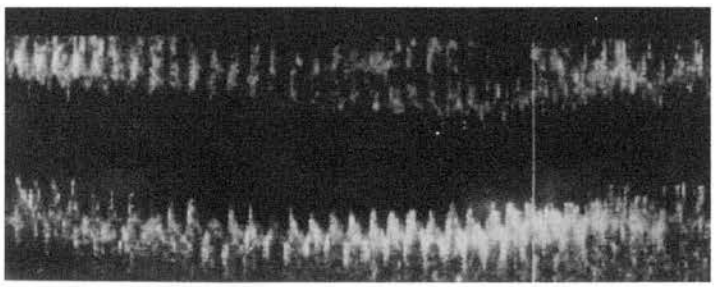

Figure 2. ***Cyclic artifacts. Longitudinal section of a coronary artery segment demonstrating sawtooth-shaped artifacts produced by vessel pulsation and movement of the IVUS catheter (reproduced with permission).***

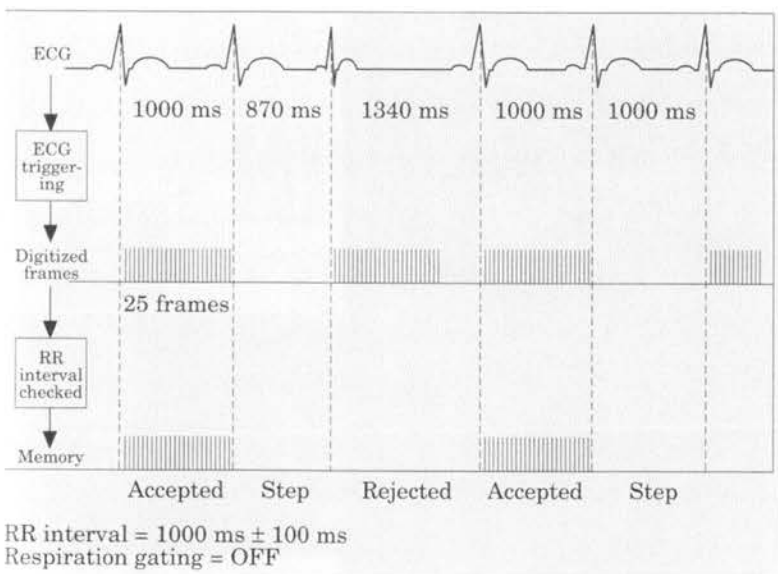

Figure 3. ***Dynamic visualization of IVUS reconstruction. An ECG-gated pullback device and dynamic three-dimensional reconstruction, using the Echoscan (TomTec) system, allows the problem of cyclic artifacts to be overcome. The range of the R-R interval is defined (1000ms±100ms) before the acquisition starts. During the pullback up to 25 images per cardiac cycle are digitized and sampled in the computer memory unless the length of the R-R interval fails to meet the pre-set range. Each time a cycle is stored, the following heartbeat is required to perform a pullback step in order to reach the adjacent scanning site (reproduced with permission).***

and vessel wall can be detected. The system is well-validated and can be used either on- or off-line. IVUS images are sampled with a digitization frame rate of 8.5 frames/sec. As the acquisition and digitization rates are fixed the length of the reconstructed coronary segment is determined by the pull-back speed. For instance, a pull-back speed of 1.0mm/sec results in the acquisition of approximately 8 cm long segments. Manual correction of the automated border detection can be performed in individual cross-sections to improve the quality of the reconstruction. The display depicts a selected cross-sectional image, a longitudinally reconstructed image and a cylindrical three-dimensional view presenting the segment opened up longitudinally. Studies can be performed within a few minutes enabling its use in the catheterization laboratory setting. Application of the algorithm may be hampered by the quality of the basic IVUS image. An additional limitation is the inability of the algorithm to detect the external elastic lamina border although manual tracing is possible.

1.5.6 *Contour detection system*

This system (Echoscan, TomTec, Munich, Germany) digitizes IVUS image frames from within a user-defined region of interest. A maximum of 200 tomographic images can be acquired. Using a continuous pull-back segments of approximately 2.5 cm can be analysed. This increases to 4 cm when an ECG-gated pull-back is employed. Reliable segmentation and three-dimensional reconstruction is possible even when image quality is not optimal. Some user interaction is required in the presence of irregular lumen shapes to accurately detect borders.

The contour detection procedure comprises three steps. Firstly the digitized IVUS images from the segment of interest are modelled within a volumetric or "voxel" space in the computer memory (Kitney *et al,* 1989). Two perpendicular cut planes running parallel to the longitudinal axis are selected. Data located at the interception of these cut planes and the voxel volume are derived to reconstruct two longitudinal images of the vascular segment. The angle and location of the cut planes is defined by the user in order to optimize the representation of the arterial segment on the longitudinal sections. Secondly, the contours of the luminal and external elastic lamina are detected in the

longitudinal images using a well-validated algorithm (Li *et al,* 1993). The optimal path of the contours is updated using dynamic programming techniques Markers can be added by the user to force the contours to pass through these sites. The contours of the longitudinal images are then depicted as points in each cross-sectional image. Finally, automated contour detection is performed in all the cross-sectional images using the four edge points, derived from the longitudinal contours, as landmarks to guide the detection (Figure 4). The accuracy of the final contours can be checked and manual corrections may be performed.

The system enables the quantitative analysis of lumen and plaque. Volumetric data can be obtained as each cross-sectional image represents a slice of the reconstructed arterial segment (von Birgelen *et al,* 1996). Displays of diameter stenosis, area obstruction and lumen symmetry along the length of the segment can be produced for in-depth analysis (Figure 5).

1.5.7 *Challenges and future directions*

Although minimal intra- and inter-observer variability for lumen and plaque volume measurements has been demonstrated (von Birgelen *et al,* 1996) there remain several technical problems which influence the accuracy and quality of the three-dimensional reconstruction. As well as IVUS image quality, the limited lateral resolution of current IVUS catheters and image distortion by non-uniform rotation or eccentric positioning of the transducer can introduce complex artifacts into the reconstruction (Benkeser *et al,* 1993; Roelandt *et al,* 1994a). Additionally, natural bends in the catheter shaft from the femoral sheath entry point, along the course of the aorta and within the coronary artery may induce differences between the movement of the distal transducer and proximal part of the catheter which is applied to the pull-back device. Furthermore, the need to use ECG-gated image acquisition to avoid cyclic motion artifacts requires a longer acquisition time (Dhawale *et al,* 1994). This may cause problems in patients with particularly severe stenoses where prolonged myocardial ischaemia may result. Finally, distortion of the reconstructed image may result from vessel curvatures resulting in over- or under-estimation of plaque volume due to the curved pullback trajectory of the IVUS

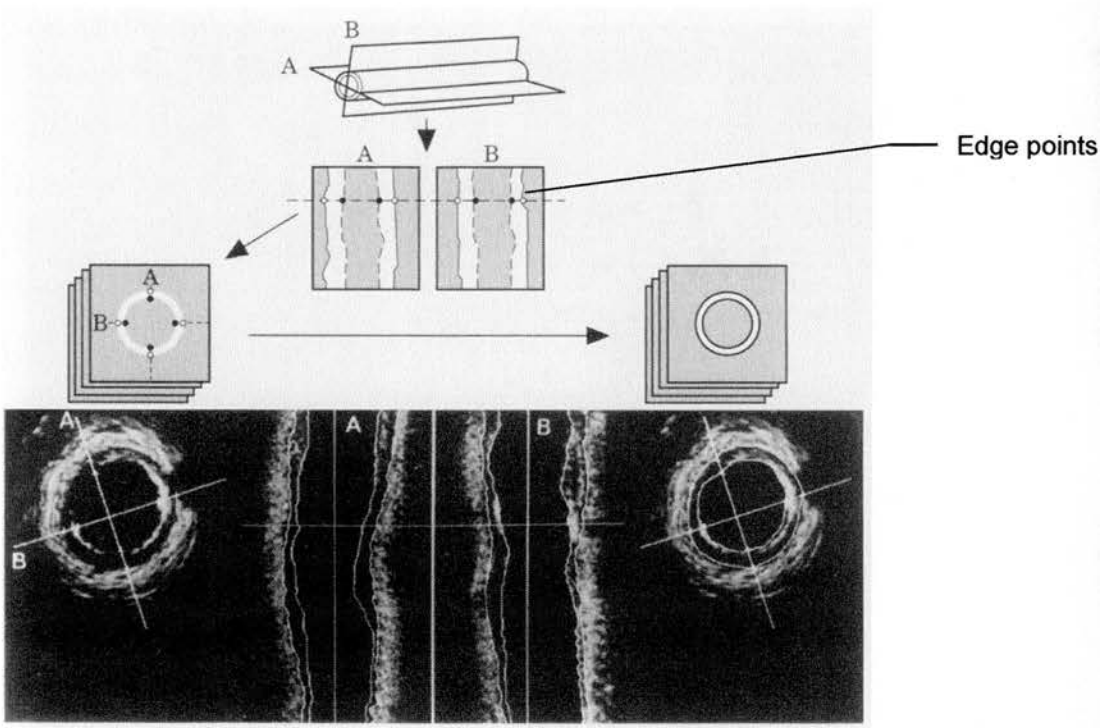

Figure 4. ***Principle of contour detection system. IVUS images obtained during pullback are stored as a 'volumetric (voxel) space'. Edge points derived from longitudinal contours, which are detected on the longitudinal reconstruction, guide and facilitate the final contour detection on the transverse IVUS images (reproduced with permission).***

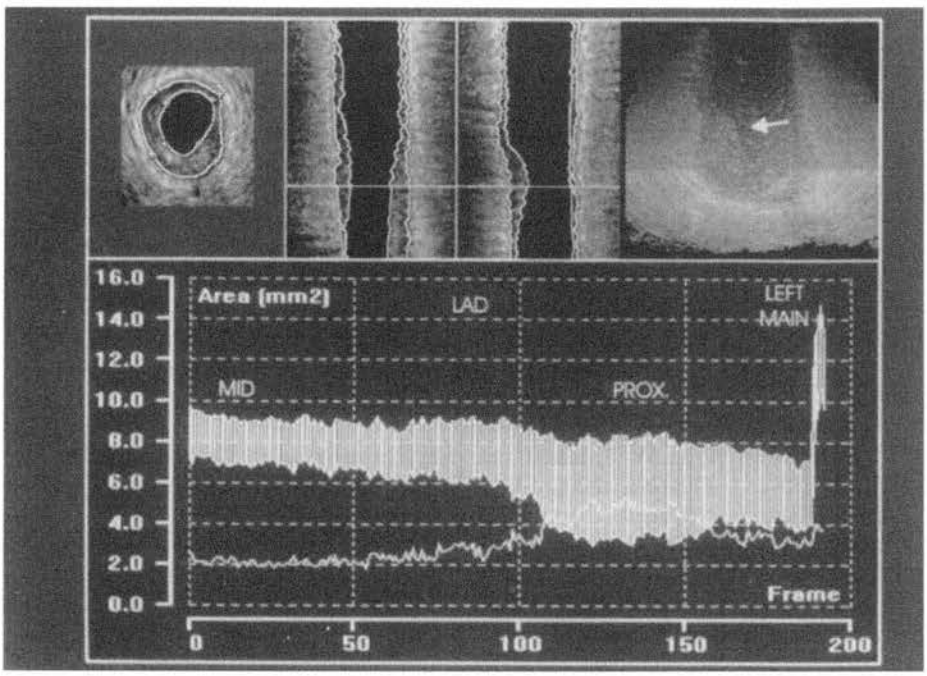

Figure 5. ***Standard display of results. Transverse and longitudinal images are displayed. The reconstructed 3-D image is demonstrated (top left panel). This view provides qualitative information regarding plaque morphology but is of no value in the quantitative analysis. Graphs of lumen, plaque and vessel area, diameter- and area-stenosis along the lesion can be displayed.***

transducer (Waligora *et al,* 1994). Recent developments combine data obtained from biplane coronary angiography and IVUS to provide information on true vessel curvatures and the orientation of the IVUS catheter (Cothren *et al,* 2000; Koch *et al,* 1993; Slager *et al,* 1995). Preliminary data suggests that this system has a high degree of accuracy in reconstructing tortuous coronary arterial segments. Some of the ongoing problems of current three-dimensional reconstruction computer systems may be overcome by further miniaturization of IVUS imaging catheters and improvements in the computer technology used.

1.5.8 Conclusion

Three-dimensional IVUS image reconstruction has clear value in the volumetric study of mechanical or pharmacological techniques in coronary atheroma regression and mechanisms of percutaneous coronary intervention such as PTCA and intracoronary stenting. This technique has largely been limited to pure research applications. With further technical improvements it is possible that its use in routine clinical practice may provide a more accurate assessment of coronary disease prior to and following percutaneous intervention.

CHAPTER 2
Methodology

2.1 Introduction

Over the last twenty years there have been numerous studies describing the composition and morphology of atherosclerotic vascular disease and the mechanisms involved when significant lesions are subjected to balloon dilatation. These have primarily been based on the histological study of human peripheral and coronary arteries or animal models of atherosclerosis. Such studies have well-documented limitations. Histological studies provide an accurate assessment of atherosclerotic plaque composition but such analysis is obviously not repeatable such that serial study before and after balloon dilatation cannot be performed. Post-mortem studies involved analysis of lesions in patients who had died as a result of the coronary balloon angioplasty procedure and therefore represented only the more severe vessel wall injury patterns rather than the range of lesion morphologies produced by balloon dilatation in routine practice (Farb *et al,* 1990). Furthermore, atherosclerotic models, developed by induction of vascular injury in peripheral arteries and administration of a lipid-rich diet, tend to involve herbivorous animals such as rabbits (Wilensky *et al,* 1995; de Smet *et al,* 1998). As a result the atherosclerotic lesions produced are predominantly lipid-rich and therefore relatively compressible compared to the more complex fibrocalcific plaques that are seen in human coronary arteries. Additionally the smaller calibre and more tortuous nature of coronary arteries compared to peripheral vessels tends to promote more eccentric plaques (Roberts *et al,* 1979). Both these factors impair the ability of such studies to accurately interpret the morphology and composition of advanced human coronary atherosclerosis and its complex response to balloon dilatation. Significant improvements in coronary artery imaging, such as the development of intravascular ultrasound imaging, have improved our ability to study coronary artery disease *in vivo* and *in vitro.* However, the accuracy of the technique requires to be validated against the histopathological appearance of atherosclerotic plaque before serial studies can be performed. Moreover these studies require to be performed in conditions which closely approximate those of *in vivo* human coronary artery disease.

The following chapter describes the preliminary studies performed to enable the development of the pulsatile flow system used to study post-mortem human coronary

arteries in the series of studies described in subsequent chapters. The primary aim of developing the system was to enable the analysis of the qualitative and quantitative accuracy of IVUS in characterizing atherosclerotic coronary artery disease in circumstances which closely approximate the clinical setting.

2.2 Development and validation of pulsatile flow system

In previous *in vitro* studies of human vascular disease using IVUS or angiographic assessment the models comprised a segment of artery suspended in a water bath with ports of access for imaging catheters. A fixed perfusion pressure was maintained by a closed loop system incorporating a bag of saline under hand-controlled pressure controlled by a pressure manometer (van der Lugt *el al,* 1995) However, other physiological factors may influence image interpretation by IVUS and also the impact of balloon dilatation of obstructive coronary lesions. The system constructed for this series of studies was designed to incorporate some of these factors so as to reproduce as accurately as possible the *in vivo* physiology of diseased human coronary arteries.

2.2.1 *Coronary flow*

The major factor responsible for coronary blood flow is aortic pressure. However, extravascular compression by contracting myocardium can cause brief reversal of flow in systole. It is generally accepted that maximal left coronary artery flow occurs during early diastole i.e. during ventricular relaxation (Kelman, 1977). This effect is less marked in the right coronary circulation due to the lower pressures exerted by the right ventricle. To imitate this phasic flow as accurately as possible a simple peristaltic pump was employed. The pump is not able to completely reproduce this characteristic flow pattern as extravascular compression cannot be reproduced in the water bath. Brief cessation rather than reversal of flow tends to occur.

Total resting coronary blood flow is approximately 200ml/min. Approximately two-thirds of this perfuses the left coronary artery. Typically, total flow within the left

anterior descending coronary artery under normal physiological conditions is between 50-80ml/min (Kelman, 1977). The peristaltic pump can be altered to produce cycle rates of between 0-250 per minute. A simple study was performed to determine the optimum cycle rate to reproduce normal coronary flow. Over a range of cycle rates which corresponded to physiological rates (50-130 beats per minute) flow was measured by collecting the perfused fluid from the distal end of the system over a period of 5 minutes. In system 1 relatively low flow rates were achieved (Figure 1). Two problems were identified. Firstly, the tubing within the closed loop system was too long. Since flow is inversely proportional to the length of a given tube at constant pressure and radius a reduction in length was made. Secondly, there were marked reductions in luminal diameter between the tubing (10mm) and the arterial sheath sidearm (3mm) and subsequent coronary artery segment (2.2-3.6mm). This produced significant attenuation of flow. Narrower tubing (5mm) and a more gradual reduction in luminal diameter was achieved by employing Touey-Borst adaptors connected to the proximal end of an 8F (2.67mm) angioplasty guide catheter (Figure 2). These modifications resulted in satisfactory flow rates at physiologically acceptable pump cycle rates (System 2).

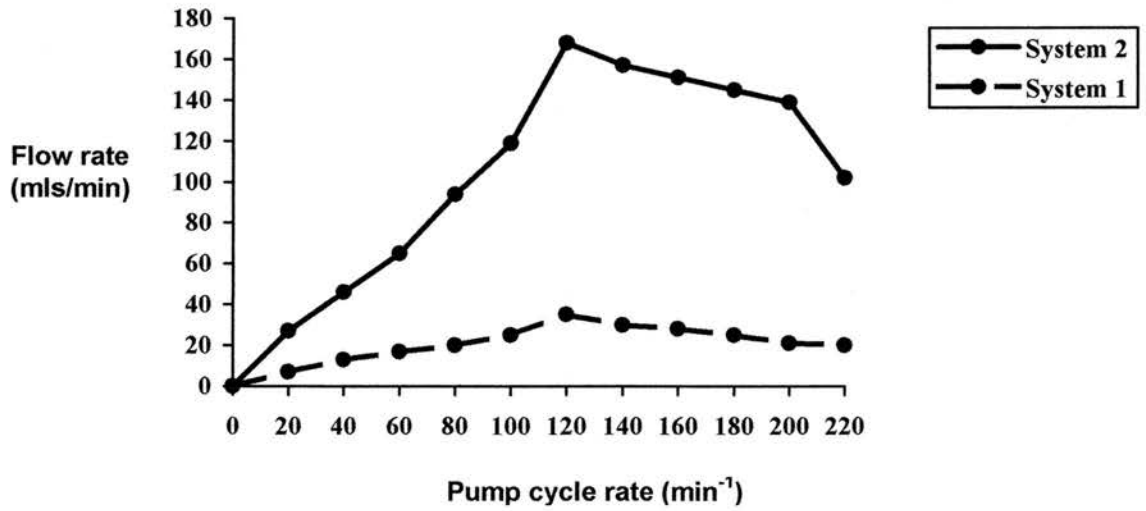

Figure 1. ***Flow rates achieved with systems 1 and 2***

2.2.2 *Perfusion pressure*

The coronary perfusion pressure is a major determinant of flow and is influenced by conditions such as hypotension and aortic stenosis. Normal coronary perfusion pressure is of the order of 100-120mmHg but varies from 40 to 220mmHg depending on factors such as autoregulation of resistance vessels and neurohormonal influences (Kelman, 1977). For the purposes of an in vitro system the perfusion pressure is only influenced by the pump cycle rate and the resistance of the flow system distal to the water bath. In the normal coronary circulation the major factors influencing peripheral resistance are due to variations in vessel radius. Arterioles provide the greatest resistance to flow due to the marked reduction in calibre at the transition point with the artery. Alterations in peripheral resistance influence the perfusion pressure and flow rates that are achieved. In an in vitro system alterations in peripheral resistance are produced by variations in the radius of the distal tubing as other factors such as fluid viscosity and the length of the tubing are constant in the system.

Once a range of pump cycle rates was determined that produced satisfactory flow rates, measurements of perfusion pressure were undertaken. An electronic pressure transducer was applied to the flow system distal to the coronary artery segment. At the defined range of flow rates (60-80mls/min, pump cycle rate 65-85/min) the maximum (systolic) perfusion was 60-80mmHg. The calibre of the distal tubing was therefore reduced (4mm) using metal clamps to externally compress the tubes. In addition, by placing several smaller calibre tubes (1mm diameter) in parallel distal to the water bath the resistance was further enhanced (see Figure 2). Repeated recordings following these manipulations produced maximum perfusion pressures of 80-100mmHg whilst optimal flow rates were maintained at a cycle rate of 75-85/min).

2.2.3 *Vessel distensibility*

Normal coronary arteries exhibit significant dimensional changes during systole and diastole. A 10-20% increase in lumen dimensions during systole has been demonstrated with ICUS. Atherosclerotic coronary arteries are less distensible due to the restriction of

a thickened intimal layer and especially in the presence of densely fibrous or calcified plaque. However, minor phasic variation in lumen dimensions of 2-10% still occurs (Alfonso *et al,* 1994). Furthermore, eccentric areas of plaque produce regional distensibility of the coronary lumen which results in significant distortion of the coronary lumen (Umeno *et al,* 1994). It is important to be aware of this factor particularly when taking serial quantitative measurements.

To determine whether the pulsatile flow system accurately replicates phasic changes in coronary lumen dimensions a post-mortem segment of right coronary artery was prepared and mounted. Pulsatile flow was established at a pump cycle rate of 72/min and perfusion pressure of 90mmHg. IVUS imaging revealed only mild eccentric plaque. It was noted that there was a 16% increase in lumen dimensions in the 'systolic' phase. Just prior to the in vitro study the IVUS catheter had been used in a diagnostic procedure in the cardiac catheterization laboratory. In this study segments of mildly diseased coronary artery demonstrated a 13% increase in distensibility in systole thus demonstrating the accurate reproduction of the *in vivo* setting using the system.

2.2.4 *Saline perfusion*

Isotonic saline was used to perfuse the flow system. The use of whole blood has been previously demonstrated to provide IVUS imaging which is identical to the clinical situation since the speckle pattern created by red blood cells is reproduced with very clear demarcation of the intima-lumen border. Moreover, it is likely that the greater viscosity of whole blood may influence flow patterns within the coronary lumen. However, differences in imaging quality between blood and isotonic saline are relatively small and changes in gain settings often compensate for the discrepancy (Peters *et al,* 1994b). Isotonic saline was used in preference to whole blood as it provided a cleaner, more practical and more readily available fluid which provided acceptable image quality for the purposes of the study.

2.3 Harvesting and preparation of coronary artery specimens

Post-mortem human coronary artery specimens were obtained from the Department of Pathology. All specimens were prepared and studied within 24 hours of death and within 3 hours of harvesting. No fixative agents were used as this practice has been demonstrated to significantly affect the composition of the atherosclerotic plaque and also the accuracy of quantitative measurements in subsequent IVUS studies (Park *et al*, 1993). Each specimen was of at least 5cm in length and of sufficient calibre to accommodate an IVUS catheter (>2mm). The arterial segments were dissected from the post-mortem hearts surrounded by a 1cm thick block of tissue (myocardium and pericardial fat mainly). The reasons for this were twofold. Firstly, without the support of surrounding tissue, and despite the buoyancy of the saline in the flow system, specimens would be subject to sagging of the middle third. This results in artificial alterations in luminal dimensions whilst stretching of the specimens would alter arterial wall anatomy and abolish normal vessel tortuousity which has an important influence on the accuracy of IVUS image interpretation and the response of the artery to balloon dilatation. Secondly, arterial distensibility is likely to be overestimated without the restriction of surrounding tissues.

The coronary specimens are perfused intermittently with saline and side-branches identified and tied off with silk sutures. Not all side-branches required tying off to maintain adequate perfusion pressure. Therefore transient occlusion of the lumen by the balloon during PTCA studies does not cause excessive pressure build-up in the proximal segment of the artery which could cause artificial damage to the intimal lining. Once prepared the specimen is mounted on two guide catheter supports within the water bath. Care was taken during this process to avoid stretching and twisting of the specimen so as to avoid plaque and vessel wall disruption. A 0.014" floppy-tipped guidewire was passed through the specimen. This enables the smooth passage of the IVUS catheter along the arterial segment in the studies described in subsequent chapters.

2.4 Histological analysis

Following IVUS examination of each specimen, the water bath was emptied and then filled with 10% buffered formalin. The perfusate was also replaced with formalin. The distal guide catheter port was occluded and a constant pressure of 80mmHg was maintained across the specimen (pressure fixation). Pressure fixation was carried out for at least 12 hours to ensure no significant shrinkage of the specimen prior to histological sectioning and analysis. Following sectioning of the regions of interest within the coronary segment sections were decalcified in a standard solution and stained with haematoxylin-eosin and elastic von Gieson stains to enable clear identification of plaque constituents such as fibrous layers and calcium deposits. Depending on the study undertaken sections were obtained from specific points of interest such as the minimum lumen area or the reference segment or at intervals (typically 0.2-0.5mm) along the length of the segment. Precise correlation of sections with the corresponding recorded ICUS images was carried out using clearly identifiable landmarks such as side-branches or focal calcium deposits, or the use of a reference needle placed in the adventitial distal to the stenosis (see Chapter 3).

Specific methodology will be described in each chapter.

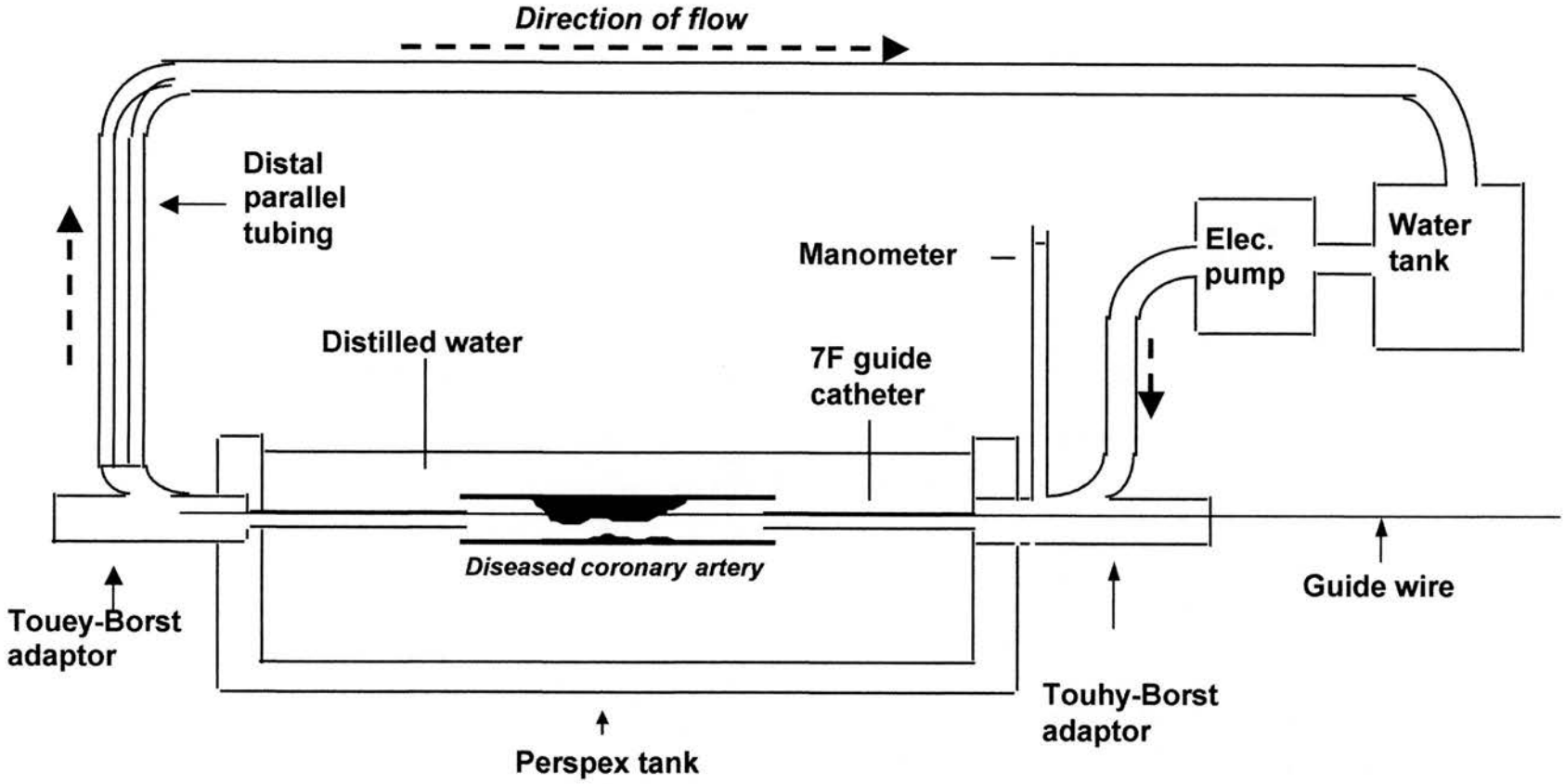

Figure 2. ***Schematic diagram of pulsatile flow system.***

CHAPTER 3

Analysis of coronary atheromatous plaque by intravascular ultrasound. Reproducibility and histological correlation of lesion morphology.

3.1 Introduction

Qualitative assessment of atheromatous plaque composition in coronary arteries is performed using IVUS to guide balloon angioplasty and stent deployment. However, evidence for the reproducibility and accuracy of atheromatous lesion characterization in this setting is lacking. Early in vitro work, using peripheral and coronary arteries, demonstrated the potential of IVUS in characterizing atherosclerotic plaque (Gussenhoven *et al,* 1989; Potkin *et al,* 1990; Siegel *et al,* 1991; Nishimura *et al,* 1990; Peters *et al,* 1994c). However these early studies have limited applicability to the current clinical setting since they were performed in vitro, in conditions unlike the clinical setting and with outmoded IVUS technology. Furthermore, other factors typical of clinical IVUS studies such as vessel tortuousity and the impact of pulsatile flow were not considered. Finally, previous studies defined the sites of interest without taking into account the potential variation between observers in the selection of sites or reference regions.

Modern IVUS technology involves higher frequency transducers, typically 30MHz, and better resolution characteristics than those used in the original in vitro studies. Additional advances include miniaturization and improved flexibility of the catheters. The European Society of Cardiology (ESC) has recently proposed an IVUS classification of plaque composition in an attempt to standardize image interpretation (Di Mario *et al,* 1998). This study, incorporating this classification, was performed to determine the reproducibility and histological correlation of qualitative IVUS imaging of atheromatous coronary arteries in conditions more closely approximating the clinical setting.

3.2 Methods

Coronary artery segments (n=30) were excised from 20 human hearts of 15 men and 5 women (mean age 73 years) at post-mortem. All arteries were stored at 4°C and studied within 24 hours of death to avoid dessication. Preservatives were avoided prior to study so as to avoid important changes in tissue structure and echogenicity (Park *et al,* 1993).

Handling of specimens during preparation was minimized to avoid trauma. Segments of at least 5cm were studied. All side branches were ligated with silk sutures and the proximal and distal ends mounted on modified 7F guide catheter sections within the closed loop perfusion system described in Chapter 2. A layer of myocardium and fat was left in place to preserve the adventitia and original curvature of the vessel. The isolated vessels were perfused with normal saline at room temperature with a mean perfusion pressure of 80mmHg and flow rates of 60-80mls/min.

A commercially available IVUS system (Cardiovascular Imaging Systems Inc., Sunnyvale, California, USA) was used with 3.2F, 30MHz Ultracross (Scimed) catheters. The catheter was passed through the specimen over an 0.014" floppy guide wire, which aided catheter tracking and reduced the potential for trauma to the arterial wall. Minor adjustments of the gain settings were necessary for each artery to aid clear visualization of the luminal and external elastic lamina boundaries. An initial mechanical pullback (0.5mm/sec) along the arterial segment was performed from the distal guide catheter and the images were recorded onto super VHS videotape for offline analysis. Significant coronary stenoses, defined as an area stenosis ([mean reference lumen area – minimum lumen area] / mean reference area) of greater than 70% by planimetry, were identified from the recorded images. At a position just distal to the lesion a suture needle was inserted transversely into the arterial adventitia so as to be visible by IVUS imaging. This site was used as a reference point to enable topographic registration of the ultrasound image with the corresponding pathological cross-section. A second pullback was then performed and once the imaging was completed the reference needle was pulled through and the reference point marked with silk suture. Arterial segments were than pressure-fixed in 10% buffered formalin for 24 hours at the peak pressure achieved during pulsatile perfusion to enable subsequent histological sections to be compared accurately with corresponding IVUS images selected at the point of maximum vessel dimensions with pulsatile flow. Further thin sutures were inserted into the adventitia at sites corresponding to the reference and minimum lumen area sites. These were determined from the pullback distance between each site and the reference needle position noted on the video recording. The arterial segments were then submitted for histological preparation and analysis.

3.2.1 *IVUS image analysis*

Atheromatous plaques were characterized by their appearance at the selected minimum lumen area site and reference site according to recently proposed guidelines (Di Mario *et al,* 1998) [Figure 1]. We considered focal calcification (calcific arc $<180^0$) separately rather than incorporating it in the description of heterogenous (mixed) plaques:

Echolucent (loose fibrous plaque with lipid deposition) – lesion echogenicity less than that of the surrounding adventitia for greater than 80% of the total plaque area.

Echodense (dense fibrous plaques) – lesion echogenicity greater than that of the surrounding adventitia for greater than 80% of the plaque area.

Heterogenous (varying degrees of loose and dense fibrous plaque) – presence of echodense and echolucent regions within the plaque, all being less than 80% of the plaque area.

Calcified – lesion echogenicity greater than that of the surrounding adventitia with acoustic shadowing and reverberations for greater than a 180^o arc.

Focal calcium deposition – sites of calcium deposition, defined as highly echogenic regions with acoustic shadowing and reverberations within the plaque subtending an arc of less than 180^o on the cross-sectional IVUS image were described in a manner analogous to the hours of the clock. Depth of the deposit in relation to the luminal border was described as *superficial*, defined as no tissue between the deposit and the lumen and *deep*, all other depths. Arc subtended by the deposit was described in degrees.

Two observers independently selected and qualitatively analysed the minimum lumen area and reference sites from the recorded pullback sequences for each vessel. One observer selected and analysed all the sites on two separate occasions at least two weeks apart. To determine whether atheromatous plaque composition at the minimum lumen

area was representative of the whole lesion the same analysis was performed along the length of the lesion at 0.5mm intervals to define the predominant plaque composition.

3.2.2 *Histological analysis*

Following pressure fixation the arterial segments were decalcified in a standard solution. Sections were cut at the premarked minimum lumen area and reference sites. Each was processed for light microscopy and stained with haematoxylin-eosin and elastic Von Gieson stains. Sections were analysed under light microscopy by a pathologist (Dr A Lessells) blinded to the IVUS image interpretation. By the appearance of the atheromatous plaque a corresponding classification to the IVUS analysis was determined for *loose fibrous*, *dense fibrosis*, *calcified*, and *heterogenous* lesions. Focal calcification was described in a similar way as that for the image analysis.

3.2.3 *Statistical analysis*

Reproducibility measurement for plaque type and focal calcium takes into account the proportion of agreements occurring by chance both within and between observers and is expressed as the Kappa value where negative values indicate a worse than chance agreement, a value of zero indicates agreement no better than chance and a value of 1.00 indicates perfect agreement. The value is expressed with 95% confidence intervals. Comparison of the histological classification and the ICUS analysis is made by calculating the sensitivity, specificity and positive predictive values for each plaque type and for focal calcium deposition.

3.3 Results

Thirty human post-mortem coronary arteries were studied (left anterior descending x 16, left circumflex x 4, right coronary x 10). Nine specimens were normal (n=2) or of insufficient calibre to accommodate the IVUS catheter (n=7). The remaining 21 atherosclerotic arteries yielded a total of 50 sites suitable for analysis (minimum lumen area x 21, reference sites x 29).

3.3.1 *IVUS image quality*

A total of eight IVUS catheters were used. Non-uniform rotational distortion occurred transiently during two recorded pullbacks. Despite this a qualitative analysis was possible at the minimum lumen area and reference sites. Persistent image artefacts were noted in three pullbacks requiring a change of catheter. This precaution enabled uniformly high image quality throughout the study.

3.3.2 *Intra-observer agreement*

Fifty sites were analysed (Table 1). Overall, agreement for plaque type was reached in 90% (45/50) producing very good correlation (kappa 0.89 [0.85-0.93]). Very good agreement was observed for echodense (0.96 [0.93-0.99]), echolucent (0.91 [0.87-0.95]) and calcified (0.96 [0.94-0.98]) plaque types and good agreement for heterogenous plaque (0.78 [0.72-0.84]). For focal calcium deposition there was very good agreement (0.88 [0.84-0.92]). Selected sites in the first compared to the second analysis were on average 0.93±0.85mm apart. Selections of the reference site were noted to be significantly further apart than those of the minimum lumen area site (1.20±0.22mm vs 0.50±0.40mm, p=0.02). This resulted in less agreement for plaque type (0.79 [0.70-0.88]) and focal calcium deposition (0.78 [0.73-0.85]) at reference sites compared to minimum lumen area sites (0.94 [0.89-0.99] and 0.92 [0.89-0.95] respectively).

3.3.3 *Inter-observer agreement*

Fifty sites were analysed (Table 2). Overall agreement for plaque type was reached in 88% (44/50) with very good correlation (0.87 [0.80-0.94]). Kappa values for individual plaque types were 0.87 (0.81-0.93), 0.89 (0.86-0.92), 0.85 (0.80-0.90) and 0.82 (0.80-0.84) for echodense, echolucent, calcified and heterogenous plaques respectively. Sites selected by each observer were on average 1.00±1.20mm apart. Selections of the reference sites were significantly further apart than those of the minimum lumen area site (1.39±0.31mm vs 0.68±0.37mm, p=0.02). As a result agreement for plaque type (0.82 [0.79-0.85]) and focal calcium deposition (0.64 [0.52-0.76]) at reference sites was

less than that for minimum lumen area sites (0.93 [0.90-0.96]) and 0.84 [0.74-0.94]), respectively.

3.3.4 *Predominant plaque composition*

The predominant plaque composition for each lesion was determined for 21 lesions (Figure 2). There was agreement of plaque composition at the minimum lumen area site and the overall plaque composition of the lesion in only 62% (13/21) of lesions. Clinically important transitions of plaque type, such as calcified to soft plaque or soft to hard plaque, were frequently noted along the length of the lesion.

3.3.5 *Histological correlation to plaque type*

Only those selected sites in which agreement was demonstrated for plaque type between observers (n=44) were used for this part of the analysis. Mean percent plaque stenosis was 78.2±8.1% at minimum lumen area sites indicating significant luminal obstruction. At reference sites there was also significant disease (percent plaque stenosis 56.2±11.7%). Calcium arcs of >120° prevented this measurement at 11 sites.

Overall, complete agreement for plaque type between IVUS and histological appearances occurred at 89% of sites. Table 3 demonstrates that the specificity and positive predictive value of IVUS for identifying individual plaque types are high (greater than 90%). The sensitivity of IVUS for echodense and heterogenous plaques was moderate (78% and 85% respectively). The overall kappa value, a better descriptor of correlation, revealed very good agreement (0.84 [0.77-0.91]). Disagreement occurred at five sites, in two the pathologist described a calcified lesion on the basis of the presence of extensive speckled microcalcification which is not visible within the resolution of the IVUS transducer. Two sites with echolucent plaque and one echodense plaque were described as heterogenous by IVUS interpretation (Table 4).

3.3.6 *Focal calcium deposition*

Excellent correlation was demonstrated for the presence of focal calcium deposits with sensitivity, specificity and positive predictive values all exceeding 90%. The observed kappa value of 0.96 (0.93-0.99) confirmed this level of agreement

3.3.7 *Influence of pulsatile flow*

All the lesions studied caused significant luminal obstruction (mean percent plaque stenosis 70.8±8.1%) and were therefore subject to only small changes in vessel area during pulsatile flow. At minimum lumen area and reference sites the systolic-diastolic area difference was 0.24±0.64mm^2 and 0.65±0.71mm^2, respectively. Continuous play of the recorded ICUS pullbacks revealed no difference in lesion echogenicity between 'systole' and 'diastole' at minimum lumen area sites but significant differences at reference sites, presumably because of stretching of the arterial wall and a larger vessel-to-wall catheter distance during the 'systolic' phase. However, the lesion classification was not significantly influenced by pulsatile flow.

3.4 Discussion

Early studies demonstrated the potential for IVUS to provide a detailed and accurate analysis of atherosclerotic plaque appearances, but these were performed under highly controlled in vitro conditions designed to optimise image quality. This study has addressed the reproducibility and histological accuracy of qualitative IVUS image interpretation using modern imaging technology and in circumstances approximating the clinical situation. Arterial tortuousity was maintained which resulted in eccentric transducer positioning and the potential for tangential imaging of the coronary wall which is common to clinical studies (Waller *et al,* 1992). Areas of significant coronary atheroma rather than normal or mildly stenotic regions were studied, resulting in a greater depth of atheromatous plaque to be interrogated. The advanced age of the arterial specimens studied resulted in the presence of more complex, heterogenous plaque types compared to previous studies (Di Mario *et al,* 1992). The influence of pulsatile flow on

image interpretation and the impact of the selection of minimum lumen area and reference sites on reproducibility was also considered.

3.4.1 *Reproducibility*

This is the first qualitative IVUS study in which the observers selected minimum lumen area and reference sites independently in separate analysis sessions. The use of preselected images in previous studies assumes that there is no inter- or intra-observer difference in the selection of the site if interest. The results show that significant variation can occur, and this does affect the IVUS classification since precise correlations of plaque type were more frequent when minimum lumen area or reference sites selected by each observer were closer or coincided. The variability in the site selected for image interpretation was significantly greater for reference sites as compared to the minimum lumen area sites. This is because the most stenotic part of the lesion is easier to identify than a suitable site within the reference segment which is usually diffusely diseased (Kearney *et al,* 1997).

Although IVUS images are frequently used to determine plaque composition in the clinical setting, only two previous reports of the observer variability of qualitative image interpretation could be identified The first was limited to the detection of focal calcification and described good agreement, which was consistent with our own findings (Peters *et al,* 1994a). The second was a clinical study of the variability of the identification of the predominant plaque composition over a defined length of atheromatous coronary artery (Hodgson *et al,* 1993). These investigators found complete agreement for plaque type in only 47% of lesions using a similar classification to the ESC working group. The described study demonstrates better agreement for plaque type, with intra-observer agreement in 90% of lesions and inter-observer agreement in 88%. However, defined sites were compared and in the setting of coronary intervention it may be necessary to consider the whole lesion to optimise the choice and positioning of mechanical devices (van der Lugt *et al,* 1995).

3.4.2 *Histological correlation*

Following the initial development of IVUS technology a number of detailed studies examined the correlation of IVUS images with corresponding histological appearances. One of the earliest studies reported low sensitivity and specificity even for the detection of atheroma, using 20MHz transducers with limited image resolution and an early commercially available IVUS system (Anderson *et al,* 1992). More recent studies, using a range of plaque classifications, have demonstrated that grey-scale levels do correspond to basic plaque types. Where all plaque types were compared, high levels of agreement were reported (>90%) [Potkin *et al,* 1990; Di Mario *et al,* 1992]. In particular the presence of calcified plaques and focal calcium deposition have been demonstrated to have high specificity and sensitivity. However lower levels of sensitivity for lipid-rich (78%) and fibrous (67%) plaque types were demonstrated.

This study demonstrates better correlation of IVUS with the histological classification, with an overall agreement for plaque type of 89% and specificity and sensitivity for individual plaque types and focal calcium deposition of greater than 90%. Discrepancies were usually subtle, such as mistaking echolucent for heterogenous plaque or, in two cases, due to microcalcification, the clinical significance of which is uncertain, that could not be visualised by IVUS (Friedrich *et al,* 1994; Goel *et al,* 1992). The improved results in more recent studies are largely attributable to advances in IVUS technology including higher frequency transducers and smaller, more flexible catheters. Additionally, in the current study the recently described ESC plaque classification was used which compares the echodensity of atheromatous plaque to the surrounding adventitia which is designed to standardise image interpretation.

3.5 Limitations of the study

It may be argued that validation of the accuracy of IVUS images compared to histopathological appearances is less relevant to the current practice of percutaneous coronary intervention given the move away from lesion-specific techniques, such as rotational atherectomy. However it is generally accepted that a knowledge of lesion

composition makes an important contribution to the selection of the optimal balloon size and inflation pressure to maximise luminal gain in stented and non-stented coronary lesions. For instance the presence of calcification may encourage the use of modest inflation pressures to minimise the risk of extensive intimal tearing which commonly arises from the transition point between the calcium and plaque. However, it is unlikely that the presence of focal areas of calcification would significantly alter the intended balloon inflation pressure in the current setting where stent implantation abolishes the influence of flow-limiting dissections or tears.

The flow model does not take into account the possible effects of transducer movement in the arterial lumen due to the beating heart. Saline perfusion was used which produces slightly higher mean pixel grey levels within plaque than blood perfusion. However distinction between plaque types is not significantly different between the two methods (Peters *et al,* 1994b). No discernible differences were noticed in the image quality between the in vitro studies and those of clinical studies performed at our centre using the same IVUS system.

Lipid pools within the plaque and luminal thrombus were not considered in this study because previous studies have demonstrated that their discrimination is inconsistent using video images alone (Peters *et al,* 1994c; Peters *et al,* 1994a). More reliable distinction may be possible in the future with the use of higher frequency (40-50MHz) transducers or advanced image processing techniques such as analysis of radiofrequency data (Spencer *et al,* 1997; Chandraratna *et al,* 1991).

3.6 Conclusions

Using modern IVUS technology and an in vitro system which approximates clinical conditions this study has demonstrated that the recently proposed ESC qualitative classification of plaque composition is reproducible and correlates well with histological appearances. In the clinical setting this new classification should perform reliably in both diagnostic IVUS examinations and in the guidance of percutaneous coronary intervention. However, it should be borne in mind that analysis of the whole lesion

rather than just the most stenotic site should determine the overall plaque composition and morphology.

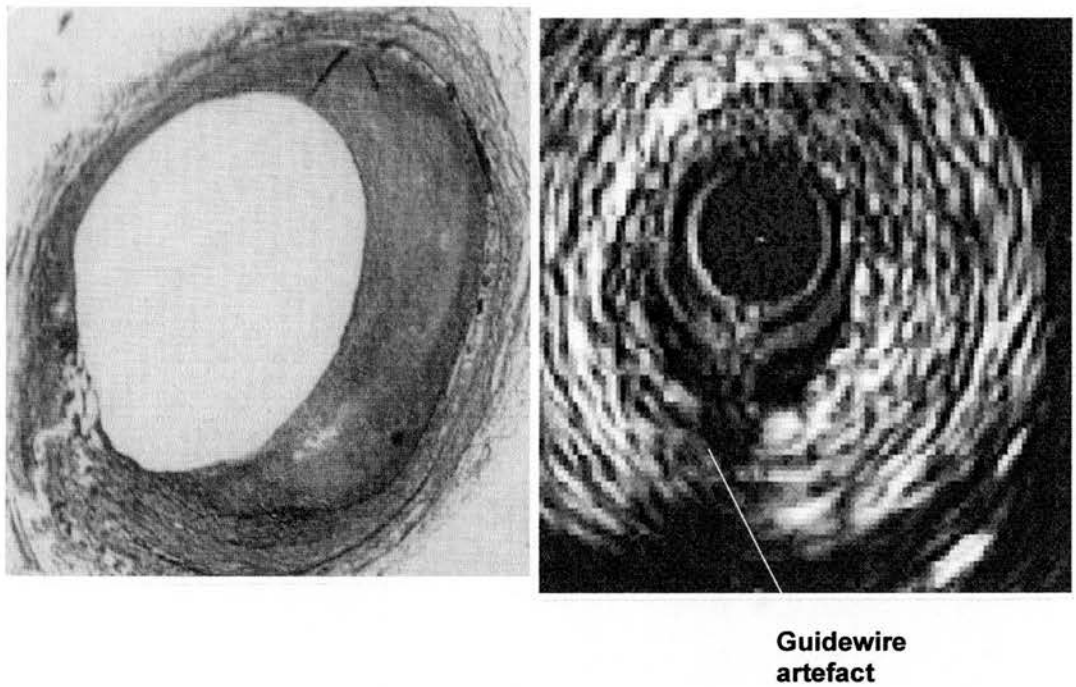

Figure 1. ***IVUS versus histology. Example of close correlation of IVUS and histology for an eccentric heterogenous (mixed) atherosclerotic plaque.***

	Kappa	%agreement
Echodense ('hard')	0.96 (0.93-0.99)	95 (18/19)
Echolucent ('soft')	0.91 (0.87-0.95)	91 (10/11)
Heterogenous ('mixed')	0.78 (0.72-0.84)	75 (6/8)
Calcified	0.96 (0.94-0.98)	92 (11/12)
Overall	**0.89 (0.85-0.93)**	**90 (45/50)**
Focal calcification	0.88 (0.84-0.92)	94 (29/31)

Table 1. ***Summary of the intra-observer reproducibility of IVUS images for coronary atherosclerotic plaque type and focal calcification using the proposed ESC classification (n=50 sites).***

	Kappa	%agreement
Echodense ('hard')	0.87 (0.81-0.93)	92 (17/19)
Echolucent ('soft')	0.89 (0.86-0.92)	89 (9/10)
Heterogenous ('mixed')	0.82 (0.80-0.84)	80 (5/6)
Calcified	0.85 (0.80-0.90)	87 (13/15)
Overall	**0.87 (0.80-0.94)**	**88 (44/50)**
Focal calcification	0.78 (0.71-0.85)	89 (26/29)

Table 2. ***Summary of the inter-observer reproducibility of IVUS images for coronary atherosclerotic plaque type and focal calcification using the proposed ESC classification (n=50 sites)***

	Specificity (%)	Sensitivity (%)	ppv	Kappa
Echodense ('hard')	95	78	94	0.90 (0.87-0.93)
Echolucent ('soft')	96	94	90	0.74 (0.69-0.79)
Heterogenous ('mixed')	94	85	92	0.79 (0.72-0.86)
Calcified	92	100	91	1.00
Overall	**94**	**89**	**92**	**0.84 (0.77-0.91)**
Focal calcification	96	99	91	0.93 (0.90-0.96)

ppv = positive predictive value

Table 3. ***Summary of the correlation of IVUS images with histology for coronary atherosclerotic plaque type and focal calcification using the proposed ESC classification (n=44 sites).***

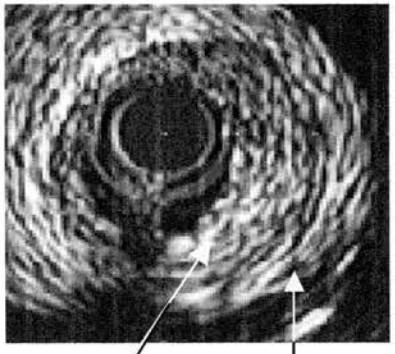

Heterogenous (mixed) plaque

Presence of echodense and echolucent regions within the plaque, all being less than 80% of the plaque area.

Focal calcification

Highly echogenic regions with acoustic shadowing and reverberations within the plaque subtending an arc of less than 180° on the IVUS image

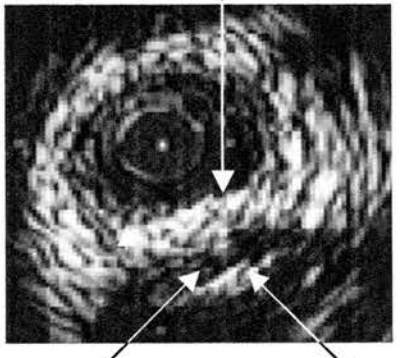

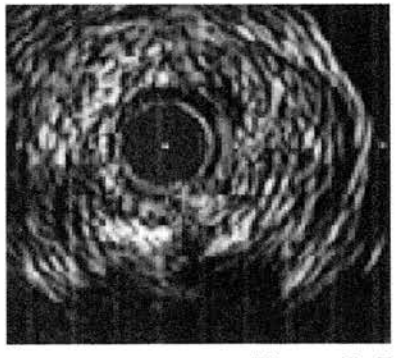

Echolucent (soft) plaque

Lesion echogenicity less than that of the surrounding adventitia for greater than 80% of the total plaque area.

Figure 2. ***Examples of atheromatous plaque types as interpreted by IVUS***

		Intravascular Ultrasound				
		Echodense	**Echolucent**	**Heterogenous**	**Calcified**	**Total**
Histology	**Echodense**	**16**	0	0	1	**17**
	Echolucent	0	**7**	0	2	**9**
	Heterogenous	2	0	**11**	0	**13**
	Calcified	0	0	0	**5**	**5**

Table 4. *Correlation of IVUS images with histology for coronary atherosclerotic plaque type.*

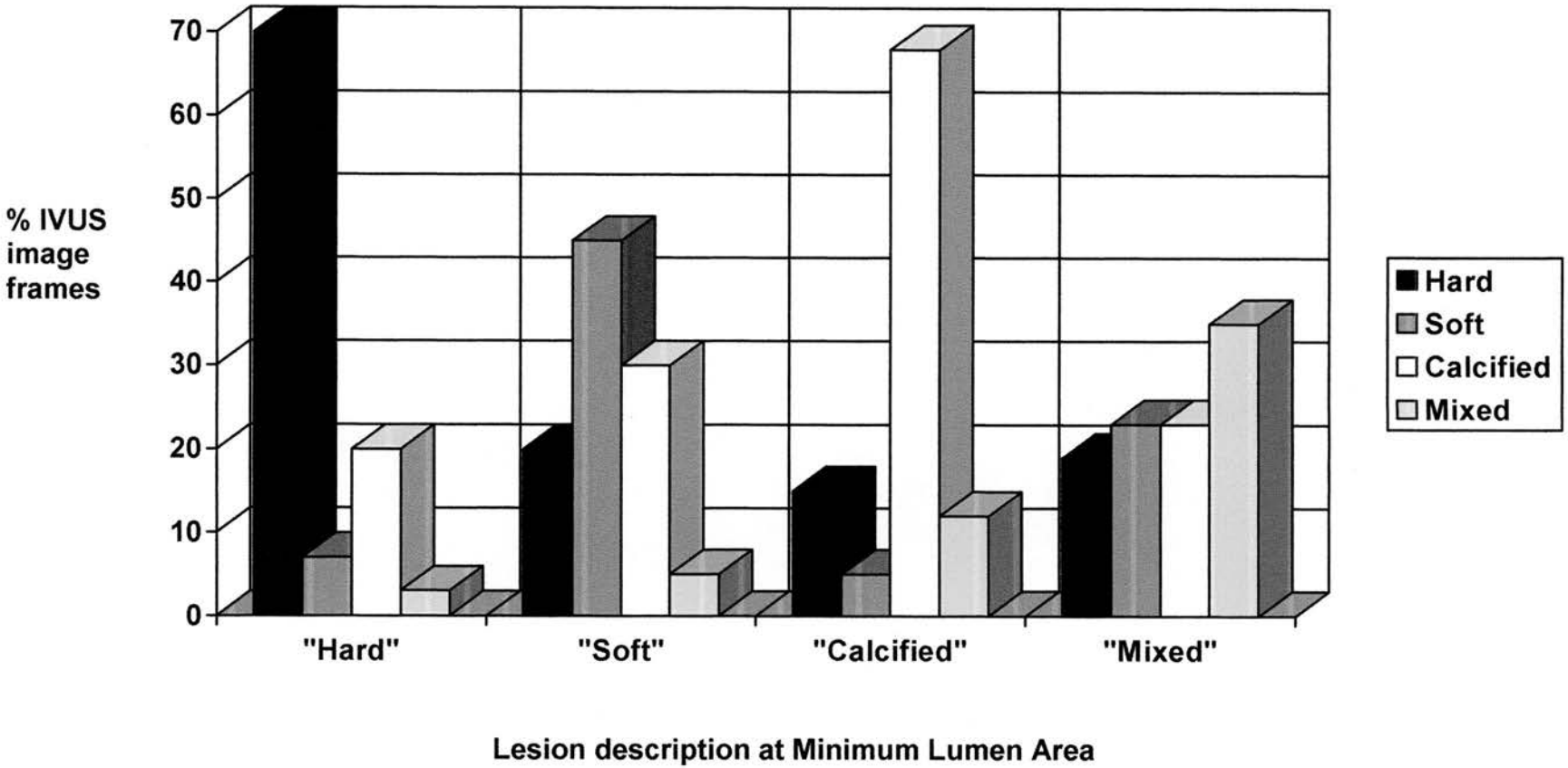

Figure 3. ***Atherosclerotic plaque type at the minimum lumen area site and plaque heterogeneity along the lesion length. For example, lesions described at the MLA as "soft" contain significant areas of hard (20%), calcified (30%) and mixed (5%) plaque along their length.***

CHAPTER 4

Clinical implications of interobserver variability in reference site selection in intravascular ultrasound-guided percutaneous intervention

4.1 Introduction

To quantitate the relatively small changes in lumen and vessel dimensions that occur during percutaneous intervention and following therapies designed to induce atheroma regression imaging techniques such as contrast angiography and intravascular ultrasound (IVUS) are required to be accurate and reproducible. For example, angiographic follow-up of 1,445 lesions at six months following successful PTCA revealed an absolute mean lumen diameter loss of only 0.28±0.52mm (Rensing *et al,* 1992). Despite the well described accuracy and reproducibility of quantitative coronary angiography (QCA) in such clinical studies the technique is based on contrast lumenography and therefore is unable to visualize changes that occur in the vessel wall. As previously described IVUS provides tomographic imaging that can quantitate vessel dimensions and also directly document the impact of vessel remodelling within the lesion and in adjacent reference segments prior to and following percutaneous intervention (Mintz *et al,* 1994a). The use of IVUS in percutaneous intervention has shifted from research (Guide Trial Investigators, 1996; Peters *et al,* 1997) to decision making in the everyday clinical setting. Recently, several studies have demonstrated the potential of IVUS to guide PTCA and stenting procedures (Stone *et al,* 1997; Colombo *et al,* 1995; de Jaegere *et al,* 1998). These studies used lumen and vessel dimensions at reference sites adjacent to the lesion to choose the balloon and stent size required in order to obtain an optimal residual lumen area following the procedure, a practice which has clearly been associated with lower restenosis rates than with angiographic guidance alone. The selection and measurement of reference sites by IVUS are operator-dependent processes and potential sources of variability (Kearney *et al,* 1997). Little has been published regarding the interobserver variability of IVUS measurements in percutaneous intervention despite the potential impact on balloon and stent sizing. It is possible that a substantial interobserver variability may confound the analysis of IVUS-guided interventions. The aim of this study was to investigate the interobserver variability of morphometric measurements of coronary stenoses and adjacent reference sites in conditions that closely approximate the clinical setting. Interobserver variability was determined in IVUS images selected and measured independently by observers. From this data we evaluated whether decisions

such as balloon sizing would significantly differ on the basis of differences in reference site selection and analysis.

4.2 Methods

Lesions were studied in the previously described in vitro pulsatile flow system and consisted of significant coronary stenoses prior to balloon angioplasty. Recorded pullbacks of the diseased, post-mortem human coronary artery specimens (n=20) studied in Chapter 3 were analysed. In brief, the specimens were prepared and mounted within the pulsatile flow system. A 0.014" floppy guide wire was used to cross the lesion. Significant lesions, defined as >70% percent plaque stenosis, were studied with 3.2 French, 30MHz mechanical IVUS catheters using a motorized pullback (0.5mm/sec). All pullbacks were recorded onto sVHS videotape for offline analysis.

4.2.1 *IVUS measurements*

From the recorded IVUS pullbacks the frame depicting the most severe site of stenosis (minimum lumen area, MLA) and a suitable reference site distal to the lesion were selected independently by two experienced operators and measured in separate analysis sessions. Reference sites were selected in a segment within 5mm of the lesion. They were defined as the most normal IVUS cross-section within the segment. Atheromatous plaque within the selected site was required to occupy less than 60% of the vessel area. Additionally there were no side-branches between the lesion and the reference site. Manual measurements were made offline using the quantitation software of the IVUS system. The largest lumen diameter during pulsatile flow was selected for quantitation. At minimum lumen area and reference sites lumen and vessel areas were measured. In addition, mean lumen and vessel diameters (minimal diameter + maximal diameter / 2) were measured at both sites. Vessel area was measured by tracing the outer border of the echolucent zone (see Figure 1) which represents the interface between media and adventitia. The endoluminal border was traced to measure lumen cross-sectional area.

Vessel area analysis at the minimum lumen area was not possible in 3 lesions due to excessive acoustic shadowing from calcification.

Interobserver variability was investigated by comparing the selection and measurement of minimum lumen area and reference sites between the two observers. In addition, the potential impact of any interobserver variability of reference site selection on the selection of optimum balloon sizes for PTCA and the determination of adequate stent deployment was assessed.

4.2.2 Statistical analysis

To assess the impact of absolute lumen and vessel dimensions on variability, and to visually assess the degree and direction of any bias, Bland-Altman plots were constructed by plotting the mean difference of measurements on the y-axis against the average of paired measurements on the x-axis (Bland *et al,* 1986). Variability was defined as the percentage difference between paired measurements of the two observers and calculated as: (difference / mean of both measurements) x 100%. Variability of 10% was considered clinically acceptable. Values are expressed with 95% limits of agreement calculated as twice the standard deviation.

4.3 Results

Interobserver variability for all measurements is summarized in Table 1. Bland-Altman plots are displayed for mean lumen diameter and lumen and vessel area at the point of maximal stenosis (Figures 2-4) and reference lumen and vessel area and mean lumen and vessel diameters (Figures 5-8).

4.3.1 *Variability of measurements at minimum lumen area*

The mean percent plaque stenosis at the minimum lumen area measured by observers 1 and 2 were 83±13% and 79±10% respectively. In general, larger lumen area measurements were made by observer 2 (0.13mm^2) and larger vessel areas were made by observer 1 (0.2mm^2). However, no statistically significant systematic bias was present for all measured parameters at the most stenotic point of the lesion. Variability, expressed as a percentage were: mean lumen diameter 0.00±4.5%, minimum lumen area 4.7±9.4% and minimum vessel area 4.5±9.1%. Analysis of selected minimum lumen area sites revealed precise concordance between observers in 90% (18/20) of the arterial specimens. In the other two cases the sites selected by each observer were separated by distances of less than 0.5mm.

4.3.2 *Variability of measurements at reference sites*

The mean percent plaque stenosis at the minimum lumen area measured by observers 1 and 2 were 38±8% and 41±8% respectively. Observer 1 had a tendency to measure a larger mean reference vessel diameter (0.1mm), lumen area (0.3mm^2) and vessel area (0.3mm^2). However, as with the previous analysis there was no significant systematic bias between observers. There was considerably less agreement between observers for all measured parameters. Variability, expressed as a percentage were: mean reference lumen diameter 10.0±20.0%, mean reference vessel diameter 10.4±20.7%, reference lumen area 14.5±29.0% and reference vessel area 13.5±26.9%. Precise concordance of reference site selection occurred in only 45% (9/20) of the arterial specimens. For these sites mean variabilities were: reference lumen diameter 6.6±6.8% and reference vessel diameter 8.8±7.4%. In the other 11 cases the sites selected by each observer were separated by a mean distance of 1.39±1.31mm. For these sites mean variabilities were: reference lumen diameter 12.7±13.1% and reference vessel diameter 11.6±12.2%.

4.3.3 *Implication of variability in IVUS measurements on balloon size selection*

The potential implication of variability in reference vessel and lumen diameter measurements on the selection of balloon sizes for percutaneous transluminal coronary angioplasty was assessed. For this part of the analysis the optimum balloon size was calculated for each lesion using mean reference vessel and lumen diameter measurements made by observer 1 and observer 2. The optimal balloon size is determined according to the CLOUT (Clinical Outcomes With Ultrasound) trial (Stone *et al,* 1997). Briefly, to allow for atherosclerotic vessel wall remodelling, the optimal balloon size is taken as halfway between the lumen and the outer adventitial layer. This is calculated at reference sites as: (mean lumen diameter + mean vessel diameter) / 2. Differences in calculated balloon sizes between observers are represented in Figure 9. In clinical practice standard balloon sizes are available in 0.25mm increments. It can be seen that in 70% (14/20) of the coronary lesions studied differences between observers in reference site selection and measurement are likely to have resulted in clinically important differences in balloon size selection in the clinical setting.

4.4 Discussion

The site of maximum coronary stenosis and adjacent reference segments can be clearly visualized on the coronary angiogram for the duration the contrast opacifies the lumen. This enables their precise identification and measurement on recorded images. However, using IVUS imaging these sites are identified from sequential tomographic images acquired as the transducer is withdrawn through the lesion. This requires observer registration and retention in memory of the vessel's changing dimensions during the pullback process. Selection of these sites is therefore a significant factor in the variability of IVUS measurements. In this in vitro study, using post-mortem diseased coronary arteries and in accurately simulated flow conditions, vessel and luminal dimensions were measured at minimum lumen area and adjacent reference sites in stenoses that would, in the clinical setting, have been suitable for percutaneous

intervention. Rather than using pre-selected frames for analysis, back and forth reviewing of the recorded IVUS pullback by each observer to identify suitable sites for analysis was performed. This practice enabled the assessment of the quantitative variability of IVUS-derived lumen and vessel dimensions at these sites in conditions which are more analogous to the clinical situation than studies based on the measurement of pre-selected frames.

For all measurements at minimum lumen area and reference sites no consistent interobserver bias was detected suggesting that systematic differences in image interpretation did not significantly contribute to interobserver variability. At minimum lumen area sites a clinically acceptable level of variability (≤10%) was observed for all measured parameters. Identical sites were frequently selected and the discordance between observers in a small number of lesions amounted to selection of sites consistently less than 0.5mm apart. This part of the study confirms that the point of maximum lumen compromise is reproducibly identified by each observer.

At reference sites a greater degree of variability was noted for all measured dimensions. Mean lumen and vessel diameter and area measurements between observers demonstrated variability of greater than 10%. Clinically acceptable variability occurred when identical reference sites were selected for analysis. However, discordance of site selection occurred in a significant proportion (55%) of lesions and, in comparison to minimum lumen areas, the selected sites were a greater distance apart. Therefore the overall variability appears mainly to be explained by differences in the selection of the reference site prior to analysis. Additionally it is likely that difficulties in measuring the endoluminal border and external elastic lamina due to ambiguous appearances may have encouraged approximating these boundaries by referring to adjacent image frames. The impact of discordance in reference site selection on the measured vessel and lumen dimensions between observers deserves some explanation since it may be anticipated that throughout the reference segment vessel and lumen dimensions are relatively constant. In clinical studies IVUS has clearly demonstrated that most reference segments that look angiographically normal are diffusely diseased with mild to moderate amounts of atherosclerotic plaque (Porter *et al,* 1993). As a result vessel and lumen dimensions

can be significantly different over relatively short distances due to marked changes in plaque content. Furthermore, there is likely to be more than one mode of vessel remodelling within each reference segment. In this study measured reference sites contained significant plaque amounting to approximately 40% of the total vessel area. Although these were post-mortem coronary arteries from subjects of a relatively advanced age the appearances are identical to those observed during clinical IVUS studies.

4.4.1 *A review of previous studies*

There are relatively few published studies of the variability of IVUS measurements. Most have described low intra- and interobserver variability for all measured parameters (Colombo *et al,* 1995; Hausmann *et al,* 1994; Foster *et al,* 1997). However, all these studies, except for one (Kearney *et al,* 1997), were performed on offline selected images at a pre-selected site. Our findings for interobserver variability in the analysis of minimum lumen area sites were similar to previous results. However, we demonstrated greater variability for reference site analysis compared to measurements of preselected sites which emphasizes the importance of frame selection in the analysis. Furthermore, some studies only report correlation coefficients >0.9 with low standard errors. The findings of these analyses are of limited applicability because clear measurement protocols were not described and the use of linear regression as a method for measuring agreement has significant limitations. A high correlation coefficient may exist despite the absence of true agreement between observers. In other words, significant differences in measurements between observers can exist in the presence of a good correlation coefficient. The use of Bland-Altman plots provides a more descriptive demonstration of variability by demonstrating the scatter of differences in measured dimensions and also reveals any systematic bias between observers.

4.4.2 *Clinical implications*

The use of IVUS is now focused on its ability to guide percutaneous coronary interventions. Many trials have used or are currently using IVUS for measurements of coronary artery dimensions for optimal balloon or stent size selection and for assessment of optimal stent deployment or post-procedural minimum lumen area, calculated as a percentage of a reference lumen area. As we have demonstrated a balloon size differing by >0.25mm would have been chosen by each observer in 70% of cases. In the clinical situation significant undersizing of semi-compliant balloons is likely to encourage the use of higher inflation pressures to increase balloon calibre. Increased barotrauma is regarded as one of the factors contributing to extensive vessel wall injury and the promotion of acute occlusion, due to flow-limiting dissection and spasm, and restenosis, due to a more profound smooth muscle proliferative response.

A further factor not specifically assessed in this study is the impact of variability in reference area measurements on the determination of procedural endpoints following PTCA and intracoronary stenting. For example, one of the well-accepted criteria for optimum stent deployment using IVUS is the achievement of a minimum intrastent lumen area greater than 90% of the mean reference lumen area. The level of variability noted in this study is clearly likely to have an impact on such assessments. These differences should be kept in mind particularly in the context of IVUS-guided trials of percutaneous intervention. The use of core laboratories to analyse data probably reduces interobserver variability. Another solution is to average the reference dimensions from a number of image slices taken within the reference segment. Also, sizing devices according to vessel dimensions within the lesion where variability negates the impact of reference segment variability. As will be demonstrated in chapter 5 we chose to calculate balloon sizes according to the mean vessel and lumen diameters at the most stenotic point of the lesion (mean vessel diameter + mean lumen diameter x 0.8) to minimize variability.

4.5 Study limitations

This was purely an IVUS study and observers did not have the benefit of angiographic information to determine the IVUS catheter position within the reference segment. Furthermore, as this was an in vitro study we relied upon selection of the maximum lumen and vessel dimensions during pulsatile flow to determine 'end-systolic' frames rather than using ECG–gated analysis. These factors could have negatively influenced the interobserver variability particularly in the assessment of reference segments. However, we suspect that systolic-diastolic variations in lumen and vessel dimensions had minimal impact on interobserver variability since all reference segments contained significant atheromatous plaque which significantly restricts the compliance of the vessel during pulsatile flow (Weissman *et al,* 1995).

This study assesses the short-term variability of IVUS measurements. We can not generalize these results to longitudinal studies of pharmacological methods of atheroma regression or restenosis following percutaneous intervention. Such assessments really require a method of reproducing the longitudinal orientation of the lesion such as three-dimensional reconstruction of vessels. This will be discussed later in the thesis.

A final consideration is the influence of the presence of negative remodeling at the point of maximal stenosis. This is one situation where optimal device sizing may be more precise at reference sites rather than within the lesion.

4.6 Conclusions

The variability of IVUS measurements at the point of maximum stenosis using independently selected image frames is low. However, within reference segments discordance of site selection results in clinically significant variability. In the clinical setting this discordance is likely to be a confounding factor in the selection of balloon sizes for PTCA and the determination of an optimal procedural endpoint particularly following intracoronary stenting. Steps to improve this quantitative variability include

the use of algorithms for sizing devices at the point of maximum stenosis rather than reference sites.

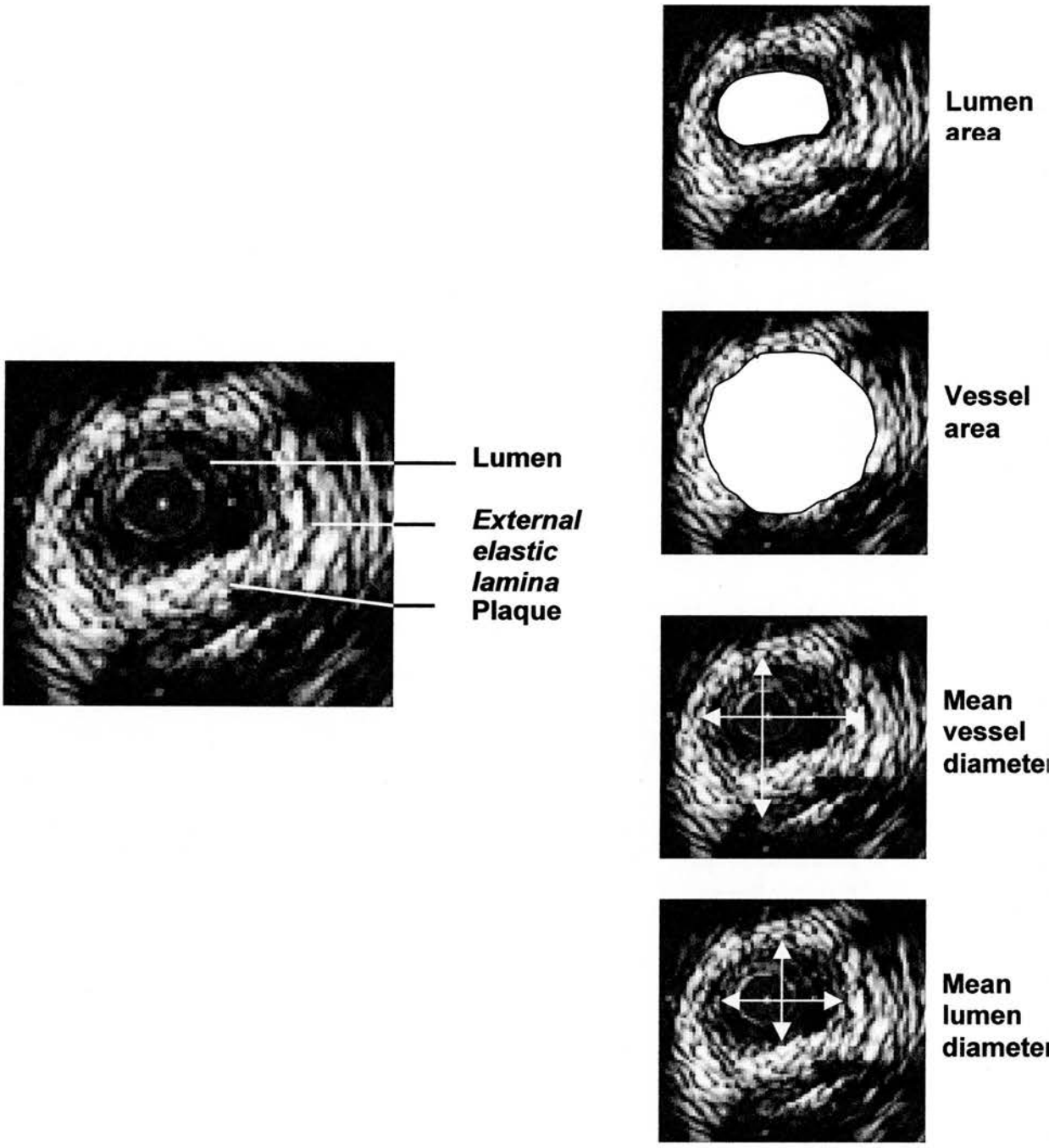

Figure 1. ***Method of measurement of lumen and vessel areas and diameters at reference sites and points of maximal stenosis***

Table 1. ***Results of the interobserver variability for the point of maximal stenosis and reference sites***

	Variability (%) (mean ± SD)
Maximal stenosis	
Mean lumen diameter	**0.0±4.5**
Lumen area	**4.7±9.4**
Vessel area	**4.5±9.1**
Reference site	
Mean lumen diameter	**10.0±20.7**
Mean vessel diameter	**10.4±20.7**
Lumen area	**14.5±29.0**
Vessel area	**13.5±26.9**

Mean lumen diameter = (maximum + minimum lumen diameter) / 2
Mean vessel diameter = (maximum + minimum vessel diameter) / 2

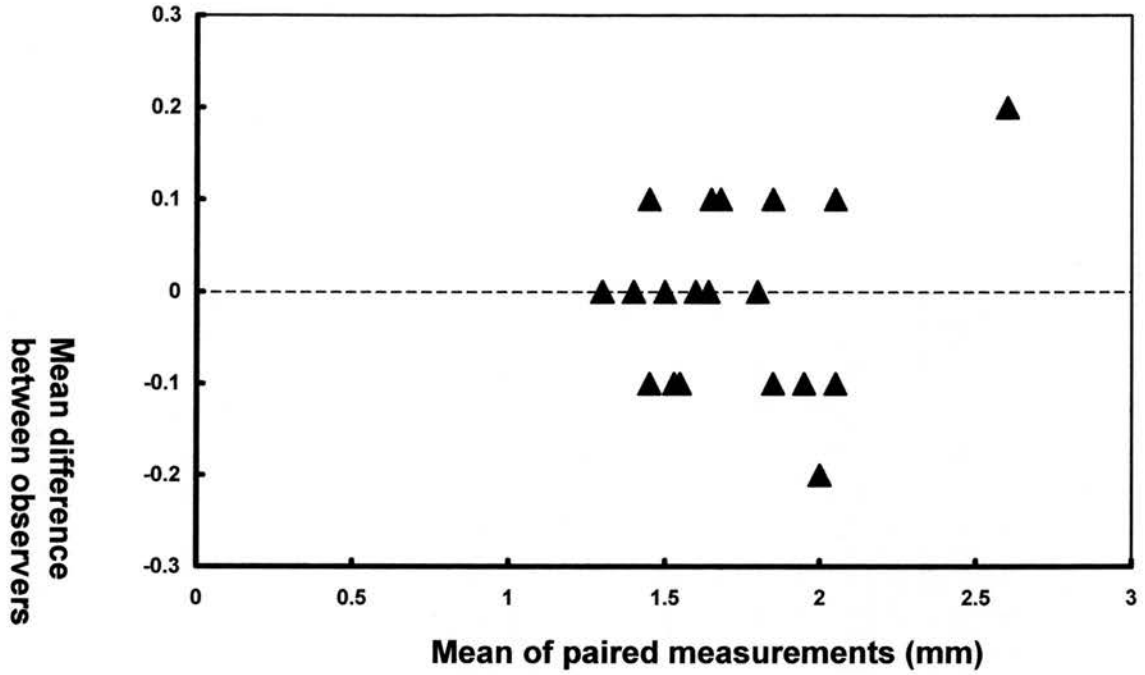

Figure 2. ***Bland-Altman plot representing the interobserver variability for lumen diameter at the point of maximal stenosis***

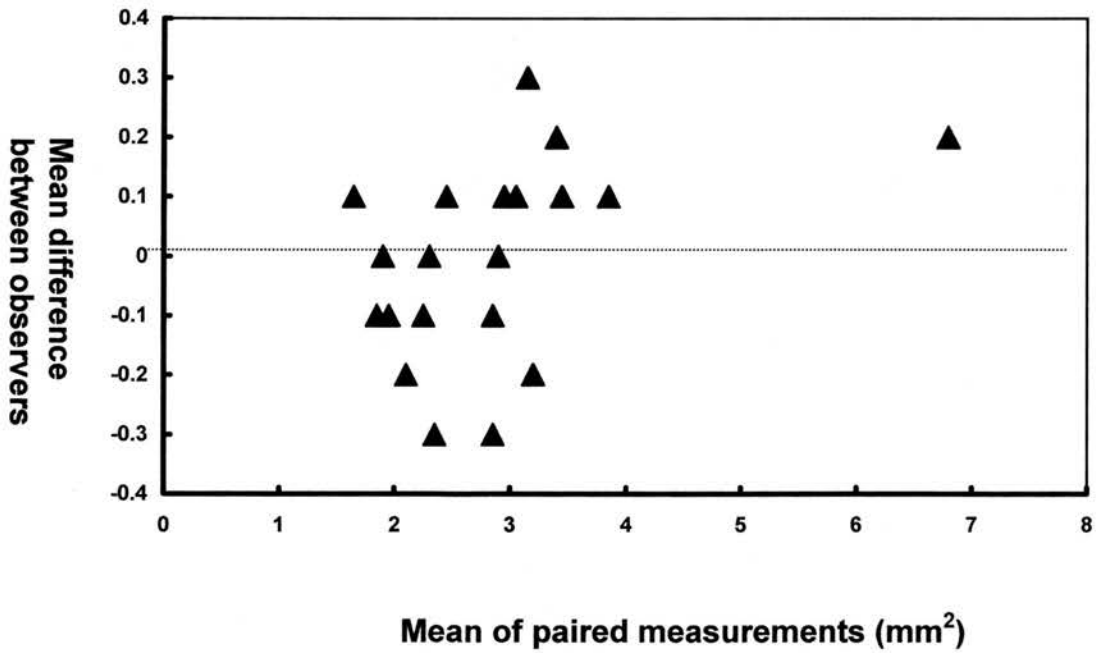

Figure 3. ***Bland-Altman plot representing the interobserver variability for lumen area at the point of maximal stenosis***

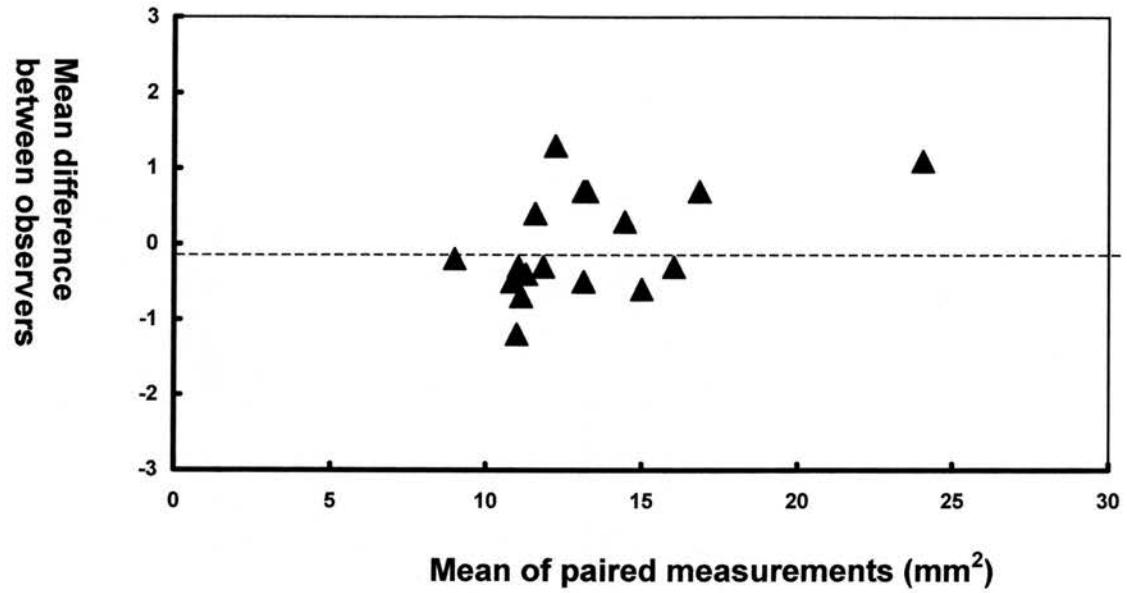

Figure 4. ***Bland-Altman plot representing the interobserver variability for vessel area at the point of maximal stenosis***

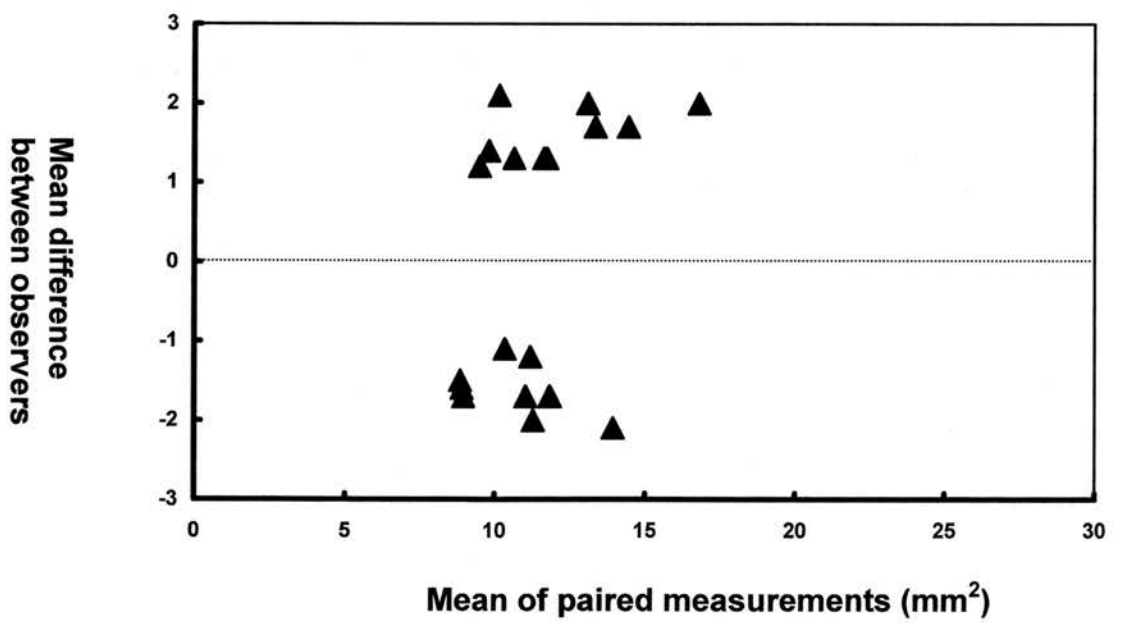

Figure 5. ***Bland-Altman plot representing the interobserver variability for reference lumen area***

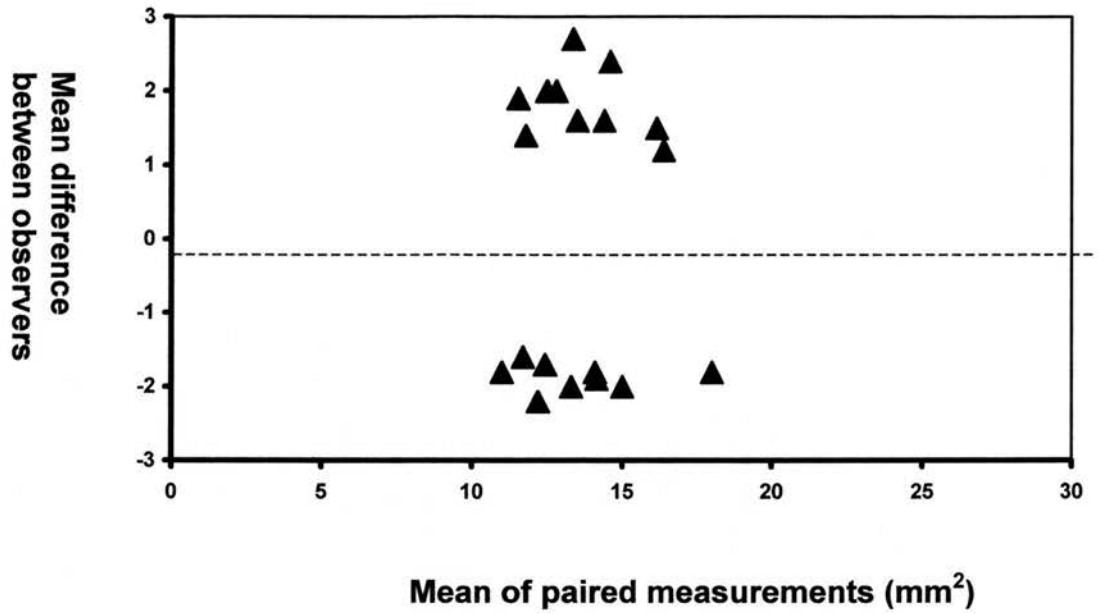

Figure 6. ***Bland-Altman plot representing the interobserver variability for reference vessel area***

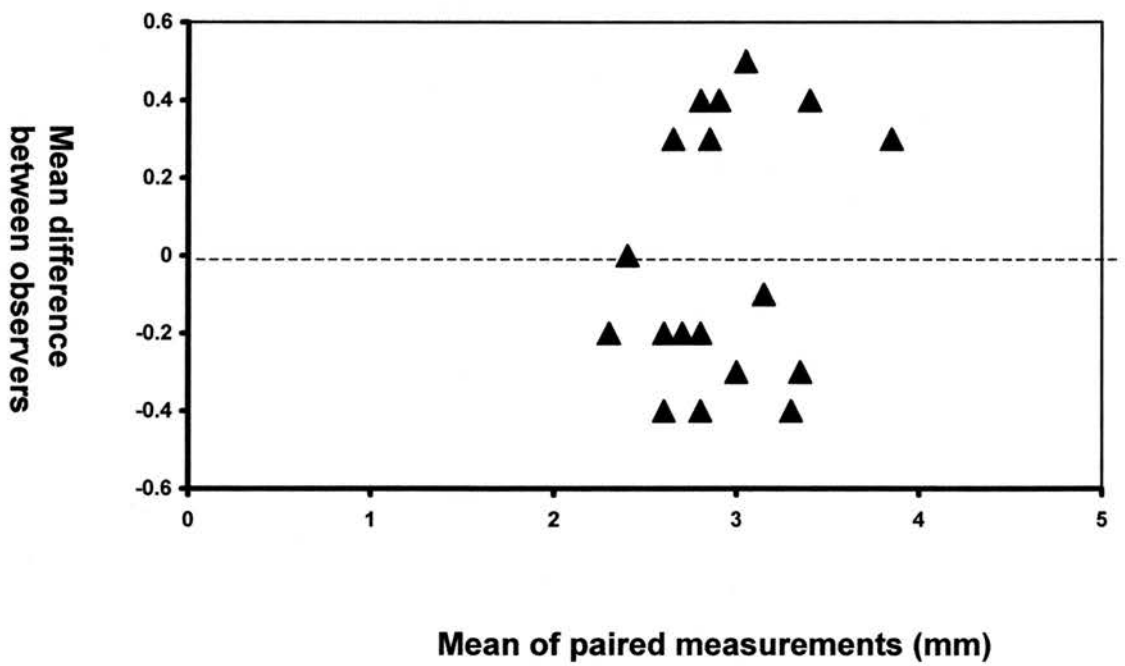

Figure 7. ***Bland-Altman plot representing the interobserver variability for reference lumen diameter***

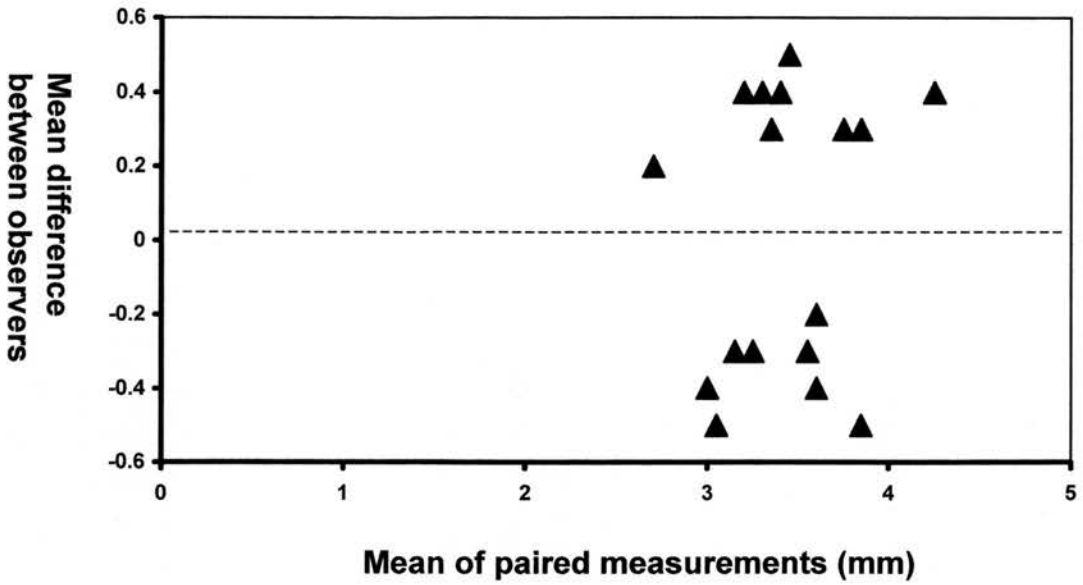

Figure 8. ***Bland-Altman plot representing the interobserver variability for reference vessel diameter***

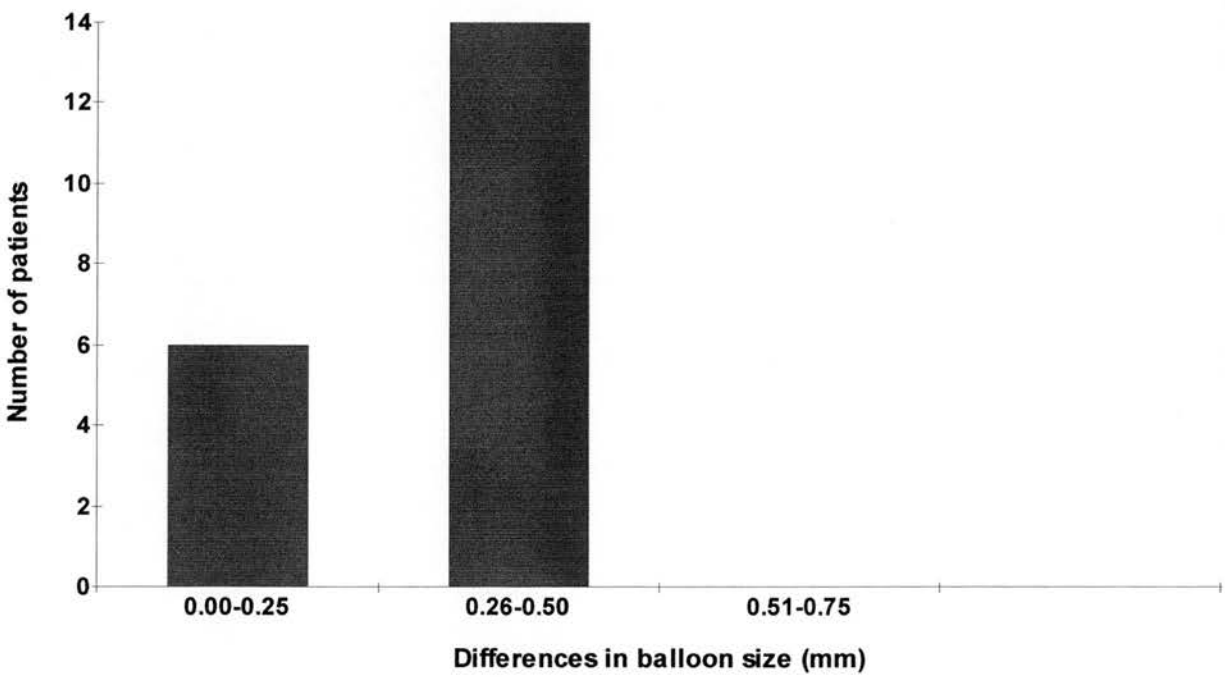

Figure 9. ***Impact on balloon size selection of interobserver variability in reference site selection and measurement using intracoronary ultrasound***

CHAPTER 5

Influence of balloon calibre and inflation pressure characteristics on arterial wall injury in intravascular ultrasound-guided percutaneous transluminal coronary angioplasty - histopathological observations

5.1 Introduction

Percutaneous transluminal coronary angioplasty (PTCA) is a widely used procedure in patients with coronary artery disease but is limited by ischaemic complications due to abrupt vessel closure and restenosis rates between 30% and 50% (Gruentzig *et al,* 1987; Nobuyoshi *et al,* 1988; Hirshfield *et al,* 1991). The influence of procedural factors such as balloon sizing and inflation pressure selection on the overall outcome of PTCA have been extensively assessed in animal and clinical studies (Meier *et al,* 1994; Roubin *et al,* 1985; Nichols *et al,* 1989). Despite this the only clear consensus of opinion was that the combination of high inflation pressures and oversized balloons tended to promote an adverse clinical outcome (Roubin *et al,* 1988). These studies were limited by their use of angiographic guidance for balloon sizing which tends to underestimate vessel dimensions (De Scheerder *et al,* 1989). More recently the use of IVUS to accurately match balloon size to true vessel dimensions has resulted in an improved clinical outcome (Stone *et al,* 1997; Haase *et al,* 1998). Avoidance of higher pressure inflations by the use of larger balloon calibres may have been a factor in the success of such trials. Furthermore, pre-interventional lesion characteristics such as plaque composition and eccentricity may be important factors when selecting the balloon calibre and inflation pressure strategy used to optimize the outcome of PTCA.

The aims of this in vitro histopathological study were: 1) to assess the incidence and extent of vessel wall injury following IVUS-guided PTCA using two different balloon calibre and inflation pressure strategies and 2) to determine whether pre-interventional lesion characteristics should influence the choice of strategy.

5.2 Methods

Atherosclerotic human coronary arteries (n=34) were harvested at post-mortem and studied within 24 hours. Each specimen was excised with a 5mm depth of surrounding tissue to help maintain the integrity of the vessel. All side-branches were tied off with sutures and the proximal and distal ends were connected to sheaths and placed in a water bath at room temperature. The closed loop pulsatile flow system described in Chapter 2

was used. Coronary flow at 80mls/min with a maximum perfusion pressure of 80mmHg was established. Distally a reference site was marked with a needle to enable accurate reproduction of balloon and IVUS catheter positions and allow correct orientation of IVUS images in serial studies. A 0.014" guide wire was negotiated through each specimen to aid catheter tracking and avoid damage to the arterial wall.

The specimens were studied with IVUS before and after PTCA using 3.2F, 30mHz catheters (CVIS Insight) with a mechanical pullback (0.5mm/sec). Pre-interventional imaging was performed to identify suitable lesions which were defined by a minimum lumen diameter <2mm, a plaque area stenosis >70%, lesion length <20mm and reference lumen diameter >2.5mm. The maximum lumen and vessel dimensions achieved during pulsatile flow were the points at which measurements were taken. The position of the minimum lumen area (MLA) was reproduced in serial studies by measuring the distance from the distal reference needle using the elapsed video time as well as landmarks such as focal areas of calcification.

The selection of optimal balloon size (OBS) was determined by measuring the mean vessel (external elastic lamina) diameter [maximum + minimum diameter / 2] at the MLA and multiplying by 0.8. A balloon to vessel ratio of 0.8 was considered optimal since this represented a final balloon size which was larger than the lumen yet just smaller than the vessel diameter [Haase et al, 1998]. Each lesion was then randomised to one of two strategies as demonstrated in Table 1. According to standard balloon compliance charts the final balloon diameter in each group is the same for each calculated OBS.

Table 1.

OBS(mm)	Group A		Group B	
	BS (mm)	Infl. Pr. (atmos.)	BS (mm)	Infl. Pr. (atmos.)
2.6-3.0	3.0	6	2.5	18
3.1-3.5	3.5	6	3.0	18
3.6-4.0	4.0	6	3.5	18

BS, balloon size; Infl. Pr., Inflation pressur

To standardise balloon dilatation profiles only one brand of balloon at a standard length of 20mm was used. No balloon had been used for more than one dilatation in a prior clinical procedure. Balloons were positioned accurately across the lesion by firstly measuring the length of IVUS catheter from the transducer, sited at the MLA, to the point where it exits the Touhy-Borst adaptor. The balloon catheter was then advanced the same distance such that the centre of the balloon is sited at the MLA. Three sixty second inflations were performed using a standard inflation device. The success of angioplasty was defined by IVUS as a luminal area gain of at least 20% relative to the external elastic membrane area.

The proximal and distal ends of the treated lesions were marked by thin sutures using the distal reference needle to aid correct orientation of subsequent histological sections. All treated arteries were then pressure-fixed at 80mmHg in 10% buffered formalin for 12 hours and decalcified in a standard solution for five hours. The arterial specimens were sectioned at 0.5mm intervals and stained using elastic von Gieson and haematoxylin eosin techniques. Qualitative and quantitative analysis of the histological sections and corresponding IVUS images along the length of the lesion was performed by independent observers.

5.3 Data and statistics

From the recorded IVUS images before intervention a qualitative assessment of plaque composition was performed at the MLA of the lesion using a well-validated classification (Di Mario *et al,* 1998). Interobserver variability of IVUS with respect to the assessment of plaque composition has been previously described (Palmer *et al,* 1999). Plaque eccentricity was determined by the ratio of minimum and maximum plaque thickness. A value of <0.5 was considered eccentric. Measurements of lumen diameter and area, total vessel diameter and area and percent plaque stenosis at the MLA were compared before and after intervention. Distal and proximal reference segments were similarly analysed. Following intervention the presence, number and depth of dissections along the length of the lesion on the IVUS cross-sections was assessed. Dissection was defined as the presence of separation of part of the plaque from the

underlying arterial wall extending in a radial and longitudinal direction. The extent of dissection was defined by the depth of plaque separation (Figure 1) [Honye *et al,* 1992]. In the corresponding histological sections the presence, and extent of dissection was similarly assessed and compared to the IVUS analysis using the kappa statistic.

Continuous variables were described by their means and standard deviations. Categorical variables were described as percentages. Comparisons between the groups were compared with the student *t* test for quantitative variables and Fishers Exact test for categorical variables. A p value <0.05 was considered statistically significant.

5.4 Results

Arterial specimens were obtained from donors of the same mean age (72±7 vs 72±6 years, p=ns) and sex distribution (males 69% vs 67%, p=ns) in each group. Pre-interventional lesion characteristics were similar between the two groups (Table 2). Significantly more eccentric stenoses were present in group A (64.7 vs 52.9%, p=0.03).

5.4.1 *Post -intervention analysis*

Quantitative - procedural success was similar in each group (Group A, 88% [15/17] vs Group B, 94% [16/17], p=ns). The mean balloon size used was 3.2±0.37mm and 3.0±0.48mm for Groups A and B respectively. No significant difference in luminal gain was noted between the groups although there was a trend towards a larger increase in total vessel area in Group A (2.0±1.2mm^2 vs 1.4±0.80mm^2, p=0.063) [Figure 2].

Qualitative - from the histological sections dissections were seen in 15 of the 17 lesions (total 15, mean 0.88±0.47) in Group A and all of the lesions in Group B (total 22, mean 1.3±0.64). Overall, in the corresponding IVUS images dissections were correctly detected in 26 cases (kappa 0.70, 0.63-0.77). More severe dissections (type C/D) were detected in Group B (11 vs 5, p<0.003) [Figure 3]. Overall, IVUS correctly detected severe dissections in 8 cases (kappa 0.31[0.25-0.37]) [Figure 4].

5.4.2 *Influence of plaque characteristics on outcome*

Each of the four different plaque types was similarly represented in Groups A and B. Deep, focal calcification was more prevalent in Group A lesions (33% vs 20%, p=0.031). Table 3 summarises the luminal area gains achieved for each plaque type in Groups A and B. With the exception of calcified plaques it can be seen that there is a non-significant trend towards an improved luminal gain for all plaque types using a large balloon, low pressure strategy. Figure 6 illustrates the number of dissections for each plaque type in Groups A and B. Severe dissections were more prevalent for all plaque types using high balloon inflation pressures. Calcified lesions had a particular tendency to develop extensive vessel wall injury using this strategy. Extension of dissection into the adventitial layer was noted in one lesion in Group A (calcified) and four lesions in Group B (three calcified, one hard).

Plaque eccentricity - In Group A 80% (12/15) dissections occurred in eccentric lesions compared to 73% (16/22) in Group B. Severe dissections occurred in the same proportions in eccentric and concentric plaques (33%[4/12] vs 33%[1/3], Group A and 50% [8/16] vs 50% [3/6], Group B).

5.5 Discussion

5.5.1 *Influence of balloon calibre and inflation pressure*

The success of PTCA depends upon a balance between the luminal gain achieved and the extent of vessel wall injury sustained. It is clear that in addition to plastic deformation or stretching of the media and adventitial layers there requires to be a degree of splitting of the intimal plaque to achieve expansion of the lumen area (Hoshino *et al,* 1987; Virmani *et al,* 1994; Braden *et al,* 1994). This 'therapeutic' dissection releases the localised constriction produced by surrounding atherosclerotic plaque enabling luminal enlargement. However, the production of deep dissection extending to the arterial media and beyond appears to be counterproductive in that the larger dissection flap contributes acutely to luminal obstruction, spasm and thrombosis and also

to a more profound smooth muscle proliferative response resulting in significant lesion restenosis (Lincoff *et al,* 1992; Ip *et al,* 1990). The selection of balloon size and inflation pressure is critical to this process. Previous animal and clinical studies of these procedural variables have demonstrated that the combination of large balloons and high inflation pressures produces an adverse morphological and clinical outcome (Roubin *et al,* 1988; Sarembock *et al,* 1989). Semi-compliant balloons enable the operator to utilize higher pressures to produce a larger balloon calibre for optimal luminal gain. This is often necessary as angiography consistently results in balloon undersizing. It has been suggested by some authors that this strategy has contributed to the high restenosis rate associated with PTCA by increasing barotrauma to the arterial wall (Marantz *et al,* 1984; Shaw *et al,* 1986). In contrast, recent studies using IVUS to guide balloon sizing according to either reference segment dimensions or vessel size within the lesion have demonstrated the success of accurate balloon oversizing, using relatively low mean balloon inflation pressures, in optimising luminal gain with low incidences of acute clinical events and one year restenosis rates equivalent to the major stenting trials (Stone *et al,* 1997; Haase *et al,* 1998).

This in vitro histopathological study using IVUS to assess vessel dimensions compares two contrasting strategies of optimal balloon sizing, oversized balloons with nominal inflation pressures, a situation analogous to IVUS-guided PTCA, and undersized semi-compliant balloons, as would be the case using angiographic measurements, with high pressure inflations. Both strategies appear to produce a similar lumen gain but a greater incidence of deep dissection is evident when higher inflation pressures are employed. This is despite the fact that more lesions in Group A were eccentric and contained deep focal calcification. In accordance with previous studies we noticed that plaque tearing tended to originate from relatively inelastic areas of plaque adjacent to a normal vessel wall or from areas of deep focal calcification (Fitzgerald *et al,* 1992). It would appear that subjecting these areas to high pressures promotes greater radial and shear forces to produce more extensive plaque disruption. Larger balloon calibres and relatively low pressures tend to produce a more controlled dissection and rely more on vessel stretch to enlarge the lumen as supported by the greater change in vessel area observed in Group A.

5.5.2 *Influence of plaque characteristics*

Using IVUS the main atherosclerotic plaque types can be readily identified and there is close correlation with the histological appearance. Previous histologic studies have suggested that vessel wall injury is related to lesion characteristics particularly plaque composition (Marsico *et al,* 1995). The potential to use IVUS to predict plaque dissection and therefore provide a lesion-specific management strategy has been explored. Van der Lugt *et al* (1997) found no significant relationship between plaque composition, defined as soft (non-calcified) and hard (calcified) plaque, and the incidence and extent of dissection using histopathological validation. Others have suggested that calcified or fibrous (non-calcified) plaques dissect more readily compared to softer, lipid-rich, lesions which tend to respond by plaque compression (The *et al,* 1992; Potkin *et al,* 1992). To our knowledge the response of the main atherosclerotic plaque types to specific balloon calibre and inflation pressure strategies has not been formally studied.

This study was performed using both histologic and IVUS assessment of vessel wall injury. In accordance with previous studies we noted that IVUS consistently underestimates both the incidence and extent of dissection when compared to histological appearances. This was despite the fact that we assessed the whole lesion rather than just the target site. A non-significant trend towards a larger luminal area gain with larger balloons and nominal pressures was noted for most plaque types. In accordance with previous studies calcified plaque required higher inflation pressures with lumen enlargement facilitated mainly by dissection and increase in total vessel area (Gil *et al,* 1996). The incidence and extent of dissection was greater for all plaque types when high pressure inflations were employed to increase balloon calibre. Particularly severe dissections occurred with calcified plaque and tended to originate at the junction between calcification and an area of fibrous plaque. Although differences existed between each group with regard to the incidence of vessel wall injury using different balloon sizes and inflation pressures a significant relationship between individual plaque types and the incidence and extent of dissection was not demonstrated. The lack of such a relationship may be due to the relatively small number of lesions studied and the fact that the primary objective of the study was a qualitative comparison rather than strictly

quantitative. Finally, contradictory IVUS results exist regarding the relationship between plaque eccentricity and dissections. Some authors have demonstrated no significant differences between eccentric and concentric plaques whereas others demonstrated that plaque fractures predominantly occur in eccentric plaques (Tenaglia *et al,* 1992). In this study plaque eccentricity did not result in a greater incidence and severity of dissection.

5.6 Study limitations

The number of lesions investigated in this study was relatively small. We therefore can only make observations rather than draw firm conclusions from the data. As the study was performed in vitro we could not determine the impact of vessel recoil following PTCA on the final lumen gain. Furthermore, despite the use of a pulsatile flow system factors such as spatial movement of the coronary artery in relation to the beating heart could not be reproduced. We did not use angiography to confirm full balloon expansion. The final balloon diameter was assumed according to standard compliance charts. However, the fact that the luminal gains achieved are similar to those achieved in clinical PTCA trials suggest that adequate balloon expansion occurred in both groups. Underdetection of dissections by IVUS may have been due to the stenting effect of the ICUS catheter which was often positioned in an eccentric position against the vessel wall. The use of three-dimensional IVUS may improve the sensitivity of IVUS to detect dissections and enable clinical studies to be performed (von Birgelen *et al,* 1996). In the future a more precise classification of plaque composition using techniques such as radiofrequency signal processing may aid the identification of plaques prone to dissect (Spencer *et al,* 1997).

5.7 Conclusions

This study provides important histological evidence that optimal lumen gain and the production of a therapeutic dissection without deeper, medial, injury occurs more frequently using oversized balloons and relatively low inflation pressures. These observations provide a possible explanation for the success of the IVUS-guided PTCA trials. However, in this study of a relatively small number of lesions plaque composition or lesion eccentricity did not predict the incidence or extent of dissection.

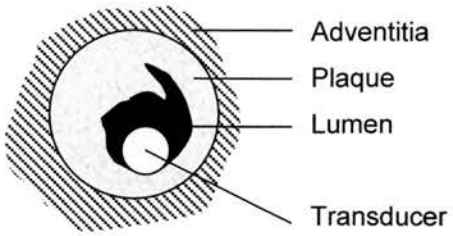

Type A
Linear, partial tear of atheroma. Doesn't extend to media.

Type B
Linear tear extending to the media but not behind plaque.

Type C
One or more tears with dissection behind the plaque subtending an arc of $<180^0$ around the circumference.

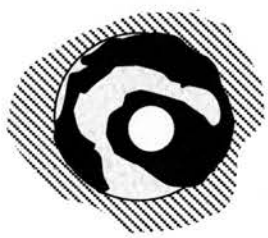

Type D
Extensive dissection. Subtends an arc of $>180^0$.

Figure 1. ***Classification of dissection type by IVUS***

Table 2. ***Donor and lesion characteristics***

	Group A (n=17)	Group B (n=17)	p
Age	72±7	72±6	
%males	69	67	
LAD (%)	53	60	
RCA (%)	41	27	0.05
LCX (%)	6	13	0.04
Lesion length (mm)	9.8±3.3	10.8±5.2	
Minimum lumen diameter (mm)	1.6±0.3	1.8±0.4	
Minimum lumen area (mm^2)	2.1±0.6	1.9±0.5	
Vessel (EEM) area (mm^2)	12.4±2.1	12.5±4.3	
Percent plaque stenosis (%)	80.7±4.6	79.5±4.1	
Eccentricity index <0.5 (%)	66	51	0.03
Plaque - soft [loose fibrous/lipid] (%)	35	29	
hard [dense fibrous] (%)	35	29	
calcified (%)	12	18	
mixed [heterogenous] (%)	18	24	
Focal calcification – superficial (%)	60	53	
deep (%)	33	20	0.03

LAD: Left anterior descending coronary artery, RCA: Right coronary artery, LCX: Left circumflex coronary artery, EEM: External elastic membrane.

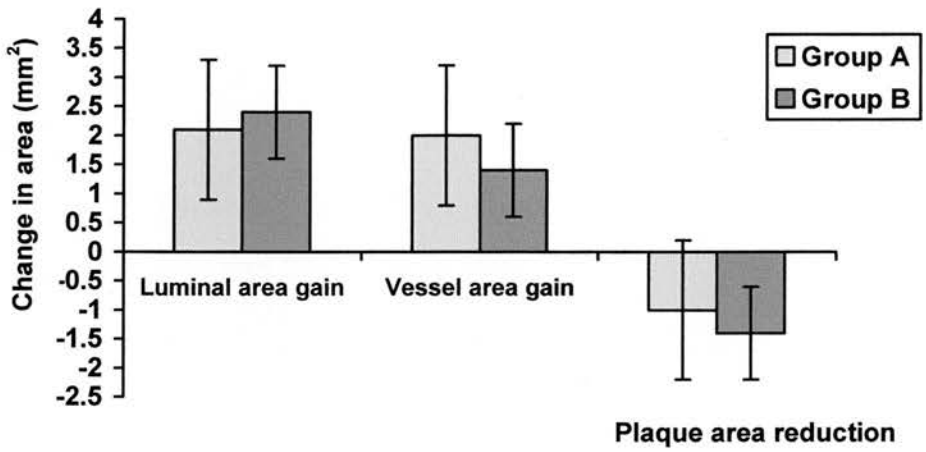

Figure 2. ***Luminal and vessel area gain and plaque area reduction after balloon dilatation, assessed by intravascular ultrasound, in Groups A and B (p=ns).***

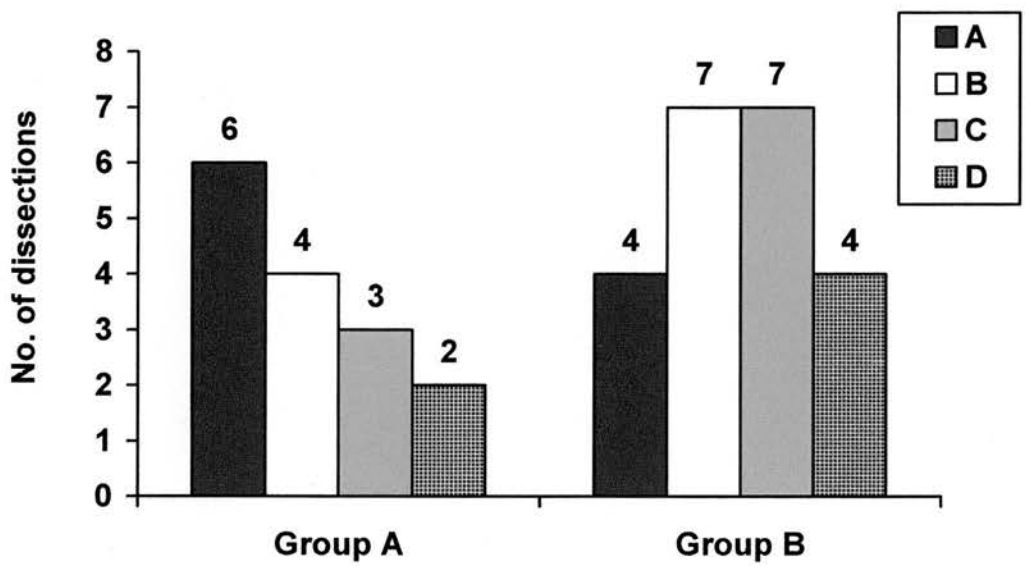

Total dissections (Group A vs Group B) – 15 vs 22, p<0.004

Figure 3. ***Number and type of dissections, assessed by histology, occurring after balloon dilatation in Groups A and B.***

a) Incidence

	Histology	IVUS	Agreement (%)	Kappa
Total dissections	**37**	**26**	**72**	**0.70(0.63-0.77)**
Type C/D dissections	**16**	**8**	**50**	**0.31(0.25-0.37)**

b) ***Severity***

		Histology			
		A	**B**	**C**	**D**
IVUS	**A**	**4**	**2**	**3**	**1**
	B	**1**	**3**	**3**	**1**
	C	**0**	**0**	**3**	**3**
	D	**0**	**0**	**1**	**1**

Figure 4. ***Correlation of IVUS and histology for incidence and severity of dissection following balloon dilatation***

Table 3. *Lumen area gain following balloon dilatation for different plaque types in Groups A and B. Values are means±SD.*

	Lumen area gain (mm^2)		p
	Group A	Group B	
Hard (dense fibrous)	1.6±0.9	1.5±1.0	0.08
Soft (loose fibrous)	1.9±1.3	1.7±1.2	0.10
Mixed (heterogenous)	2.9±1.6	2.7±1.8	0.06
Calcified	1.4±1.3	2.2±1.5	0.03

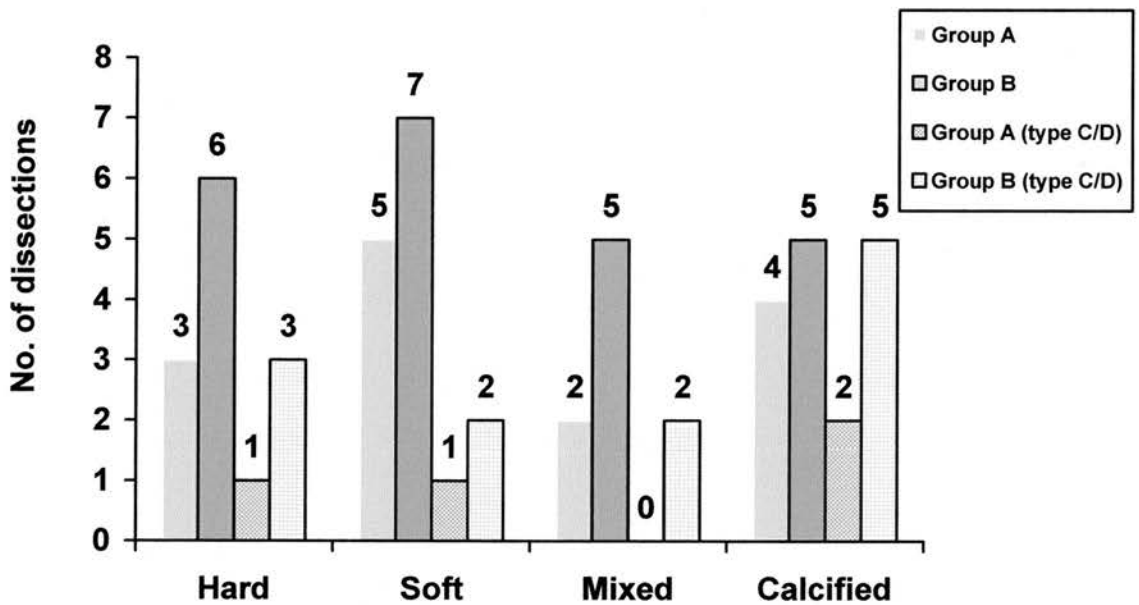

Figure 6. *Number of dissections following balloon dilatation according to plaque type. First two columns indicate total dissections, last two columns indicate severe (C/D) dissections.*

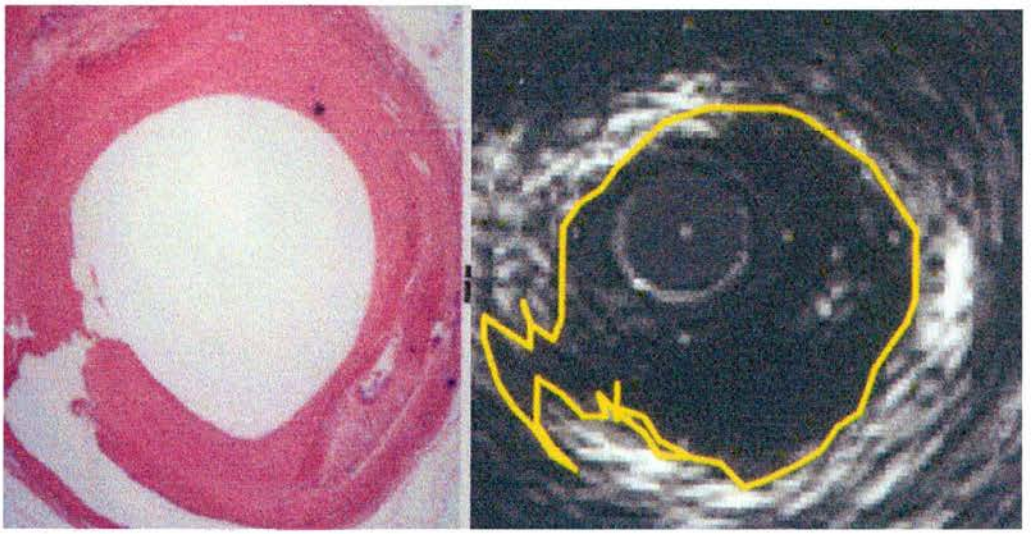

Figure 7. ***Histological analysis of arterial injury post-PTCA. Top - type A dissection (no extension to medial layer). Bottom – type C dissection (extension to medial layer but subtends arc <180^0). Corresponding IVUS image depicts point of dissection but underestimates extent of dissection plane behind plaque.***

Overview of subsequent chapters

In the final part of this thesis two studies are performed to validate three-dimensional ICUS reconstruction in the setting of coronary artery disease.

As described in Chapter 1, one limitation of the technique is the image distortion and non-uniform pullback speed produced by bends in the IVUS catheter. In *Chapter 6* a study is described which assesses the impact of naturally-occurring and induced IVUS catheter shaft angulations on the accuracy of volumetric reconstruction. This is carried out in a straight vessel phantom and a diseased tortuous coronary arterial segment, both of known dimensions.

In *Chapter 7* the potential for three-dimensional IVUS to improve accuracy in assessing vascular injury following PTCA is studied. Comparison to conventional two-dimensional IVUS imaging is made with respect to the measurement of the length, depth and classification of coronary dissections using histopathological assessment as the control.

CHAPTER 6

An analysis of the influence of catheter shaft angulation on the accuracy of volume measurement by three-dimensional intravascular ultrasound

6.1 Introduction

The accuracy of three-dimensional imaging in the measurement of lumen and vessel dimensions, using acoustic quantification or contour detection algorithms, has been confirmed in cylindrical phantom studies (von Birgelen *et al*, 1996) and also in comparisons between ultrasound and histological measurements in post-mortem peripheral and coronary arteries (Hausmann *et al*, 1994; von Birgelen *et al*, 1996). In all these studies a prerequisite for accurate assessment of dimensions is the generation of precise computerized reconstructions from good quality 2-D IVUS images. An important factor in the achievement of such images is recognizing and minimizing any distortion of the images acquired during the pullback sequence. Image distortion may be produced by a number of factors which are characteristic of IVUS systems. The most influential of these are the *rotation angle artefact* and the production of an oblique imaging plane due to *non-coaxial* and *eccentric* transducer positioning within the vessel. These and other contributory factors will be discussed in detail later. In the clinical setting the production of image distortion is more likely given the relative lack of control over the position of the transducer tip within the vessel lumen and the potential for a non-uniform pullback speed and increased transducer shaft friction due to natural angulations that occur as the catheter traverses the guide catheter within the aorta and tortuous proximal coronary artery segments. As a result the accuracy of vessel and lumen volume measurements suggested by the in vitro studies may not be truly applicable to routine clinical studies.

The following study assesses the impact of naturally occurring and induced catheter shaft angulation of different degrees and variable transducer tip position within the vessel lumen on the accuracy of volume measurement by 3-D IVUS imaging. A cylindrical vessel phantom of known lumen volume is assessed followed by a study of lumen, vessel and plaque volume in a post-mortem atherosclerotic coronary artery specimen.

6.2 Methods

In vitro phantom study. A cylindrical phantom with a pre-marked segment of known volume (589mm^3) was mounted within the water bath described in Chapter 2. The proximal section of the phantom was corrugated to enable bends to be made so as to simulate the varying angulation of the aorto-coronary ostial junction (Figure 1). The tip of a standard 8 French Judkins guide catheter was attached to the phantom. The catheter shaft was positioned on a flat surface, and using rounded objects of varying diameters, fashioned so as to reproduce the course traversed by the catheter in vivo from the femoral artery entry site, along the course of the aorta to the coronary ostium. A metal cylinder, internal diameter 12cm, was used to reproduce the curvature of the aortic arch. At the proximal end of the catheter a series of angulations (0^0, 45^0, 90^0) were made representing potential induced catheter positions prior to entry into the femoral artery. Three distal angulations (0^0, 45^0, 90^0) at the corrugated portion of the phantom were fashioned to simulate the course of the catheter in more tortuous proximal coronary arteries. A total of nine different conformations of proximal and distal angulations was therefore possible (Figure 3).

In vitro coronary artery study. A single human atherosclerotic right coronary artery was removed at post-mortem and studied within 24 hours to avoid any desiccation. A segment of the specimen measuring 25mm in length was mounted within the water bath using identical methodology to the earlier chapters. The proximal part of the segment was sutured loosely to the guide catheter tip. This enabled the artery to be angulated (0^0, 45^0, 90^0) with respect to the catheter tip as in the phantom study. The catheter shaft was positioned as described above with three proximal angulations (0^0, 45^0, 90^0) making nine possible conformations in total.

An IVUS transducer (3.2F, 30MHz) was placed at the distal end of the specimen and an initial pullback (0.5mm/sec) recorded to identify an atherosclerotic segment for analysis. A suitable segment measuring 16mm in length was identified which contained significant atherosclerotic plaque with little or no calcification. Because of marked acoustic shadowing a heavily calcified lesion would have prevented the identification of

the external elastic lamina making assessment of vessel and plaque volume impossible. Proximal and distal marker needles, visible by IVUS imaging, were sited transversely in the adventitial layer to demarcate the segment.

After the acquisition of IVUS pullback sequences in each different conformation the coronary artery specimen was fixed in 10% buffered formalin for 12 hours. The marker needles were pulled through and proximal and distal silk sutures used to demarcate the segment of interest. Using standard procedures the segment was sectioned at precise 0.2mm intervals along its length. All sections were mounted on slides for histomorphometric analysis. For each cross-section lumen and external lamina borders were clearly identified enabling computer-assisted planimetry to measure *lumen area*, *total vessel area* [area bounded by external elastic lamina] and *plaque area* [area bounded by external elastic lamina and lumen border]. Vessel, lumen and plaque volumes for the segment of interest were then calculated as:

$$\mathbf{V} = \sum_{i=1}^{n} A_i . H$$

where V = volume; A = area of lumen, vessel or plaque in a certain cross-section; H = thickness of the section (0.2mm); and n = number of histological cross-sections within the region of interest. Three calculations each were made for lumen volume, plaque volume and total vessel volume. The mean value was taken for comparison to volume measurements made by 3-D IVUS for each conformation of catheter angulation.

6.2.1 *Imaging methodology*

In both studies a high torque 0.014" guidewire was passed along the guide catheter shaft and negotiated through the phantom or coronary artery segment. This was to enable smooth IVUS catheter tracking during the pullback imaging sequence.

Two fresh 3.2F, 30MHz (Cardiovascular Imaging Systems, Insight) IVUS catheters were used for all studies. For each conformation of proximal and distal angulation three recorded pullbacks (0.5mm/sec) of the IVUS catheter across the pre-marked segment of interest in the phantom and coronary artery specimen were performed. In all cases a pullback duration of at least 5 seconds was allowed prior to imaging of the segment of interest to ensure a uniform pullback speed was attained and any slack in the IVUS catheter shaft eliminated. Optimal image quality was ensured by careful adjustment of gain settings and flushing of the IVUS catheter between each pullback.

6.2.2 *Three-dimensional image reconstruction and volume measurement*

A commercially available dynamic image acquisition system with automated contour detection was used (Echoscan, TomTec). The methodology for this system is described in chapter 1. The acquired raw data from each recorded sequence was digitized from a maximum of 200 recorded IVUS images at 0.2mm intervals. From the acquired data the segment of interest was identified by the recorded needle marker positions. Post-processing of the reconstruction discarded unwanted data from proximal and distal to the segment of interest. Appropriate perpendicular, longitudinal cut planes were selected and external elastic lamina and endoluminal borders detected and displayed using the computer algorithm. Automated contour detection, with some manual correction, on serial cross-sectional images was performed using the four contour points derived from the longitudinal contours. From the processed images, phantom lumen and coronary vessel, lumen and plaque volumetric data was derived and displayed by the system.

Volume measurement for the phantom and coronary artery segment was made three times for each parameter and the mean value calculated for further analysis. Therefore a total of 54 reconstructions were performed and analysed. All measurements were recorded and entered onto a computer spreadsheet for later comparison to histomorphometric data. Additionally, IVUS catheter tip position within the vessel lumen was noted from each recorded IVUS pullback sequence and was defined as

concentric, lying centrally within the lumen, or *eccentric*, lying peripherally in the lumen, often against the vessel wall. All data acquisition and analysis was performed by one observer experienced in 3-D IVUS imaging techniques. Intra- and interobserver variability in the measurement of volume by IVUS has previously been shown to be low (von Birgelen *et al*, 1996).

6.2.3 *Data analysis and statistics*

The impact of the position, degree and number of catheter shaft angulations on volumetric analysis by 3-D IVUS was firstly assessed by comparison of the mean phantom lumen volume for each conformation to the true phantom volume which was of uniform cross-sectional area throughout. Secondly, a comparison with histomorphometric measurement was made for IVUS-derived vessel, plaque and lumen volume measurements of the coronary artery segment which, due to the presence of atherosclerotic plaque, had more complex vessel and lumen morphology. In a separate analysis a comparison of the influence of transducer position within the lumen was made by comparing measurements made in similar catheter shaft conformations from concentric and eccentrically positioned transducer tips.

Statistical analysis – Comparisons between phantom and coronary artery volumes and true values were assessed by determining the mean±SD of the between-method differences (Bland and Altman, 1986). Variability in volume measurements of ±10% was considered clinically significant.

6.3 Results

6.3.1 *Phantom study*

In general phantom volume measurements were overestimated by 3-D IVUS (Table 1). Although image distortion was not quantitatively assessed it was noted that elliptical IVUS cross-sectional images occurred frequently during the pullback sequences

particularly with more severe and complex catheter angulations. Although variability was low there was a tendency for greater inaccuracy of volume measurement by IVUS when an increased severity and number of angulations was present. Minimal angulation (confirmation 1) of the IVUS catheter shaft was most accurate at reproducing the true lumen volume with low variability (3.2±0.0%). Distal angulations (conformations 2 & 3) demonstrated similarly low variability (5.2±0.8%). However proximal angulations (conformations 4 & 5) and multiple severe angulations (conformation 9) produced the greatest, although still clinically acceptable, variability (9.0±0.9% & 10.0±0.0% respectively).

6.3.2 *Coronary artery study*

The length of the coronary artery segment of interest was 16mm. At the most stenotic point of the lesion the mean lumen diameter was 1.1mm with a maximum percent plaque stenosis of 77%. Mean reference diameter [proximal reference + distal reference / 2] was 3.1mm. The atherosclerotic plaque comprised mainly dense fibrous tissue with two areas of superficial focal calcification which did not affect the detection and measurement of lumen and external elastic lamina borders. Histomorphometric assessment of 80 cross-sections revealed mean volumes of **95.6mm^3** [total vessel], **45.2mm^3** [plaque] and **50.1mm^3** [lumen].

As in the phantom study 3-D IVUS assessment consistently overestimated volume measurements (Tables 2a-c). Minimal catheter angulation (conformation 1) produced clinically acceptable variability (<10%) for vessel (-7.9%), lumen (-6.0%) and plaque volume (-8.5%) respectively. Distal angulations (conformations 2&3) produced variability of just over 10%. However proximal angulations produced significantly greater overestimation of vessel, lumen and plaque dimensions. Once again, variability was greatest when multiple severe angulations (conformation 9) were applied (-19.0%, -17.7% and -21.3% respectively).

6.3.3 Influence of transducer tip position

A predominantly concentric IVUS transducer tip position within the lumen was uncommon. Of the 54 pullback sequences recorded the transducer was mainly eccentrically positioned in 75.9% (41/54) of cases. A concentric position occurred more often in the phantom study (33.3% [9/27]) compared to the coronary artery study (14.8% [4/27]). Surprisingly, there was no relationship between the number and severity of catheter shaft angulations and eccentric catheter position.

To compare variability between different transducer tip positions, comparison of pullback sequences in the coronary artery study was made. Volumetric measurements from four pullbacks with predominantly eccentric catheter tip positioning were compared to corresponding pullbacks of the same conformations of catheter shaft angulation with predominantly concentric positioning (Tables 3a-c). In general eccentric catheter tip positioning produces significantly greater variability in vessel (mean 16.8±2.6% vs 14.2±3.1%, $p<0.01$), lumen (mean 16.5±2.9% vs 11.8±3.2%, $p<0.01$) and plaque volume (18.1±2.8% vs 15.3±3.5%, $p<0.01$) measurement compared to a concentric position.

7.4 Discussion

In clinical IVUS studies optimal image quality is important for accurate measurement of vessel dimensions. In mechanical IVUS systems image quality is frequently compromised by geometric distortion of images due to a number of factors. There are few studies which have assessed the impact of these factors on the accuracy of lumen and vessel quantitation with conventional 2-D IVUS imaging. No formal studies have yet been performed to assess their effect on volume measurement by computerized 3-D reconstruction of IVUS images. In this setting one might expect greater inaccuracy due to the cumulative effect of consecutive distorted cross-sectional IVUS images. This in vitro study assessed the impact of commonly encountered causes of IVUS image distortion on volume measurement by IVUS using a phantom of known volume and a segment of diseased human post-mortem coronary artery.

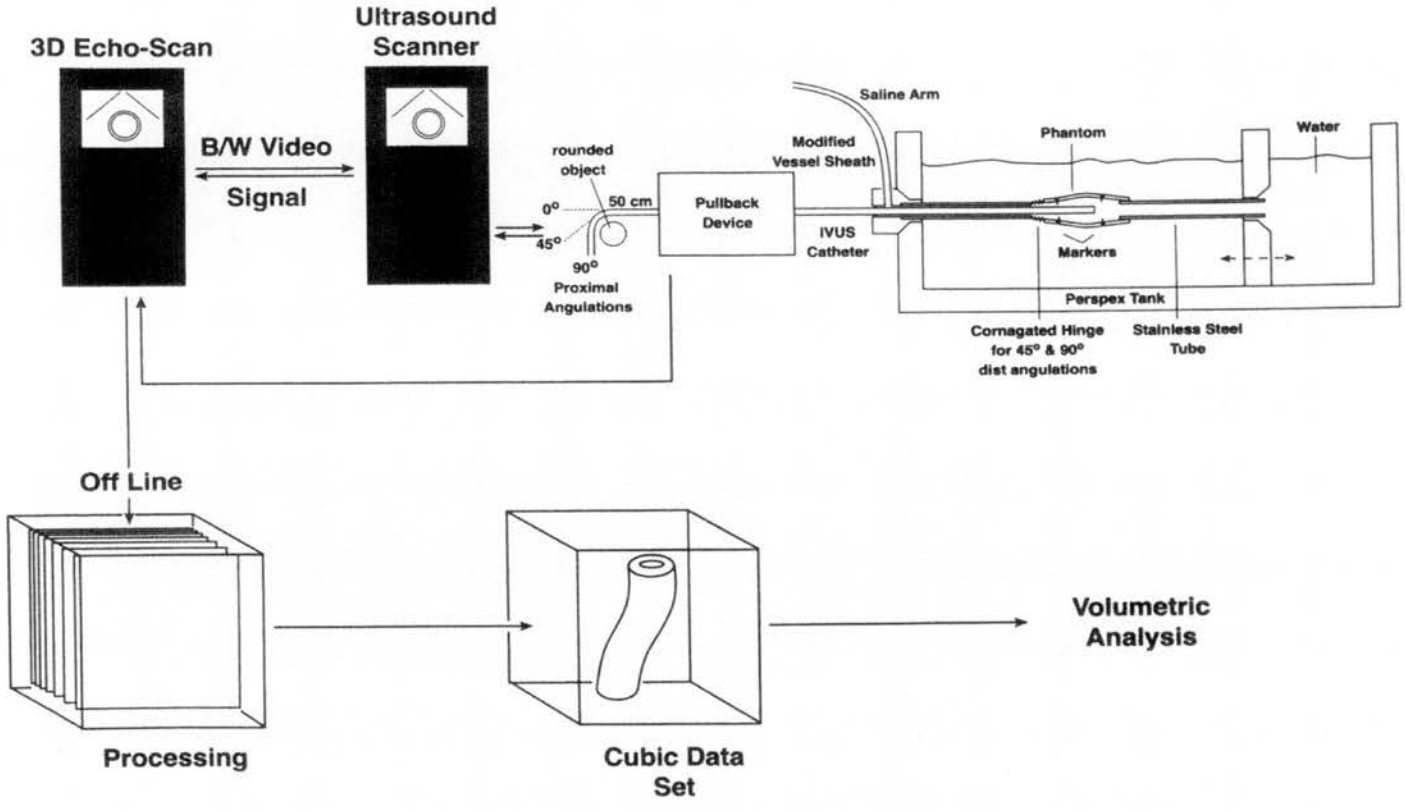

Figure 2. ***Schematic diagram of volumetric reconstruction***

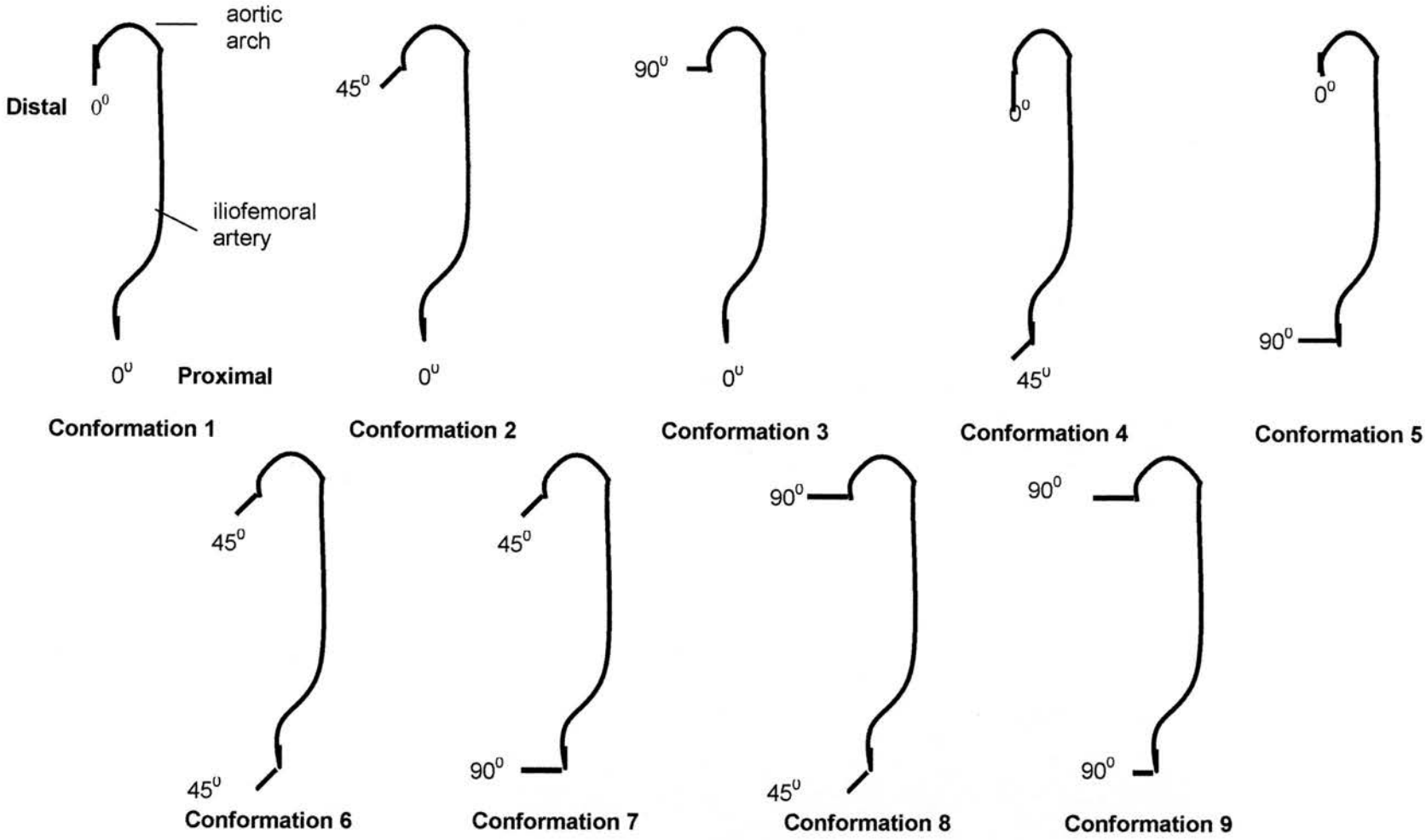

Figure 3. ***Catheter angulation conformations***

	Mean IVUS volume (mm^3)	Δ (ICUS – True)	Variability (%) (Δ / ([ICUS+True] / 2))
Control	**608.2±22.1**	**-19.2±0.0**	**-3.2±0.0**
Distal	**620.2±27.8**	**-31.2±4.8**	**-5.2±0.8**
Proximal	**644.6±34.2**	**-55.6±5.8**	**-9.0±0.9**
Multiple	**651.1±35.6**	**-62.1±0.0**	**-10.0±0.0**

All values are mean values ± SD
IVUS = intravascular ultrasound; Δ = between-method difference
Control = conformation 1; Distal = conformations 2&3, Proximal = conform. 4&5;
Multiple = conformation 9.

Table 1. ***Mean volumes and between-method differences for 3-D IVUS versus true phantom volume (589mm^3)***

	Mean vessel volume (mm^3)	Δ (IVUS-histo)	Variability (%) (Δ / ([IVUS + histo] / 2))
Control	**103.4±13.4**	**-7.8±0.0**	**-7.9±0.0**
Distal	**106.7±14.6**	**-11.1±1.3**	**-11.0±1.3**
Proximal	**108.8±14.2**	**-13.2±2.1**	**-12.9±2.1**
Multiple	**115.7±16.5**	**-20.1±0.0**	**-19.0±0.0**

All values are mean ± SD
IVUS=intravascular ultrasound; Δ=between-method difference;
histo= histomorphometry
Control = conformation 1; Distal = conformations 2&3;
Proximal = conformations 4&5; Multiple = conformation 9.

Table 2a. ***Mean vessel volume and between-method differences for 3-D IVUS versus histomorphometry (mean 95.6mm^3)***

	Mean lumen volume (mm^3)	Δ (IVUS-histo)	Variability (%) (Δ / ([IVUS + histo] / 2))
Control	**53.2±8.3**	**-3.1±0.0**	**-6.0±0.0**
Distal	**56.0±9.2**	**-5.9±1.0**	**-11.1±1.9**
Proximal	**56.7±8.6**	**-6.6±0.9**	**-12.4±1.7**
Multiple	**59.8±9.3**	**-9.7±0.0**	**-17.7±0.0**

All values are mean ± SD
IVUS=intravascular ultrasound; Δ=between-method difference;
histo = histomorphometry
Control = conformation 1; Distal = conformations 2&3;
Proximal = conformations 4&5; Multiple = conformation 9.

Table 2b. ***Mean lumen volume and between-method differences for 3-D IVUS versus histomorphometry***

	Mean plaque volume (mm^3)	Δ (IVUS-histo)	Variability (%) (Δ / ([IVUS + histo] / 2))
Control	**49.2±6.8**	**-4.0±0.0**	**-8.5±0.0**
Distal	**50.6±7.5**	**-5.4±1.9**	**-11.3±3.4**
Proximal	**52.4±7.6**	**-7.2±1.2**	**-14.8±2.5**
Multiple	**56.0±8.4**	**-10.8±2.1**	**-21.3±4.2**

All values are mean ± SD
IVUS=intravascular ultrasound; Δ=between-method difference;
histo = histomorphometry
Control = conformation 1; Distal = conformations 2&3;
Proximal = conformations 4&5; Multiple = conformation 9.

Table 2c. ***Mean plaque volume and between-method differences for 3-D IVUS versus histomorphometry***

	Concentric			Eccentric		
	Vessel vol. (mm^3)	Δ	Var. (%)	Vessel vol. (mm^3)	Δ	Var. (%)
Conf. 1	103.4	-7.8	-7.8	109.4	-13.8	-13.5
Conf. 4	107.7	-12.1	-11.9	109.0	-13.4	-13.1
Conf. 7	114.7	-19.1	-18.2	116.2	-20.6	-19.5
Conf. 9	115.1	-19.5	-18.5	117.8	-22.2	-20.8
Mean	110.2	-14.6±3.2	-14.2±3.1	113.1	-17.5±2.8	-16.8±2.8*

*p<0.01 vs concentric
Δ = between-method difference; var. = variability; conf. = conformation

Table 3a. ***Mean vessel volumes and between-method difference for concentric versus eccentric transducer tip position***

	Concentric			Eccentric		
	Plaque vol. (mm^3)	Δ	Var. (%)	Plaque vol. (mm^3)	Δ	Var. (%)
Conf. 1	49.6	-4.4	-9.3	52.0	-6.8	-14.0
Conf. 4	52.2	-7.0	-14.4	53.3	-8.1	-16.4
Conf. 7	53.2	-8.0	-16.3	54.9	-9.7	-19.4
Conf. 9	55.6	-10.4	-20.6	56.5	-11.3	-22.2
Mean	52.7	-7.5±1.7	-15.3±3.5	54.2	-9.0±1.4	-18.1±2.8

*p<0.01 versus concentric
Δ=between-method difference; var.=variability; conf.=conformation

Table 3b. ***Mean plaque volumes and between-method differences for eccentric versus concentric transducer tip position***

	Concentric			Eccentric		
	Lumen vol. (mm^3)	Δ	Var. (%)	Lumen vol. (mm^3)	Δ	Var. (%)
Conf. 1	**54.1**	**-4.0**	**-7.7**	**56.3**	**-6.2**	**-11.7**
Conf. 4	**55.6**	**-5.5**	**-10.4**	**56.7**	**-6.6**	**-12.3**
Conf. 7	**57.6**	**-7.5**	**-13.9**	**61.5**	**-11.4**	**-20.4**
Conf. 9	**58.2**	**-8.1**	**-15.0**	**61.8**	**-11.7**	**-20.9**
Mean	**56.4**	**-6.3±1.7**	**-11.8±3.2**	**59.1**	**-9.0±1.6**	**-16.5±2.9***

*p<0.01 versus concentric
Δ=between-method difference; var.=variability; conf.=conformation

Table 3c. ***Mean lumen volumes and between-method differences for eccentric versus concentric transducer tip position***

6.4.1 *Impact of catheter conformation*

For all measurements it was noted that lumen, plaque and vessel volumes tended to be overestimated by 3-D IVUS rather than underestimated. This is probably explained by the frequent production of elliptical image cross-sections due to eccentric and non-coaxial catheter tip positioning. In the phantom study we observed a trend towards greater variability of lumen volume measurement when multiple catheter bends were introduced. Additionally it was noted that variability was greater for proximal angulations compared to those made at the catheter tip. However, the differences were relatively small in relation to the phantom volume and this is reflected by the lack of clinically significant variability for all measurements in this part of the study. The most obvious explanation for the relatively low variability is that the phantom was straight and uniformly cylindrical. Therefore, image distortion was less commonly encountered because the catheter tip position was more frequently concentric and the luminal border was consistently well-defined. Furthermore, the phantom was of relatively high volume compared to diseased segments of coronary artery. As a result the overestimation of lumen volume by IVUS had less impact on the final lumen volume. Imaging and volumetric reconstruction of diseased coronary arteries by IVUS presents additional difficulties. As well as the problem of guide catheter tip angulations as the coronary ostium is entered, the transducer shaft undergoes further distortion as it traverses tortuous proximal coronary artery segments. This commonly results in eccentric transducer tip positioning and non-coaxial alignment of the imaging plane particularly as the transducer is withdrawn across a curved segment. Furthermore, despite attempts to straighten the transducer shaft prior to imaging of the segment of interest a non-uniform pullback speed may occur intermittently due to slack introduced into the transducer shaft as it is withdrawn.

In the coronary artery study significantly greater variability was noted for lumen, plaque and vessel volumes when multiple catheter shaft angulations were present. These values reached clinical significance. However, as with the phantom study it was noted that proximal angulations had a greater, and more clinically significant impact, than those at the catheter tip. This was particularly the case for measurement of plaque volume.

6.4.2 *Impact of transducer tip position*

Although not quantitatively assessed it was noted that image distortion, particularly of the vessel wall, was more frequently encountered when the transducer tip was eccentrically positioned. As a result significantly greater variability was noted for measurement of lumen, plaque and volume measurement compared to a concentric transducer tip position. It was noted that transducer tip position had a greater impact on the variability of volume measurement in the control conformation and distal angulations. Where multiple, or just proximal angulations, were present it was clear that significant image distortion was present even when the transducer tip was concentrically positioned confirming that other factors had a role.

6.4.3 *Explanation of findings*

The presence if imaging artifacts and geometric distortion of IVUS images using mechanical systems has long been recognized yet seldom studied in a formal manner. The frequency and impact of these factors during clinical, conventional IVUS studies in diseased coronary arteries is largely unknown. The most informative study was that of Kearney *et al* (1995) which provided a comprehensive overview of the impact of catheter shaft angulation and eccentric geometric image distortion on lumen diameter and area measurements in a custom-built phantom. Greater image distortion was noted for a greater number and degree of catheter shaft angulations although the differences in quantitation were relatively small. Important differences were noted between eccentrically and concentrically placed transducer tips. Over 70% of images acquired with eccentrically located catheters were subject to geometric distortion resulting in significantly greater quantitative inaccuracy. The results from our study tend to support this data although the differences noted were larger due to the cumulative error of assessing multiple IVUS cross-sectional images.

The most important technical factors involved in IVUS image distortion deserve further explanation. The Rotation Angle Artefact (RAA) is unique to mechanical IVUS systems and most likely results from non-uniform rotation of the transducer shaft due to

intermittent friction between the rotating drive shaft and the outer sheath or external constriction usually due to excessive tightening of the Touey-Borst adaptor. This results in intermittent slowing of transducer rotation with binding of the catheter shaft which disrupts the acquisition of ultrasound data from a segment of the arterial cross-section (Chae *et al* 1992). Data from the last scan line emitted during normal rotation speed fills the remaining sector of the image resulting in inaccurate representation of the arterial cross-section. Where there is persistent slowing and acceration of transducer rotation there is variation in the number of scan lines emitted from adjacent segments of the cross-section. Production of 2-D IVUS images assumes a uniform rotation speed such that scan lines are distributed evenly throughout the cross-section regardless of the source of each scan line. The resultant image is therefore not truly representative of the arterial cross-section. This effect is much more marked when the transducer tip is situated eccentrically in the lumen particularly in irregular arterial segments which contain eccentric atherosclerotic plaque (Chae *et al*, 1992). Non-uniform rotation can result from friction due to excessive catheter shaft angulation or less frequently as the transducer is advanced across a severe stenosis or along a particularly tortuous arterial segment.

Accurate reproduction of arterial cross-sections by IVUS imaging requires positioning of the transducer such that the imaging plane lies at right angles to the rotating imaging core (Peters *et al*, 1994). Angulation of the transducer tip reduces the insonation angle such that the returning sound wave amplitude is diminished. This situation frequently occurs in clinical practice due to eccentric catheter positioning and tortuous vessels resulting in suboptimal luminal border definition which can influence the accuracy of vessel and lumen quantitation. Furthermore, angulations of the transducer relative to the long axis of the vessel (non-coaxial alignment) results in the production of an elliptical shaped cross-section as the arterial section is imaged obliquely. Not only does this tend to overestimate vessel dimensions there is significant degradation of image quality of the contralateral arterial wall due to a significant fall in lateral resolution (McKay *et al*, 1989). All the above factors operate in routine IVUS studies and clearly influence the accuracy of volume measurement. Additional characteristics unique to volumetric reconstruction by IVUS include non-uniformity of transducer pullback speed due to

tortuous vessels. In practice this has the least influence on the accuracy of measurements since previous clinical studies have demonstrated accurate length measurements in coronary arteries using mechanical pullback (Fuessel *et al,* 1996). Furthermore, in the present study low variability in lesion length was noted and there was only marginal overestimation when multiple catheter angulations were introduced.

6.4.4 *Clinical implications*

Three-dimensional reconstruction of IVUS images is increasingly being employed in longitudinal clinical studies assessing mechanical or pharmacological therapies aimed at regression of coronary atherosclerosis (Schortl *et al,* 2001; Palmer *et al,* 1998). Such data requires to be extremely accurate considering the relatively small volume changes that may result. Knowledge of the potential sources of inaccuracy due to geometric distortion of IVUS images is essential. Where excessive image distortion is evident during a pullback acquisition sequence care must be taken in interpreting the data. The influence of factors such as catheter shaft angulation can be minimized by the maintenance of a straight extraarterial catheter course and appropriate selection of proximal coronary artery segments to be studied. The problem of eccentric and non-coaxial transducer tip positioning is more difficult to address. Future developments may see the introduction of transducer tip micromotors enabling manual or automated correction of transducer position as it is withdrawn along the arterial segment.

6.5 Conclusions

The production of accurate vessel, plaque and lumen volume measurement by computerised three-dimensional IVUS reconstruction in clinical studies is influenced by the quality of the conventional images produced. Technical factors such as catheter shaft angulation and transducer tip position significantly influence the degree of image distortion. Recognition of these factors is important particularly in longitudinal studies of atheroma regression.

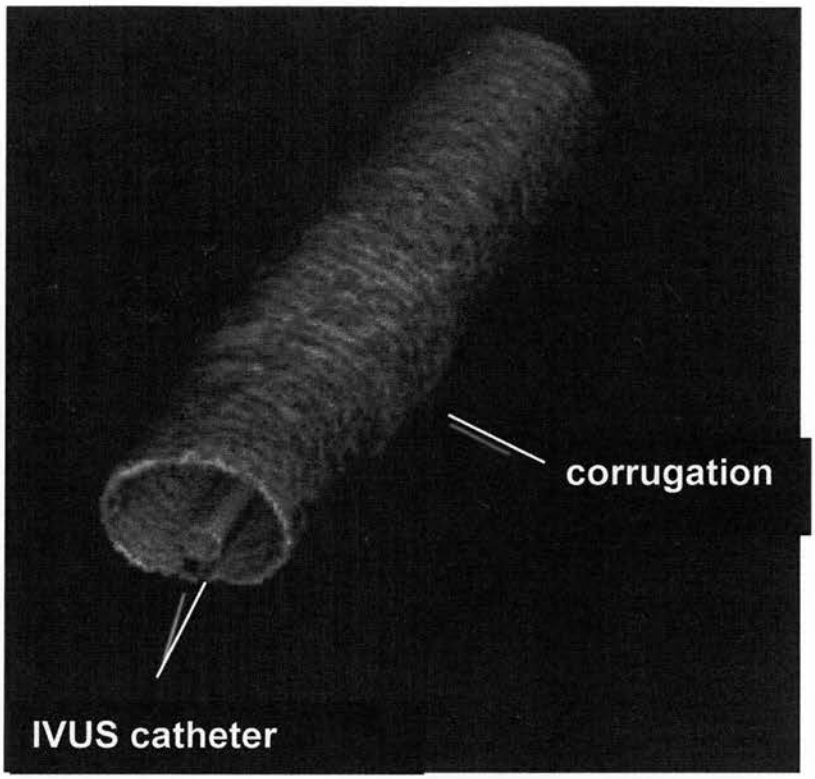

Figure 3. ***Illustration of 3-D reconstructed phantom. The IVUS catheter shaft and corrugation, used to form distal angulations, are clearly visualised***

CHAPTER 7

Evaluation of arterial wall dissections in coronary angioplasty: a comparison of two-and three-dimensional intravascular ultrasound imaging

7.1 Introduction

Prior to the introduction of IVUS there were few substantial clinical studies of the extent of balloon-induced vascular damage following PTCA due to the difficulty in visualizing and quantifying tears and dissections. Data initially originated from post-mortem studies performed in patients who had died following PTCA (Soward *et al,* 1985; Farb *et al,* 1990). These findings were subject to considerable bias since the frequent findings of vessel occlusion, extensive dissection and thrombosis clearly represented the most severe end of the spectrum of morphological changes occurring during balloon-dilatation. Furthermore, the atherosclerotic plaques tended to be "younger" comprising lipid-rich, soft plaque which responds to balloon dilatation very differently to typical coronary stenoses encountered in everyday clinical practice.

Assessment of coronary dissections by coronary angiography relies upon extravasation of contrast into the area of plaque and medial disruption which does not always occur. Dissections are often poorly visualized despite the use of multiple orthogonal view planes (Arnett *et al,* 1979). Depth and longitudinal extent of damage is frequently underestimated largely due to spiral dissections which track out of the plane of view. The severity of a dissection is often inferred from the luminal encroachment seen adjacent to the dissection plane or the presence of thrombus or persistent spasm (Keane *et al,* 1995). With IVUS the arterial wall can be visualized in considerable detail using modern, high resolution transducers. Changes in luminal and vessel dimensions as a result of PTCA can be made with serial studies (Yock *et al,* 1991; Braden *et al,* 1994). Following PTCA intimal disruption and extension into the plaque and medial layers can be clearly seen as a break in the endoluminal border with evidence of blood-speckling, often enhanced with a contrast injection, into the false lumen beyond. A mobile dissection flap is also frequently seen. The radial extent of dissection can be clearly visualized and measured. As a result IVUS has provided further insights into the arterial response to balloon inflation in PTCA. However, as demonstrated in Chapter 5, arterial damage occurs along the entire length of the treated segment and analysis of the tomographic slice at the point of maximal stenosis alone will underestimate the true extent of dissections (van der Lugt *et al,* 1995). Furthermore, the most severe arterial damage often occurs proximal or distal to this point. The use of a controlled pullback of

the IVUS transducer between predetermined sites distal and proximal to the stenosis enables serial tomographic slices to be studied. Such analysis requires to some degree a mental reconstruction of the recorded tomographic slices. Although the linear extent of arterial damage can be assessed there remains the problem of underestimating dissection length and depth due to factors such as superficial focal calcification obscuring a dissection plane for several slices, and abrupt changes in dissection depth between adjacent image slices. The development of computer algorithms that enable three-dimensional reconstruction of serial tomographic IVUS images allows visualization of an entire arterial segment (Roelandt *et al,* 1994; von Birgelen *et al,* 1995). The purpose of this study was to compare the accuracy of two-dimensional IVUS imaging and combined information from two- and three-dimensional IVUS imaging in determining the linear extent, continuity and depth of arterial dissections induced by coronary balloon angioplasty.

7.2 Methods

Atherosclerotic human coronary arteries (n=24) were studied. These comprised the video-recorded IVUS images of the 17 specimens that constituted Group B (high inflation pressure) in Chapter 5 and an additional 7 specimens harvested specifically for this study. These arterial specimens were prepared and studied using identical methodology to that described in Chapter 5. Following pre-interventional IVUS imaging the stenoses were subjected to dilation with balloons sized on the basis of the mean vessel diameter ([maximum + minimum vessel diameter / 2] x 0.8) at the minimum lumen area. All arterial segments were subjected to a minimum of one inflation at a pressure of 18 atmospheres to encourage the production of arterial dissection for further study. A final controlled IVUS pullback (0.5mm/sec) was recorded. All treated arteries were then pressure-fixed at 80mmHg in 10% buffered formalin for 12 hours and decalcified in a standard solution for five hours. The arterial specimens were sectioned at 0.2mm intervals and stained. Qualitative and quantitative analysis of the histological sections was performed by an independent observer.

7.2.1 *Three-dimensional IVUS image reconstruction*

A commercially available dynamic image acquisition system with automated contour detection was used (Echoscan, TomTec). The methodology for image acquisition and reconstruction is fully described in Chapter 1. In brief, IVUS pullbacks were performed using 2.9F catheters. Pullbacks were performed from pre-defined points proximal and distal to the lesion, marked by curved needles inserted into the adventitial layer. Care was taken to start the pullback at least 5 seconds before the segment to be studied to allow for straightening of the imaging core inside the catheter in order that a constant pullback speed was attained. A frame grabber digitized the predefined region of interest from a maximum of 200 recorded IVUS images at 0.2mm intervals. Appropriate perpendicular, longitudinal cut planes were selected and external elastic lamina and endoluminal borders detected and displayed using a computer algorithm. Automated contour detection, with some manual correction, on serial cross-sectional images was performed using the four contour points derived from the longitudinal contours. Vessel and lumen volumetric data was derived from the processed images.

7.2.2 *IVUS image analysis*

2-D IVUS imaging – from conventional video recordings of the IVUS pullback along the length of each treated lesion the plaque and medial layers were inspected for the presence of dissection. Dissection was defined as the presence of separation of part of the plaque from the underlying arterial wall extending in a radial and longitudinal direction. The extent of dissection was defined by the *depth* of plaque separation and classified as previously described (Figure 1) [Honye *et al,* 1992]. By scrolling along the recording of serial tomographic slices proximal and distal extents of dissections were estimated and changes in dissection depth and continuity identified. With knowledge of the pullback speed (0.5mm/sec) and using the time elapsed from distal and proximal ends of the dissection the dissection *length* was calculated. This analysis was performed three times for each identified dissection and the mean dissection length calculated for comparison to three-dimensional imaging and histopathological assessment.

3-D IVUS imaging - following three-dimensional reconstruction the longitudinal representations of the arterial segment were examined in several different planes to identify arterial dissections. Slight changes in the cut plane were necessary to trace spiral dissections and determine any abrupt changes in depth that occurred. Additional information on dissection depth was derived from serial IVUS cross-sectional images displayed simultaneously with the longitudinal view. Using this combined data the length of dissection was measured by the number of frames from the distal to proximal end and depth measured by dedicated quantitation software. In addition the type of dissection was determined by a classification derived from 2-D IVUS data (Figure 1). All quantitative assessments were carried out three times and mean values calculated.

All IVUS analysis was carried out by a single observer experienced in the interpretation of post-intervention IVUS images. This was so as to avoid any interobserver variability in image interpretation.

7.2.3 *Histopathological analysis*

An independent observer examined serial histological cross-sections along the length of each lesion. The number of dissections and type according to the above classification were recorded. Dissection length was determined by counting the number of slices, sectioned at 0.2mm intervals, which clearly contained evidence of plaque separation which was, by its situation on the cross-section, clearly contiguous with the preceding dissection plane. Maximum dissection depth was measured by histomorphometry.

7.2.4 *Statistical analysis*

The kappa statistic was used to compare the magnitude of agreement between histopathologic interpretation of dissection type and (1) 2D IVUS assessment and (2) combined 2D and 3D IVUS assessment (Cohen *et al,* 1960). A kappa of 0 indicates only chance agreement between methods, a value of 1 indicates perfect agreement. In general, values >0.75 indicate excellent agreement, values of 0.4-0.75 indicate good agreement and a value of <0.4 indicates only marginal agreement. Linear regression analysis was

performed to assess the correlation between each imaging method and histomorphometry with respect to dissection depth and length. Mean values were compared by students t test and expressed as mean±SD. A p value of <0.05 was considered statistically significant.

7.3 Results

Conventional IVUS imaging was possible in all of the seven additional coronary arterial specimens used specifically for this study. Overall, recorded pullbacks of treated lesions were available for all 24 arterial segments which originated from the left anterior descending coronary artery (n=15), right coronary artery (n=6) and left circumflex coronary artery (n=3). Prior to balloon dilatation the presence of moderate to severe stenoses at the most stenotic point of the lesion was confirmed in all segments (mean percent plaque area 82.3±7.3%).

7.3.1 *Dissection type*

From the histopathological analysis 20 of the 24 arterial segments were confirmed to have areas of dissection of varying severity. A total of 25 individual dissections were identified. Five vessels had more than one area of dissection. The findings were compared to 2D IVUS and 2D + 3D combined information.

Histopathology versus 2D IVUS – assessment of serial IVUS cross-sections revealed dissections in 11 of the 20 arterial segments known to contain dissection (55%). Overall, 2-D IVUS correctly detected 52% (13/25) of all dissections. Two individual dissections per lesion were detected by 2-D imaging in three arterial segments. However, in two of these cases histopathological analysis, and 3-D imaging confirmed the presence of one long, continuous dissection plane rather than separate areas of injury. The overall kappa value for correlation of dissection type was 0.29 (0.23-0.35) indicating marginal agreement (Figure 2).

Histopathology versus 2-D and 3-D IVUS – for 2-D and 3-D IVUS combined information agreement on the presence of dissection was reached in 90% (18/20) of arterial segments. Overall, correct detection of all dissections occurred in 76% (19/25). The overall kappa value for correlation of dissection type was 0.64 (0.57-0.71) indicating good agreement (Figure 3).

7.3.2 *Dissection length and depth*

Of the 25 dissections identified by histopathology, 12 were detected by both 2-D IVUS and 2-D + 3-D IVUS information. These were used to compare the accuracy of dissection and depth measurement using each imaging method.

Histopathology versus 2-D IVUS – 2-D IVUS consistently underestimated dissection length (3.52±1.75mm vs 6.54±2.42mm, $p<0.001$) and depth (0.61±0.24mm vs 0.92±0.32mm, $p=0.001$). Reasonable correlation was found between the methods for each parameter ($r=0.78$, $p=0.002$ & $r=0.64$, $p=0.025$) [Figures 4 & 5].

Histopathology versus 2-D + 3-D IVUS – Measurements using information from 2-D and 3-D IVUS produced accurate dissection length (6.13±2.29mm vs 6.54±2.42mm, $p=0.09$) and depth (0.86±0.32mm vs 0.92±0.32mm, $p=0.28$) estimations. High correlation was noted between the methods for both measured parameters ($r=0.98$, $p<0.001$ & $r=0.85$, $p<0.001$) [Figures 6 & 7].

7.4 Discussion

Balloon-induced atherosclerotic plaque disruption, manifesting as superficial cracks or deep radial tears, occurs in the majority of lesions treated by PTCA. For instance, Gerber et al demonstrated that plaque rupture with or without dissection was the main mechanism of luminal enlargement in 83% of patients (Gerber *et al,* 1992). Coronary dissection generally results from deep radial tears and in eccentric plaques where weakness at the base of the plaque causes its separation from the underlying medial layer (Richardson *et al,* 1989; Fitzgerald *et al,* 1992). Depending on the strength and integrity

of the deep layers the dissection may extend radially into the adventitial layer and can track longitudinally usually between the plaque and medial layers. The extent of dissection may critically affect the outcome of PTCA. Numerous animal and post-mortem studies have demonstrated that the acute and long-term success of the technique is intrinsically related to the acute improvement in luminal gain and the extent of vascular damage occurring during the procedure (Block *et al,* 1980; Hoshino *et al,* 1987). Localised 'therapeutic' dissections appear to be a prerequisite for improving lumen gain by releasing the constriction of the atherosclerotic plaque and medial layer (Losordo *et al,* 1992). However studies of patients who died early after PTCA suggest that deeper injury to the arterial wall promotes acute closure due to spasm and flow-limiting dissections (Lincoff *et al,* 1992). A more profound smooth muscle proliferative response appears to occur when the injury extends beyond the media-adventitia border resulting in late restenosis (Faxon *et al,* 1987). The assessment of arterial dissection is therefore an important process following PTCA. IVUS has overcome the clear limitations of contrast angiography by providing a detailed analysis of changes in vessel wall morphology following balloon dilatation. However, the accurate assessment of dissection by conventional IVUS imaging is inhibited by the lack of complete visualization of the whole lesion in single image frames. The mental process of identifying and tracking dissection planes, particularly in highly echogenic plaques, from serial tomographic image slices is prone to error. The goal of this study was to validate and compare the accuracy of conventional IVUS imaging and combined information from computer-generated 2-D and 3-D information with respect to identifying the severity, depth and length of balloon-induced coronary dissections in coronary lesions that would, in the clinical setting, have been suitable for PTCA. Histopathological appearances, with histomorphometric assessment of the dimensions of the dissection, were used as the gold standard with which to compare the imaging methods. Correlation of the presence and extent of dissection with histopathological appearances was significantly better using information from longitudinal reconstruction of IVUS images compared to recorded serial cross-sectional images alone. There was a clear advantage in the ability to directly visualize the whole lesion from the computerized reconstruction. Dissection planes were easily tracked despite abrupt changes in depth and their tendency to spiral out of the plane of view. Discrepancy between histopathology and 3-D IVUS

resulted from the difficulty encountered when dissections extended deep to calcified areas due to acoustic shadowing. Additionally plaque tears originating adjacent to superficial calcification were difficult to identify. Another explanation for the discrepancy is the probability that the IVUS transducer caused a degree of splinting such that the dissection flap was compressed against the lumen wall.

Conventional IVUS imaging provides a reasonably good correlation with histomorphometry for maximum dissection depth and length although the mean values demonstrate a tendency to underestimate true dimensions. Superior correlation is achieved with 3-D IVUS imaging and mean values for each measured parameter are not significantly different.

7.4.1 *Previous studies*

The accuracy of three-dimensional, volumetric, reconstruction of IVUS images has been well-validated against histomorphometry for lumen, plaque and vessel volume (von Birgelen *et al* 1996; Mehran *et al* 1998). Only one study has validated the accuracy of the technique in the assessment of arterial injury following PTCA. Coy *et al* (1992) assessed the accuracy of dissection length and depth estimations in different vessel types. Three-dimensional IVUS detected over 90% of dissections in normal and fibrous arteries although only 69% of calcified vessels. Dimensions were categorized as extension to intima, media or adventitia (depth) and length >5mm or <5mm. Using the kappa statistic excellent correlation was noted for both parameters in normal and fibrous vessels (kappa 0.72-1.0). Marginal correlation was noted for calcified vessels. With respect to dissection type our findings compare favourably to these results in coronary vessels containing the severity and complexity of lesion seen in clinical practice rather than a proportion of normal vessels where delineation of arterial wall structures by ultrasound is somewhat easier. Furthermore, the study compared depth and length measurements rather than defined categories for each parameter which provides a more precise assessment of the value of 3-D IVUS over conventional IVUS imaging.

7.4.2 *Study limitations*

Comparison of dissection length and depth between histopathology and 2-D and 3-D IVUS in this study involved a small number of dissections which may affect the degree of correlation observed. Future studies involving a larger number of arterial specimens may be necessary to substantiate this data. Although histopathological appearances were used as the gold standard for comparison it is possible that some arterial trauma occurred during the sectioning process making the diagnosis of balloon-induced dissection problematic in some specimens. However in Chapter 3 no significant arterial disruption was noted during the sectioning process. Finally, 30MHz mechanical IVUS catheters were used in the imaging protocol. Although these provided acceptable image quality it is possible that the use of currently available, higher frequency transducers (40MHz) may have further improved image resolution and enabled more accurate detection of the extent of dissection.

7.4.3 *Clinical implications*

The use of 3-D IVUS to reconstruct coronary arterial lesions treated by PTCA provides an accurate assessment of arterial injury. In the clinical setting, the ability of the technique to precisely delineate dissection depth and extent may be of benefit in two particular areas. Firstly, the proximal and distal extent of a dissection flap may not be accurately quantified by angiography. Inadequate cover by a stent can predispose to new lesions on either side of the stent due to enhanced smooth muscle proliferation at the site of arterial trauma. On the other hand overestimation of length leads to implantation of longer stents which increases the likelihood of in-stent restenosis. Secondly, there are clinical situations in which stent implantation provides less favourable results such as in small calibre arteries and diabetic coronary disease.

The ability to determine the severity of dissection may help differentiate those lesions that would benefit from stent implantation from lesions with minor dissections that are unlikely to cause acute or long-term problems when treated by PTCA alone.

7.5 Conclusions

Using histopathological information as the gold standard, this study demonstrates the improved accuracy over conventional two-dimensional IVUS imaging of computerized three-dimensional reconstruction of recorded IVUS pullbacks with respect to the detection and classification of arterial dissection and measurement of length and depth. These observations suggest that, in the clinical setting, three-dimensional IVUS imaging would be a useful adjunct to angiography for the precise assessment of vascular injury following PTCA to aid clinical decision-making.

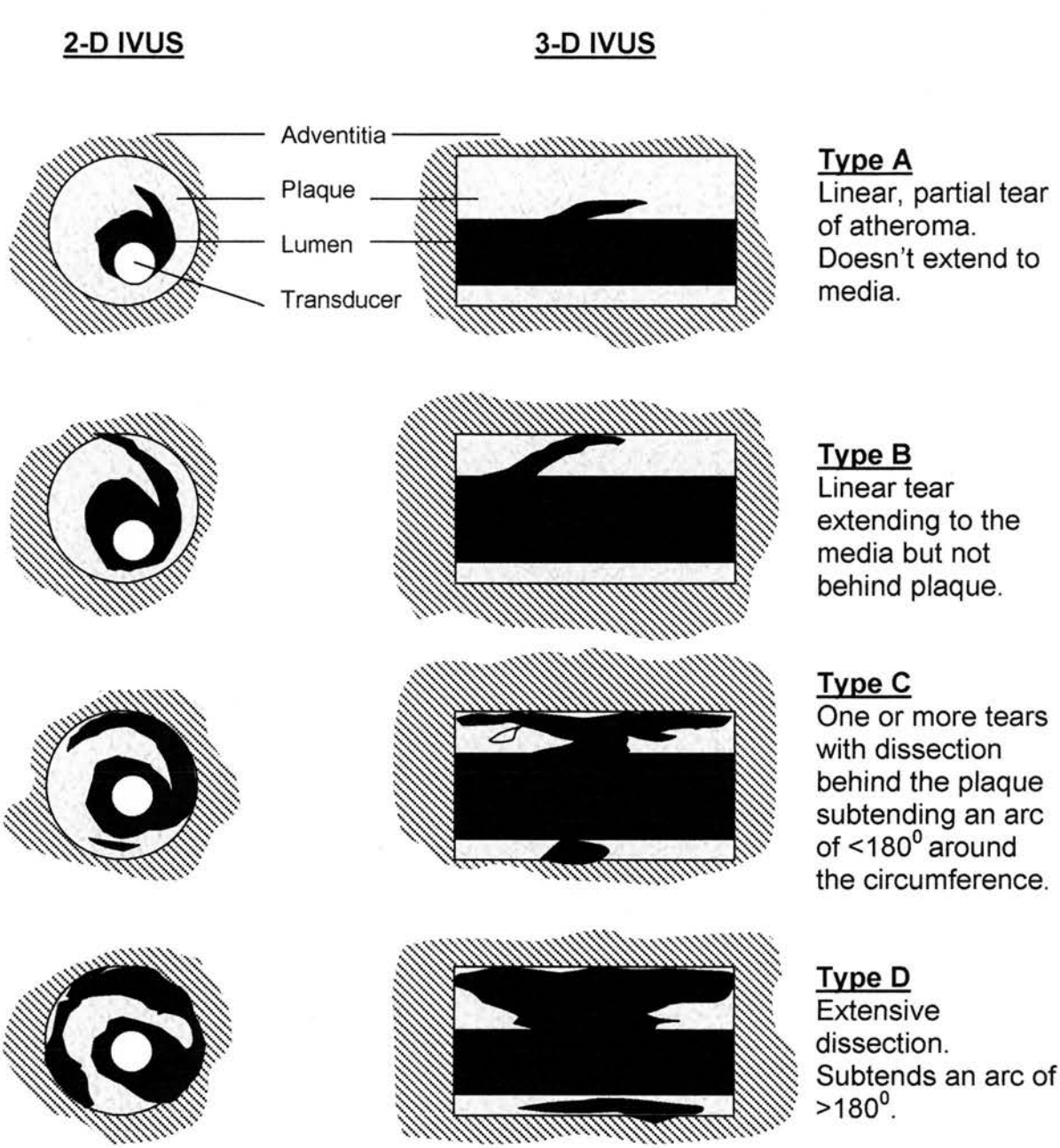

Figure 2. ***Classification of dissection type by 2D and 3-D IVUS***

		Histology				
		A	B	C	D	
IVUS	A	2	0	2	0	4
	B	0	3	2	1	6
	C	0	0	1	2	3
	D	0	0	0	0	0
		2	3	5	3	13

Figure 2. ***Correlation between histology and 2-D IVUS for dissection type (kappa = 0.29)***

		Histology				
		A	B	C	D	
IVUS	A	3	0	2	0	5
	B	0	4	1	0	5
	C	0	1	4	1	6
	D	0	0	0	3	3
		3	5	7	4	19

Figure 3. ***Correlation between 2D and 3-D IVUS and histology for dissection type (kappa=0.64)***

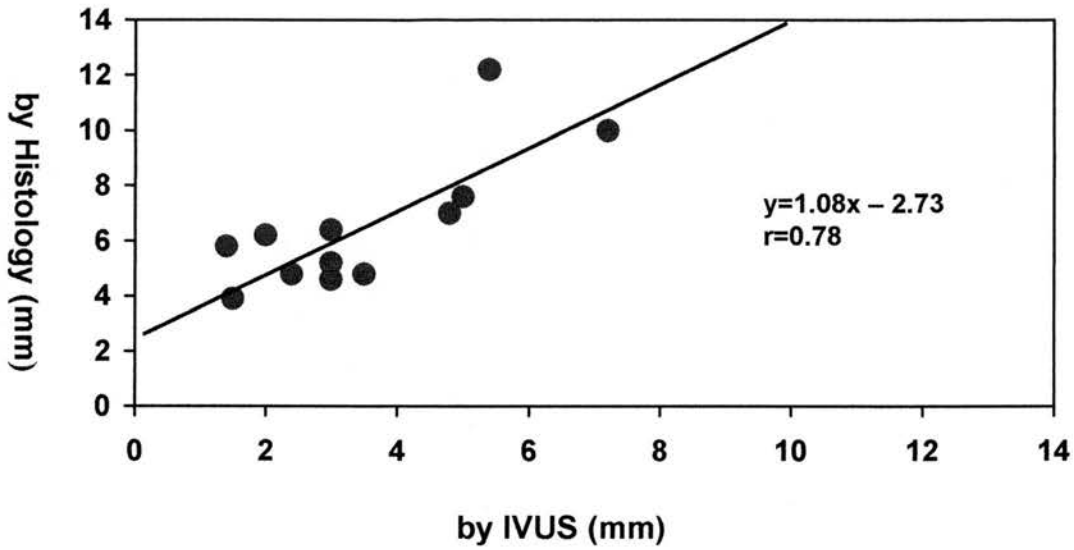

Figure 4. ***Linear regression plot comparing measurement of dissection length between 2-D IVUS and histology***

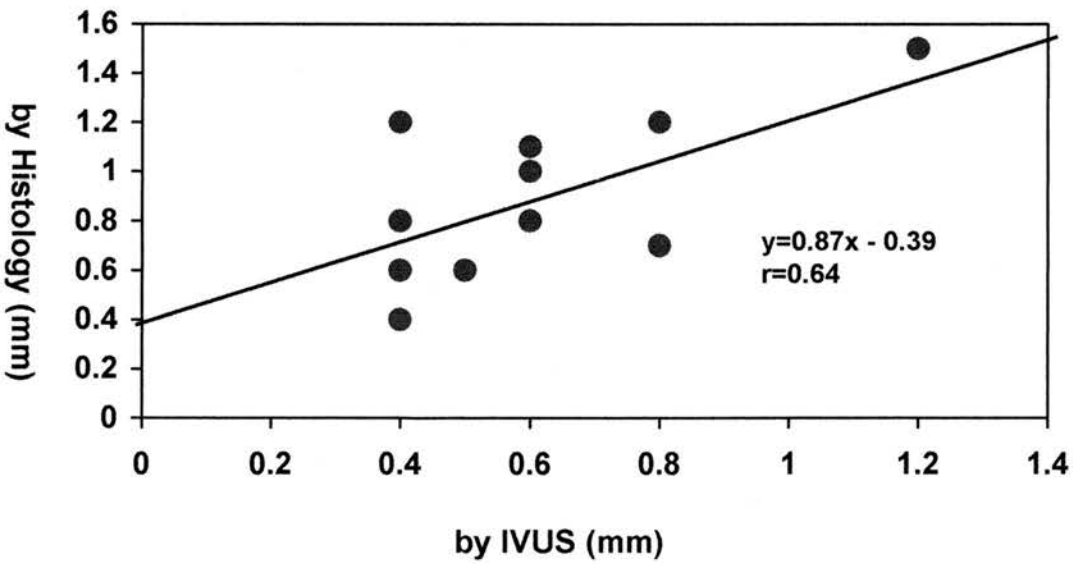

Figure 5. ***Linear regression plot comparing measurement of dissection depth between 2-D IVUS and histology***

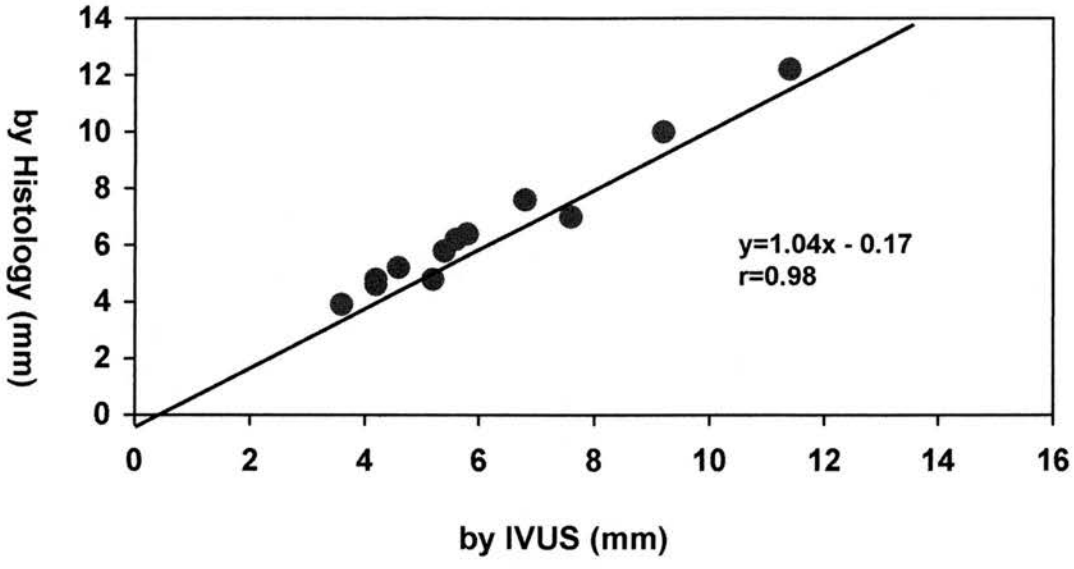

Figure 6. *Linear regression plot comparing measuremont of dissection length by 2-D and 3-D IVUS and histology*

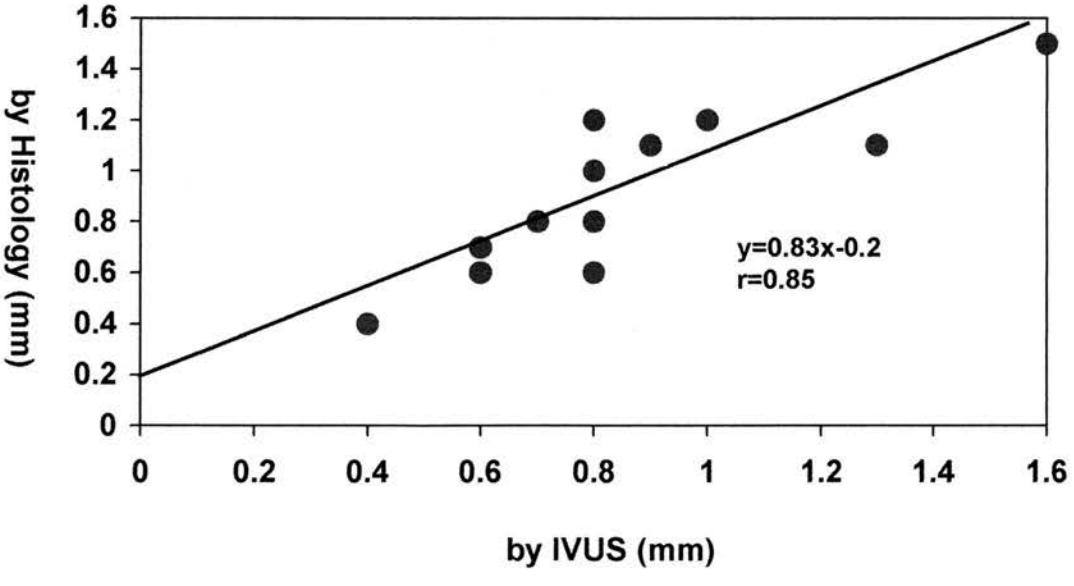

Figure 7. Linear regression plot comparing measurement of dissection depth between 2-D and 3-D IVUS and histology

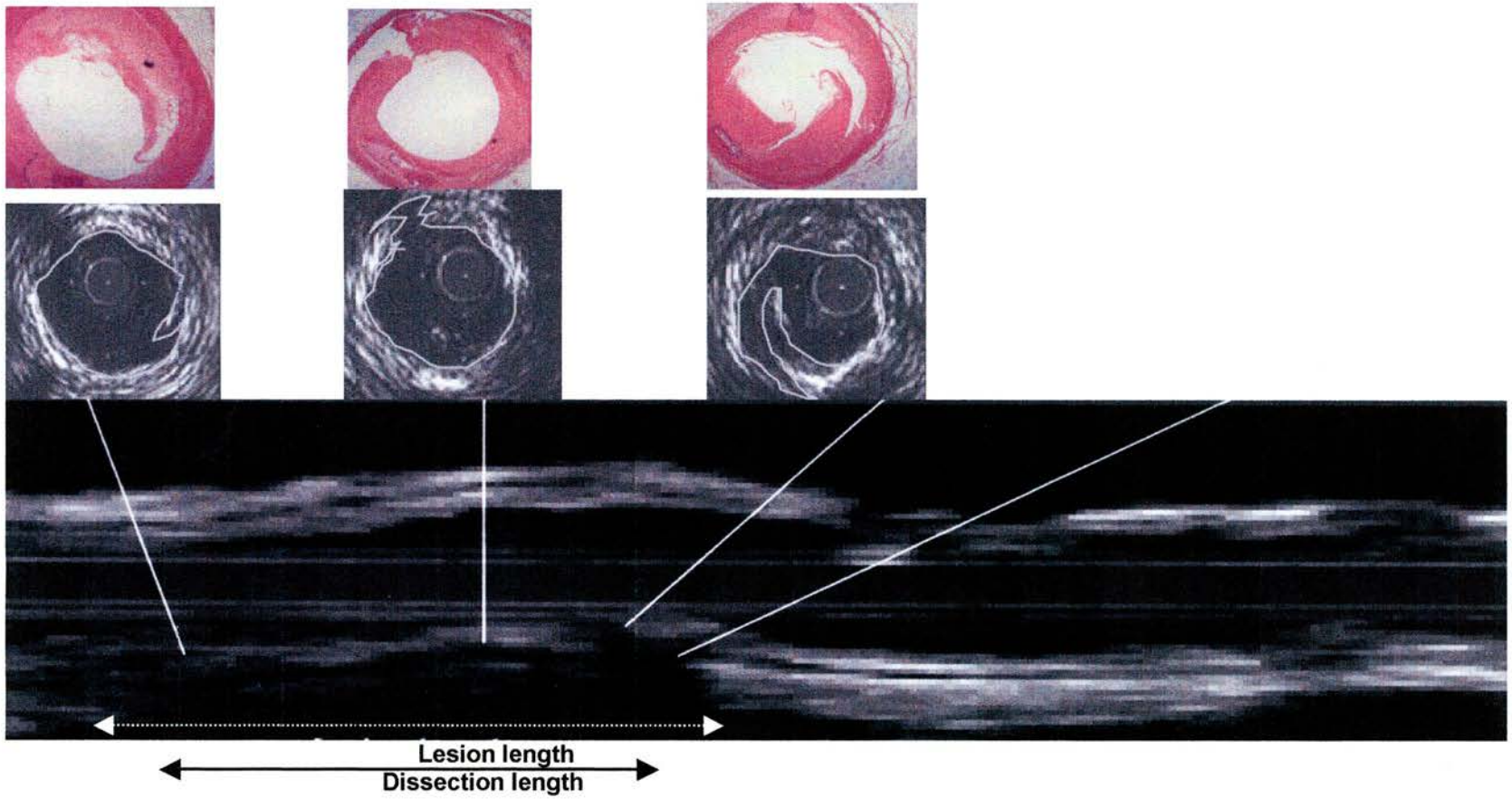

Figure 8. ***2-D versus 3-D IVUS. The longitudinal image demonstrates a long dissection plane extending into the medial layer (type C). Corresponding histological sections demonstrate that 2-D IVUS images underestimate the linear extent and depth.***

CHAPTER 8
General Conclusions

8.1 General Conclusions

The work presented in this thesis has investigated a number of areas which are relevant to the clinical application of intravascular ultrasound. They have been extensively discussed within each chapter, however the following points represent a summary of the findings:-

1) One of the important advantages of IVUS in comparison to coronary angiography is its ability to depict the vessel wall. In particular, the quantitative and qualitative assessment of atherosclerotic plaque provides useful information in diagnostic IVUS studies and also prior to percutaneous intervention. The behaviour of a coronary stenosis to balloon dilatation or alternative techniques is critically dependent on the composition and extent of atherosclerotic plaque. Previous studies provided some evidence for the accuracy of intravascular ultrasound in determining plaque composition in coronary and peripheral vessels using human and animal models. The data in this thesis was obtained in conditions closely approximating the clinical setting and demonstrated the close correlation of IVUS images to corresponding histological sections using a relatively simple classification developed by the European Society of Cardiology. Although a more precise determination of plaque components is necessary for atheroma regression studies the classification can be applied with confidence in routine clinical studies.

2) During percutaneous coronary intervention the sizing of balloons used to dilate atherosclerotic coronary lesions is an important factor in determining the degree of lumen enlargement and extent of vascular injury. Both of these factors are critical determinants of the incidence and degree of restenosis. Determination of balloon size, and also optimal deployment of intracoronary stents, depends upon a comparison of the balloon size, or minimum stent area, with adjacent reference arterial segments. IVUS provides a clear advantage over angiography in accurately determining reference dimensions. Previous studies have demonstrated low interobserver variability of IVUS in determining lumen and

vessel dimensions in clinical studies. However, the data presented in this thesis confirms that interobserver differences in the *selection* of suitable reference segments, results in clinically significant variability in their measurement particularly in areas containing diffuse atheromatous disease. Potentially important differences in balloon size selection and determination of optimal stent deployment may result. Clinical studies would be necessary to determine the true clinical relevance of these findings.

3) The use of IVUS to accurately size balloons has resulted in markedly improved outcomes following PTCA. Restenosis rates have compared favourably to those following intracoronary stenting. In this thesis the histopathological basis for these observations is suggested. The data provides evidence of reduced arterial injury and maximal lumen enlargement using larger balloons combined with relatively low inflation pressures. It therefore appears that excessive barotrauma is the predominant factor in determining the degree of plaque disruption occurring within a lesion. Furthermore, with the exception of heavily calcified lesions, these observations appear to be independent of the composition and morphology of the stenotic plaque.

4) The use of computer algorithms to process serial tomographic IVUS frames has enabled the longitudinal reconstruction of arterial segments. Volumetric analysis has demonstrated clinical and research applications particularly in the study of atheroma regression. Although volumetric measurement of lumen, vessel and plaque has been shown to be accurate in in vitro models confounding factors such as natural and induced angulations of the IVUS catheter shaft may influence the precision of clinical studies. The data in this thesis demonstrates that multiple angulations of the catheter shaft cause clinically significant variability in plaque volume measurement. However, the accuracy of measurements appears to be predominantly influenced by induced angulations of the catheter shaft outwith the femoral artery entry site. This confirms the need for a disciplined imaging protocol particularly for any serial clinical study of atheroma regression.

5) The use of conventional IVUS imaging to assess vascular injury following PTCA has confirmed the basic mechanisms suggested by early histopathological studies. The natural progression from this is the longitudinal reconstruction of dilated coronary artery segments to assess vascular injury. The provision of a third dimension to view the axial extent of plaque disruption avoids the potential error inherent in the process of mentally reconstructing the injured segment. In this thesis the improved accuracy of three-dimensional IVUS over conventional imaging in assessing the length and depth of injury is demonstrated suggesting a role for the technique in routine PTCA procedures. Realistically, it is unlikely that such an approach will gain widespread acceptance in the clinical setting since the technique is currently time-consuming and the costs of additional computer software are prohibitive. However, this technique provides an important research tool and, in the future, more efficient computer algorithms may enhance its use in this setting. Finally, precise assessment of vascular injury is of less importance in current clinical practice due to the exponential rise in the use of intracoronary stents which provide fairly complete coverage of a diseased segment. However, the accurate assessment of vascular injury using three-dimensional ultrasound techniques is important in studies of restenosis and the investigation of pharmacological agents such as cell cycle inhibitors on this process.

All the studies described in this thesis have been specifically designed to validate clinically relevant technical aspects of IVUS imaging and demonstrate the application of the technique in the assessment of vascular injury following PTCA. Clearly, clinical conditions cannot be precisely reproduced in the in vitro setting. However, the important physiological properties of diseased coronary arteries have been carefully considered in the design of the pulsatile flow system. Furthermore, the use of histopathological correlation to confirm the accuracy of IVUS imaging in a number of the described studies ensures that it can be applied with confidence in the clinical setting.

CHAPTER 9
Bibliography

9.1 Bibliography

Abizaid A, Mehran R, Pichard AD et al. Results of high pressure ultrasound guided 'oversized' balloon PTCA to achieve stent-like results. *J Am Coll Cardiol* 1997; 29 (Suppl A): 280A.

Abizaid A, Mintz GS, Leon MB et al. Clinical, intravascular ultrasound, and quantitative angiographic determinants of the coronary flow reserve before and after percutaneous transluminal coronary angioplasty. *Am J Cardiol* 1998; 82: 423-428.

Adelman AG, Cohen M, Kimball BP et al. Canadian coronary atherectomy trial. A randomized comparison of directional coronary atherectomy and percutaneous transluminal coronary angioplasty for lesions of the proximal left anterior descending artery. *N Engl J Med* 1993; 329: 228-234.

Albiero R, Rau T, Colombo A et al. Comparison of immediate and intermediate-term results of intravascular ultrasound versus angiography guided Palmaz-Schatz stent implantation in matched lesions. *Circulation* 1997; 96: 2997-3005.

Alfonso F, Macaya C, Hernandez R et al. Determinants of coronary compliance in patients with coronary artery disease: An intravascular ultrasound study. *J Am Coll Cardiol* 1994; 23: 879-884.

Andersen HR, Maeng M, Falk E et al. Remodelling rather than neointimal formation explains luminal narrowing after deep vessel wall injury. Insights from a porcine coronary restenosis model. *Circulation* 1996; 93: 1716-1724.

Anderson MH, Simpson IA, Ward DE et al. Intravascular ultrasound imaging of the coronary arteries: an in vitro evaluation of measurement of area of the lumen and atheroma characterization. *Br Heart J* 1992; 68: 276-281.

Arnett EN, Ismer JM, Redwood CR et al. Coronary artery narrowing in coronary artery disease: comparison of cineangiographic and necropsy findings. *Ann Intern Med* 1979; 91: 350-356.

Baim DS, Faxon DP. Coronary angioplasty. In: Grossman W, ed. Cardiac Catheterization and Angiography. Philadalphia: Lea & Febiger, 1986: 473-492.

Becker J. Atherosclerosis – a lesion in search of a definition. *Int J Cardiol* 1985; 8: 375-377

Belli G, Whitlow PL, Gross L et al. Intracoronary stenting without oral anticoagulation: the Cleveland Clinic registry. *Circulation* 1995; 92 (Suppl I): I-796.

Benkeser PJ, Churchwell AL, Abouelnasr DM et al. Resolution limitations in intravascular ultrasound imaging. *J Am Soc Echocardiogr* 1993; 6: 158-165.

Bertrand M, Lablanche M, MacFadden E et al. Discordant results of visual and quantitative estimates of stenosis severity before and after coronary angioplasty. *Cathet Cardiovasc Diagn* 1993; 28: 1-6.

Bland JM, Altman DG. Statistical methods for assessing agreement between two methods of clinical measurement. *Lancet* 1986; 2: 307-310.

Block PC, Baughman KL, Pasternak RC. Transluminal angioplasty: correlation of morphologic and angiographic findings in an experimental model. *Circulation* 1980; 61: 778-785.

Bom N, ten Hoff H, Lancee CT et al. Early and recent intraluminal ultrasound devices. *Int J Cardiac Imag* 1989; 4: 79.

Braden GA, Herrington DM, Little WC et al. Qualitative and quantitative contrasts in the mechanisms of lumen enlargement by coronary balloon angioplasty and directional coronary atherectomy. *J Am Coll Cardiol* 1994; 23: 40-48.

Bruining N, von Birgelen C, Di Mario C et al. Dynamic three-dimensional reconstruction of ICUS images based on an ECG gated pull-back device. In: Computers in Cardiology 1995, Los Alamitos: IEEE Computer Society Press, 1995: 633-636.

Chae JS, Brisken AF, Siegel RJ et al. Geometric accuracy of intravascular ultrasound imaging. *J Am Soc Echocardiogr* 1992; 5: 577-587.

Chandraratna PAN, Choudhury S, Yitiger E et al. Differentiation between fatty plaque and thrombus by quantitative ultrasonic methods. *Circulation* 1991; 84: II-702.

Chandrasekaran K, D'Adamo AJ, Sehgal CM. Three-dimensional reconstruction of intravascular ultrasound images. In: Yock PG, Tobis JM, eds. Inntravascular Ultrasound Imaging. New York: Churchill-Livingstone, 1992: 141-147.

Chenzbraun A, Pinto FJ, Alderman EL et al. Distribution and morphologic features of coronary artery disease in cardiac allografts: an intracoronary ultrasound study. *J Am Soc Echocardiogr* 1995; 8: 1-8.

Choi JW, Goodreau LM, Davidson CJ et al. Resource utilization and clinical outcomes of coronary stenting: a comparison of intravascular ultrasound and angiographical guided stent implantation. *Am Heart J* 2001; 142(1): 112-118.

Cohen J. A coefficient of agreement for nominal scales. *Educational and Psychological Measurement* 1960; 20: 37-46.

Colombo A, Hall P, Nakamura S et al. Intracoronary stenting without anticoagulation accomplished with intravascular ultrasound guidance. *Circulation* 1995; 91: 1676-1688.

Cothren RM, Shekhar R, Nissen SE et al. Three dimensional reconstruction of the coronary artery wall by image fusion of intravascular ultrasound and bi-plane angiography. *Int J Card Imaging* 2000; 16(2): 69-85.

Coy KM, Park JC, Siegel RJ et al. In vitro validation of three-dimensional intravascular ultrasound for the evaluation of arterial injury after balloon angioplasty. *J Am Coll Cardiol* 1992; 20: 692-700.

Davidson CJ, Sheikh KH, Bashore TM et al. Intravascular ultrasonography versus digital subtraction angiography: a human in vivo comparison of vessel size and morphology. *J Am Coll Cardiol* 1990; 16: 633-636.

Davies MJ, Richardson PD, Maas J et al. Risk of thrombosis in human atherosclerotic plaques: role of extracellular lipid: macrophage, and smooth muscle cell content. *Br Heart J* 1993; 69: 377-381.

Davies MJ, Thomas AC. Plaque fissuring: the cause of acute myocardial infarction, sudden ischaemic death and crescendo angina. *Br Heart J* 1985; 53: 363-373.

de Jaegere P, Mudra H, van Es GA et al. IVUS guided optimized stent deployment. Immediate and 6 months clinical and angiographical results from the multicentre ultrasound stenting in coronaries study (MUSIC study). *Eur Heart J* 1998; 8: 1214-1223.

De Scheerder I, De Man F, Wilczek K et al. Inntravascular ultrasound versus angiography for measurement of luminal diameters in normal and diseased coronary arteries. *Am Heart J* 1994; 127: 243-251.

de Smet BJGL, van der Zande J, Post MJ et al. The atherosclerotic Yucatan animal model to study the arterial response after balloon angioplasty: the natural history of remodelling. *Cardiovasc Res* 1998; 39: 224-232.

Dhawale PJ, Wilson DL, Hodgson JMcB. Optimal data acquisition for volumetric intracoronary ultrasound. *Cathet Cardiovasc Diagn* 1994; 32: 288-299.

Di Mario C, Gil R, Camenzind E et al. Quantitative assessment with intracoronary ultrasound of the mechanism of restenosis after percutaneous transluminal balloon angioplasty and directional coronary atherectomy. *Am J Cardiol* 1995; 75: 772-777.

Di Mario C, Gorge G, Peters RJG et al. Clinical application and image interpretation in intracoronary ultrasound. *Eur Heart J* 1998; 19: 207-229.

Di Mario C, Madretsma S, Linker D et al. The angle of incidence of the ultrasonic beam: A critical factor for the image quality in intravascular ultrasonography. *Am Heart J* 1993; 126: 76-85.

Di Mario C, The SHK, Madretsma S et al. Detection and characterization of vascular lesions by intravascular ultrasound: an in vitro study correlated with histology. *J Am Soc Echocardiogr* 1992; 5: 135-146.

Ehrlich S, Honye J, Tobis J et al. Unrecognized stenosis by angiography documented by intravascular ultrasound imaging. *Catheterization and cardiovasc diagn* 1991; 23: 198-201.

Erbel R, Ge J, Ashry M et al. Intravascular ultrasound: diagnostic applications. In: De Feyter PJ, Di Mario C, Serruys PW, eds. Quantitative Coronary Imaging. Delft: Barjesteh, Meeuwes & Co, 1995: 211-223.

Erbel R, Ge J, Kearney P et al. Value of intracoronary ultrasound and Doppler in the differentiation of angiographically normal coronary arteries: A prospective study in patients with angina pectoris. *Eur Heart J* 1996; 17: 880-889.

Falk E. Morphologic features of unstable atherothrombotic plaques underlying acute coronary syndromes. *Am J Cardiol* 1989; 63: 1141-1201.

Farb A, Virmani R, Kolodgie FD et al. Plaque morphology and pathologic changes in arteries from patients dying after coronary balloon angioplasty. *J Am Coll Cardiol* 1990; 16: 1421-1429.

Faxon DP, Sanborn TA, Haudenschild CC. Mechanism of angioplasty and its relation to restenosis. *Am J Cardiol* 1987; 60: 5B-9B.

Fischman DL, Leon MB, Baim DS et al. A randomized comparison of coronary stent placement and balloon angioplasty in the treatment of coronary artery disease. *N Engl J Med* 1994; 331: 496-501.

Fitzgerald PJ, Muhlberger VA, Moes NY et al. Calcium location within plaque as a predictor of atherectomy tissue retrieval: an intravascular ultrasound study. *Circulation* 1992; 86: I-516.

Fitzgerald PJ, Oshima A, Hayase M et al. Final results of the can routine ultrasound influence stent expansion (CRUISE) study? *Circulation* 2000; 102: 523-530.

Fitzgerald PJ, Ports TA, Yock PG et al. Contribution of localized calcium deposits to dissection after angioplasty. An observational study using intravascular ultrasound. *Circulation* 1992; 86: 64-70.

Foster GP, Mittelman MA, Zarich SW et al. Variability in the measurement of intracoronary ultrasound images: implications for the identification of atherosclerotic plaque regression. *Clin Cardiol* 1997; 20: 11-15.

Friedrich GJ, Moes NY, VA et al. Detection of intralesional calcium by intracoronary ultrasound depends on the histologic pattern. *Am Heart J* 1994; 128: 435-441.

Fuessel RT, Mintz GS, Pichard AD et al. In vivo validation of intravascular ultrasound length measurements using a motorized transducer pullback system. *Am J Cardiol* 1996; 77: 1115-1118.

Fuster V, Badimon I, Cheseboro JH et al. The pathogenesis of coronary artery disease and the acute coronary syndromes. *N Engl J Med* 1992; 326: 242-250, 310-318.

Ge J, Chirillo F, Erbel R et al. Screening of ruptured plaques in patients with coronary artery disease by intravascular ultrasound. *Heart* 1999; 81(6): 621-627.

Ge J, Erbel R, Rupprecht HJ et al. Comparison of intravascular ultrasound and angiography in the assessment of myocardial bridging. *Circulation* 1994; 89: 1725-1732.

Ge J, Erbel R, Zamorano J et al. Coronary artery remodelling in atherosclerotic disease: an intravascular ultrasonic study in vivo. *Coron Artery Dis* 1993; 4: 981-986.

Ge J, Fengqi L, Erbel R et al. Angiograpjically 'silent' plaque in the left main coronary artery detected by intravascular ultrasound. *Coron Artery Dis* 1995; 6: 805-810.

Gerber TC, Erbel R, Meyer J et al. Classification of morphologic effects of percutaneous transluminal coronary angioplasty assessed by intravascular ultrasound. *Am J Cardiol* 1992; 70: 1546-1554.

Gerber TC, Erbel R, Meyer J et al. Extent of atherosclerosis and remodelling of the left main coronary artery determined by intravascular ultrasound. *Am J Cardiol* 1993; 73: 666-671.

Gil R, Di Mario C, Serruys PW et al. Influence of plaque composition on mechanisms of percutaneous transluminal coronary balloon angioplasty assessed by ultrasound imaging. *Am Heart J* 1996; 131(3): 591-597.

Glagov S, Weisenberg E, Zarins CK et al. Compensatory enlargement of human atherosclerotic coronary arteries. *N Engl J Med* 1986; 316: 1371-1375.

Goel M, Honye J, Nakamura S et al. Significance of coronary calcification by ultrafast computed tomography: comparison with intravascular ultrasound. *Circulation* 1992; 86: I-476.

Gruentzig AR, King III SB, Siegenthaler W et al. Long term follow up after percutaneous transluminal coronary angioplasty: the early Zurich experience. *N Engl J Med* 1987; 316: 1127-1132.

Gruentzig A, Senning A, Siegenthaler WE. Non-operative dilatation of coronary artery stenosis: percutaneous transluminal angioplasty. *N Engl J Med* 1979; 301: 61-68.

Guide Trial Investigators. IVUS-determined predictors of restenosis in PTCA and DCA: final report from the GUIDE trial, Phase II. *J Am Coll Cardiol* 1996; 29 (Suppl A): 156A.

Gurley J, Nissen S, DeMaria A et al. Influence of operator and patient dependent variables on the suitability of automated quantitative coronary arteriography for routine clinical use. *J Am Coll Cardiol* 1992; 19: 1237-1243.

Gussenhoven EJ, Essed CE, Bom N et al. Arterial wall characteristics determined by intravascular ultrasound imaging: an in vitro study. *J Am Coll Cardiol* 1989; 14: 947-952.

Gussenhoven EJ, Essed CE, Freitman P et al. Intravascular echographic assessment of vessel wall characteristics: a correlation with histology. *Int J Card Imaging* 1989; 4: 105-116.

Haase KK, Athanasiadis A, Karsch KR et al. Acute and one year follow-up results after vessel size adapted PTCA using intracoronary ultrasound. *Eur Heart J* 1998; 19: 263-272.

Hausmann D, Erbel R, Alibelli-Chemarin MJ et al. The safety of intracoronary ultrasound. A multicentre survey of 2207 examinations. *Circulation* 1995; 91: 623-630.

Hausmann D, Friedrich G, Sudhir K et al. 3D intravascular ultrasound imaging with automated border detection using 2.9F catheters. *J Am Coll Cardiol* 1994; 23: 174A.

Hausmann D, Lundkvist AJ, Yock PG et al. Intracoronary ultrasound imaging: Intraobserver and interobserver variability of morphometric measurements. *Am Heart J* 1994; 128: 674-680.

Hermiller J, Cusma J, Bashore T et al. Quantitative and qualitative coronary angiographic analysis: review of methods, utility and limitations. *Cathet Cardiovasc Diagn* 1992; 25: 110-131.

Hiro T, Leung CY, Guzman S et al. Are 'soft echoes' really soft?: ultrasound assessment of mechanical properties in human atherosclerotic tissue. *Circulation* 1995; 92: I-649.

Hirshfield JW Jr, Schwartz JS, Jugo R et al and the M-Heart Investigators. Restenosis after coronary angioplasty: a multivariate statistical model to relate lesion and procedure variables to restenosis. *J Am Coll Cardiol* 1991; 18: 647-656.

Hodgson J McB, Graham SP, Eberle MJ et al. Clinical percutaneous imaging of coronary anatomy using an over-the-wire ultrasound catheter system. *Int J Card Imaging* 1989; 4: 187-193.

Hodgson J McB, Reddy KG, Sheehan HM et al. Intracoronary ultrasound imaging: correlation of plaque morphology with angiography, clinical syndrome and procedural results in patients undergoing coronary angioplasty. *J Am Coll Cardiol* 1993; 21: 35-44.

Honye J, Mahon DJ, Tobis JM et al. Morphologic effects of coronary balloon angioplasty in vivo assessed by intravascular ultrasound imaging. *Circulation* 1992; 85: 1012-1025.

Hoshino T, Yoshida H, Takayama S et al. Significance of intimal tears in the mechanism of luminal enlargement in percutaneous transluminal coronary angioplasty: correlation of pathologic and angiographic findings in post-mortem hearts. *Am Heart J* 1987; 114: 503-510.

Ip JH, Fuster V, Cheesebro JH et al. Syndromes of accelerated atherosclerosis: Role of vascular injury and smooth muscle cell proliferation. *J Am Coll Cardiol* 1990; 15: 1667-1687.

Isner JM, Donaldson RF, Clarke RH et al. Attenuation of the media of coronary arteries in advanced atherosclerosis. *Am J Cardiol* 1986; 58: 937-939.

Jain SP, Jain A, Collins TJ et al. Predictors of restenosis: a morphometric and quantitative evaluation by intravascular ultrasound. *Am Heart J* 1994; 128: 664-673.

Johnson DE, Alderman EL, Schroeder JS et al. Transplant coronary artery disease: Histopathological correlations with angiographic morphology. *J Am Coll Cardiol* 1991; 17: 449-457.

Keane D, Melkert R, Herrman JP et al and the Benestent Investigators. Quantitative coronary angiography endpoints: a valid surrogacy for clinical endpoints? In: De Feyter PJ, Di Mario C, Serruys PW, eds. Quantitative Coronary Imaging. Delft: Barjesteh, Meeuwes & Co, 1995: 211-223.

Kearney PP, Erbel R, Ge J et al. Assessment of spontaneous coronary artery dissection by intravascular ultrasound in a patient with unstable angina. *Cathet Cardiovasc Diagn* 1994; 32: 58-61.

Kearney PP, Koch L, Erbel R et al. Differences in morphology of stable and unstable coronary lesions and their impact on the mechanism of angioplasty. An in vivo study.with IVUS. *Eur Heart J* 1996; 17: 721-730.

Kearney PP, Ramo MP, Sutherland GR et al. Analysis of the reproducibility of reference lumen quantitation with intravascular ultrasound in stented coronary arteries. *Cathet Cardiovasc Diagn* 1997; 40: 1-7.

Kearney PP, Ramo MP, Sutherland GR et al. How important are image distortion artifacts when using mechanical ultrasound transducers? *Br Heart J* 1995; 73(suppl 3): 17.

Kelman GR. Physiology of coronary blood flow. In: Kelman GR: *Applied Cardiovascular Physiology (2nd Ed.)*. Butterworths, London; 1977: 1-20.

Kitney R, Moura L, Straughan K. 3-D visualization of arterial structures using ultrasound and voxel modelling. *Int J Cardiac Imag* 1989; 4: 134-143.

Koch L, Kearney P, Erbel R et al. Three-dimensional reconstruction of intracoronary ultrasound images: roadmapping with simultaneously digitized coronary angiograms. In: Computers in Cardiology 1993, Los Alamitos: IEEE Computer Society Press, 1993: 89-91.

Kovach JA, Mintz GS, Pichard AD et al. Sequential intravascular ultrasound characterization of the mechanisms of rotational atherectomy and adjunct balloon angioplasty. *Am J Cardiol* 1993; 22: 1024-1032.

Lee DY, Nishioka T, Siegel RJ et al. Effect of intracoronary imaging on clinical decision making. *Am Heart J* 1995; 129: 1084-1093.

Lincoff AM, Popma JJ, Topol EJ et al. Abrupt vessel closure complicating coronary angioplasty: clinical, angiographic and therapeutic profile. *J Am Coll Cardiol* 1992; 19: 926-935.

Li W, Bosch JG, Zhong Y et al. Image segmentation and 3D reconstruction of intravascular ultrasound images. In: Wei Y, Gu B, eds. Acoustical Imaging , Vol. 20. New York: Plenum Press, 1993: 489-496.

Li W, Gussenhoven EJ, Zhong Y et al. Temporal averaging for quantification of lumen dimensions in intravascular ultrasound images. *Ultr Med Biol* 1994; 20: 117-122 (a).

Li W, von Birgelen C, Di Mario C et al. Semi-automatic contour detection for volumetric quantification of intracoronary ultrasound. In: Computers in Cardiology 1994, Los Alamitos: IEEE Computer Society Press, 1994: 277-280 (b).

Losordo DW, Rosenfield K, Isner J et al. How does angioplasty work? Serial analysis of human iliac arteries using intravascular ultrasound. *Circulation* 1992; 86: 1845-1858.

Losordo DW, Rosenthal K, Isner JM et al. Focal compensatory enlargement of human arteries in response to progressive atherosclerosis. *Circulation* 1994; 89: 2570-2577.

Lyon RT, Zarins CK, Glagov S et al. Vessel, plaque and lumen morphology after transluminal balloon angioplasty. Quantitative study in distended human arteries. *Arteriosclerosis* 1987; 7: 306-314.

Marantz T, Williams DO, Most AS et al. Predictors of restenosis after successful angioplasty. *Circulation* 1984; 70: II-176.

Marsico F, Kubica J, Specchia G et al. Influence of plaque morphology on the mechanism of luminal enlargement after directional coronary atherectomy and balloon angioplasty. *Br Heart J* 1995; 74: 134-139.

McKay CR, Griggith J, Marcus ME at al. Factors influencing intraluminal ultrasound image quality and arterial wall morphology. *Circulation* 1989; 80: II-2305.

McPherson DD, Hiratzka LF, Brandt B et al. Delineation of the extent of coronary atherosclerosis by high frequency epicardial echocardiography. *N Engl J Med* 1987; 316: 304-309.

Mehran R, Mintz GS, Leon MB et al. Validation of the in vivo intravascular ultrasound measurement of in-stent neointimal hyperplasia volumes. *J Am Coll Cardiol* 1998; 32: 794-799.

Meier B, Gruentzig A, King S et al. Higher balloon dilatation pressure in coronary angioplasty. *Am Heart J* 1984; 107: 619-622.

Mintz GS, Kovach JA, Leon MB et al. Geometric remodelling is the predominant mechanism of clinical restenosis after coronary angioplasty. *J Am Coll Cardiol* 1994; 23: 138A (a).

Mintz GS, Pichard AD, Kovach JA et al. Impact of preintervention intravascular ultrasound imaging on transcatheter treatment strategies in coronary artery disease. *Am J Cardiol* 1994; 73: 423-430.

Mintz GS, Popma JJ, Pichard AD et al. Intravascular ultrasound predictors of restenosis following percutaneous transcatheter coronary revascularisation. *J Am Coll Cardiol* 1996; 27: 1678-1687.

Mintz GS, Popma JJ, Pichard AD et al. Limitations of angiography in the assessment of plaque distribution in coronary artery disease. A systematic study of target lesion eccentricity in 1446 lesions. *Circulation* 1996; 93: 924-931.

Moussa I, Moses J, Colombo A et al. Stenting after optimal lesion debulking (SOLD) registry. Angiographic and clinical outcome. *Circulation* 1998; 98(16): 1604-1609.

Mudra H, Klauss V, Blasini R et al. Ultrasound guidance of Palmaz Schatz intracoronary stenting with a combined intravascular ultrasound balloon catheter. *Circulation* 1994; 90: 1252-1261.

Mudra H, Macaya C, Zahn R et al. Interim analysis of the "optimization with ICUS to reduce stent restenosis" (OPTICUS) trial [abstract]. *Circulation* 1999; 98 (suppl): 1908.

Nakamura S, Colombo A, Gaglione A et al. Intracoronary ultrasound observations during stent implantation. *Circulation* 1994; 89: 2026-2034.

Nichols AB, Smith R, Powers ER et al. Importance of balloon size in coronary angioplasty. *J Am Coll Cardiol* 1989; 13: 1094-1100.

Nishimura RA, Edwards WD, Tajik AJ et al. Intravascular ultrasound imaging: in vitro validation and pathologic correlation. *J Am Coll Cardiol* 1990; 16: 145-154.

Nissen SE, Grines CL, DeMaria AN et al. Application of a new phased array ultrasound imaging catheter in the assessment of vascular dimensions. *Circulation* 1990; 81: 660-666.

Nobuyoshi M, Kimura T, Nosaka H et al. Restenosis after successful percutaneous transluminal coronary angioplasty: serial angiographic follow-up of 229 patients. *J Am Coll Cardiol* 1988; 12: 616-623.

Palmer ND, Northridge DB, Fox KAA et al. In vitro analysis of coronary atheromatous lesions by intravascular ultrasound. Reproducibility and histological correlation of lesion morphology. *Eur Heart J* 1999; 20: 1701-1706.

Palmer ND, McLeod A, Uren NG et al. Rationale and protocol for the Coronary Atheroma Regression with Atorvastatin (CARA) study. Personal communication.

Park JC, Siegel RJ, Demer LL. Effects of calcification and formalin fixation on in vitro distensibility of femoral arteries. *Am Heart J* 1993; 125: 344-349.

Pasterkamp G, Wensing PJW, Post MJ et al. Paradoxical arterial wall shrinkage may contribute to luminal narrowing of human atherosclerotic femoral arteries. *Circulation* 1995; 91: 1444-1449.

Pasterkamp G, Borst C, Gussenhoven EJ et al. Remodelling of de novo atherosclerotic lesions in femoral arteries: impact on mechanism of balloon angioplasty. *J Am Coll Cardiol* 1995; 26: 422-428.

Peters RJG, Ge J, Yock PG et al. Observer agreement on qualitative analysis of intracoronary ultrasound. *Circulation* 1994; 90: I-551 (a).

Peters RJG, Kok WEM, Bom N, for the PICTURE Study Group. Prediction of restenosis after coronary balloon angioplasty. *Circulation* 1997; 95: 2254-2261.

Peters RJG, Kok WEM, Visser CA et al. Characterisation of plaque components with intracoronary ultrasound imaging: an in vitro quantitative study with videodensitometry. *J Am Soc Echocardiogr* 1994; 7: 616-623 (b)

Peters RJG, Kok WEM, Visser CA et al. Determinants of echodensity at the intima-media interface with intracoronary ultrasound imaging. *J Am Soc Echocardiogr* 1994.

Peters RJG, Kok WEM, Visser CA et al. Histopathologic validation of intracoronary ultrasound imaging. *J Am Soc Echocardiogr* 1994; 7:230-241 (c).

Pinto FJ, Chenzbraun A, St Goar FG et al. Feasibility of serial intracoronary ultrasound imaging for assessment of progression of intimal proliferation in cardiac transplant recipients. *Circulation* 1994; 90: 2348-2355.

Pinto FJ, St Goar FG, Alderman EL et al. Immediate and one year safety of intracoronary ultrasonic imaging. Evaluation with serial quantitative angiography. *Circulation* 1993; 88: 1709-1714.

Porter TR, Radio SJ, Xie F et al. Composition of coronary atherosclerotic plaque in the intima and media affects intravascular ultrasound measurements of intimal thickness. *J Am Coll Cardiol* 1994; 23: 1079-1084.

Porter TR, Sears T, Shurmur S et al. Intravascular ultrasound study of angiographically mildly diseased coronary arteries. *J Am Coll Cardiol* 1993; 22: 1858-1865.

Post MJ, Borst C, Kuntz RE. The relative importance of arterial remodelling compared with intimal hyperplasia in lumen narrowing after balloon angioplasty. *Circulation* 1994; 89: 2816-2821.

Potkin BN, Bartorelli AL, Roberts WC et al. Coronary artery imaging with intravascular high-frequency ultrasound. *Circulation* 1990; 81: 1575-1585.

Potkin BN, Keren G, Leon MB et al. Arterial responses to balloon coronary angioplasty: An intravascular ultrasound study. *J Am Coll Cardiol* 1992; 20: 942-951.

Rensing B, Hermans W, Serruys PW et al. Lumen narrowing after percutaneous transluminal coronary balloon angioplasty follows a near Gaussian distribution: A quantitative angiographic study in 1,445 successfully dilated lesions. *J Am Coll Cardiol* 1992; 19: 939-945.

Richardson PD, Davies MJ, Born GVR. Influence of plaque configuration and stress distribution on fissuring of coronary atherosclerotic plaques. *Lancet* 1989; 2: 941-944.

Rickenbacher PR, Pinto FJ, Chenzbraun A et al. Incidence and severity of transplant coronary artery disease early and up to 15 years after transplantation as detected by intravascular ultrasound. *J Am Coll Cardiol* 1995; 25: 171-177.

Rickenbacher PR, Pinto FJ, Lewis NP et al. Prognostic importance of intimal thickness measured by intracoronary ultrasound after cardiac transplantation. *Circulation* 1995; 92: 3445-3452.

Roberts WC, Jones AA. Quantitation of coronary arterial narrowing at necropsy in sudden cardiac death: analysis of 31 patients and comparison with 25 control subjects. *Am J Cardiol* 1979; 44: 39-45.

Roelandt JRTC, Di Mario C, Pandian NG et al. Three-dimensional reconstruction of intracoronary ultrasound images: Rationale, approaches, problems and directions. *Circulation* 1994; 90: 1044-1055(a).

Roelandt JRTC, ten Cate FJ, Taams MA et al. Ultrasonic dynamic three-dimensional visualization of the heart with a multiplane transoesophageal imaging transducer. *J Am Soc Echocardiogr* 1994; 7: 217-229(b).

Roubin GS, Douglas JS, Gruentzig AR et al. Influence of balloon size on initial success, acute complications, and restenosis after percutaneous transluminal coronary angioplasty. A prospective randomized study. *Circulation* 1988; 78: 557-565.

Roubin GS, Leimgruber PP, Gruentzig A et al. Influence of balloon size on outcome after coronary angioplasty (PTCA). *Circulation* 1985; 72(suppl III): III-400.

Russo RJ, Attubato MS, Davidson CJ et al. Angiography versus intravascular ultrasound-directed stent placement: final results from AVID [abstract]. *Circulation* 1999; 100(suppl I): I-234.

Saremberk IJ, LaVeau PJ, Ezekowitz MD et al. Influence of inflation pressure and balloon size on the development of intimal hyperplasia after balloon angioplasty. *Circulation* 1989; 80: 1029-1040.

Schortl M, Bocksch W, Gross M et al. Use of intravascular ultrasound to compare effects of different strategies of lipid-lowering therapy on plaque volume and composition in patients with coronary artery disease. *Circulation* 2001; 104(4): 387-392.

Serruys PW, de Jaegere P, Kiemeneij et al. on behalf of the Benestent Study Group. A comparison of balloon-expandable stent implantation with balloon angioplasty in patients with coronary artery disease. *N Engl J Med* 1994; 331: 489-495.

Shaw RE, Myler RK, Topol EJ et al. Clinical and morphological factors in prediction of restenosis after multiple vessel angioplasty. *J Am Coll Cardiol* 1986; 7: 63A.

Siegel RJ, Ariani M, Fishbein MC et al. Histopathologic validation of angioscopy and intravascular ultrasound. *Circulation* 1991; 84: 109-117.

Siegel RJ, Chae JS, Fishbein MC et al. Histopathologic correlation of the layered intravascular ultrasound appearance of normal adult human muscular arteries. *Am Heart J* 1993; 126: 872-878.

Simonton CA, Leon MB, Kuntz RE et al. Acute and late clinical and angiographic results of directional atherectomy in the optimal atherectomy restenosis study (OARS). *Circulation* 1995; 92: I-545.

Slager CJ, Laban M, von Birgelen C et al. ANGUS: A new approach to three-dimensional reconstruction of geometry and orientation of coronary lumen and plaque by combined use of coronary angiography and ICUS. *J Am Coll Cardiol* 1995; 25: 144A.

Soward AL, Essad CE, Serruys PW et al. Coronary arterial findings after accidental death immediately after successful percutaneous transluminal coronary angioplasty. *Am J Cardiol* 1985; 6: 369-375.

Spencer T, Ramo MP, Salter DM et al. Characterisation of atherosclerotic plaque by spectral analysis of intravascular ultrasound: an in vitro methodology. *Ultr Med Biol* 1997; 23: 191-203.

Stiel GM, Stiel LSG, Mathey DG et al. Impact of compensatory enlargement of atherosclerotic coronary arteries on angiographic assessment of coronary artery disease. *Circulation* 1989; 80: 1603-1609.

Stone GW, Hodgson JM, St Goar FG et al. for the clinical outcomes with ultrasound trial (CLOUT) investigators. Improved procedural results of coronary angioplasty with intravascular ultrasound guided balloon sizing. *Circulation* 1997; 95: 2044-2052.

Stone P, Gibson M, Sacks F et al. Natural history of coronary atherosclerosis using quantitative angiography in men, and implications for clinical trials of coronary regression. *Am J Cardiol* 1993; 71: 766-772.

Sumitsuji T, Suzuki T, Katoh O et al. for the ABACUS investigators. Restenosis mechanism after aggressive directional coronary atherectomy assessed by intravascular ultrasound in adjunctive balloon angioplasty following coronary atherectomy study (ABACUS). *J Am Coll Cardiol* 1997; 129A.

Takagi A, Tsurumi Y, Kasanuki H et al. Clinical potential of intravascular ultrasound for physiological assessment of coronary stenosis: relationship between quantitative ultrasound tomography and pressure-derived fractional flow reserve. *Circulation* 1999; 100: 250-255.

Tamura A, Mikinya Y, Nasu M. Effect of pravastatin (10mg/d) on progression of coronary atherosclerosis in patients with serum total cholesterol from 160 to 220mg/dl and angiographically documented coronary artery disease. Coronary Artery Regression Study (CARS) Group. *Am J Cardiol* 1997; 79(7): 893-896.

Tenaglia AN, Buller CE, Davidson CJ et al. Mechanisms of balloon angioplasty and directional coronary atherectomy as assessed by intracoronary ultrasound. *J Am Coll Cardiol* 1992; 20: 685-691.

The SHK, Gussenhoven EJ, Bom N et al. Effect of balloon angioplasty on the femoral artery evaluated with intravascular ultrasound imaging. *Circulation* 1992; 86: 483-493.

Tuczu EM, Berkalp B, DeFranco AC et al. The dilemma of diagnosing coronary calcification: Angiography versus intravascular ultrasound. *J Am Coll Cardiol* 1996; 27: 832-840.

Umans VA, Baptista J, Di Mario et al. Angiographic, ultrasonic, and angioscopic assessment of the coronary artery wall and lumen area configuration after directional atherectomy: the mechanism revisited. *Am Heart J* 1995; 130: 217-227.

Umeno T, Yamagishi M, Uematsu M et al. Intravascular ultrasound evidence for the importance of plaque distribution in determining regional coronary vessel distensibility. *Circulation* 1994; 90: I-164.

van der Lugt A, Gussenhoven EJ. Comparison of intravascular ultrasonic findings after coronary balloon angioplasty evaluated in vitro with histology. *Am J Cardiol* 1995; 76: 661-666.

van der Lugt A, Gussenhoven EJ, Pieterman H et al. Failure of intravascular ultrasound to predict dissection after balloon angioplasty by using plaque characteristics. *Am Heart J* 1997; 134: 1075-1081.

Velican D, Velican C. Comparative study on age-related changes and atherosclerotic involvement of the coronary arteries of male and female subjects up to 40 years of age. *Atherosclerosis* 1981; 38: 39-50.

Virmani R, Farb A, Burke AP. Coronary angioplasty from the perspective of atherosclerotic plaque: Morphologic predictors of immediate success and restenosis. *Am Heart J* 1994; 127: 163-179.

von Birgelen C, Di Mario C, Li W et al. Morphometric analysis in three-dimensional intracoronary uktrasound: an in-vitro and in-vivo study using a novel system for the contour detection of lumen and plaque. *Am Heart J* 1996; 132: 516-527.

von Birgelen C, Mintz GS, Roelandt JRTC et al. Reconstruction and quantification with three-dimensional intracoronary ultrasound: an update on techniques, challenges and future directions. *Eur Heart J* 1997; 18: 1056-1067.

von Birgelen C, Slager CJ, Serruys PW et al. Volumetric intracoronary ultrasound: a new maximum confidence approach for the quantitative assessment of progression-regression of atherosclerosis. *Atherosclerosis* 1995; 118: S103-113.

von Birgelen C, van der Lugt A, de Feyter PJ et al. Computerized assessment of coronary lumen and atherosclerotic plaque dimensions in three-dimensional intravascular ultrasound correlated with histomorphometry. *Am J Cardiol* 1996; 78: 1202-1209.

Waligora MJ, Vonesh MJ, McPherson DD et al. Effect of vascular curvature on three-dimensional reconstruction of intravascular ultrasound images. *Circulation* 1994; 90: I-227.

Waller BF. Morphologic correlates of coronary angiographic patterns at the site of percutaneous transluminal coronary angioplasty. *Clin Cardiol* 1988; 11: 817-822.

Waller BF, Pinkerton CA, Slack JD. Intravascular ultrasound: a histological study of vessels during life. The new 'gold standard' for vascular imaging. *Circulation* 1992; 85: 2305-2310.

Waters D, Lesperance J, Gillam LD et al. Advantages and limitations of serial coronary angiography for the assessment of progression and regression of coronary atherosclerosis. Implications for clinical trials. *Circulation* 1993; 87: II-38-II-47.

Weissman NJ, Palacios IF, Weyman AE. Dynamic expansion of the coronary arteries: implications for intravascular ultrasound measurements. *Am Heart J* 1995; 130: 46-51.

Wilensky RL, March KL, Sandusky G et al. Vascular injury, repair and restenosis after percutaneous transluminal coronary angioplasty in the atherosclerotic rabbit. *Circulation* 1995; 92: 2995-3005.

Wong SC, Hong MK, Chuang YC et al. The antiplatelet treatment after intravascular ultrasound guided optimal stent expansion (APLAUSE) trial. *Circulation* 1995; 92 (Suppl I): I-795.

Yock PG, Fitzgerald PJ, Linker DT et al. Intravascular ultrasound guidance for catheter-based coronary interventions. *J Am Coll Cardiol* 1991; 17(Suppl B): 39B-45B.

Yock PG, Tohnson EL, Linker DT. Intravascular ultrasound: development and clinical potential. *Am J Card Imaging* 1988; 2: 185-193.

Zir LM, Miller SW, Dinsmore RE et al. Interobserver variability in coronary angiography. *Circulation* 1976; 53: 627-632.